Porcine Blood in Forensic Bloodstain Pattern Analysis: Hemorheological Issues

Masterarbeit

Zur Erlangung des akademischen Grades

Master of Science in Biomedical Sciences

der Fachhochschule FH Campus Wien

Vorgelegt von:

Andreas Sparer, BSc

Personenkennzeichen:

1430003016

Erstgutachterin:

Ao. Univ.-Prof.in Mag.a Dr.in Ursula Windberger, BSc

Zweitgutachter:

Assoc.-Prof. Ing. Mag. Dr. Fabian Kanz

Eingereicht am:

01. September 2016

Erklärung:

Ich erkläre, dass die vorliegende Masterarbeit von mir selbst verfasst wurde und ich keine anderen als die angeführten Behelfe verwendet bzw. ich mich auch sonst keiner unerlaubter Hilfe bedient habe.

Ich versichere, dass ich diese Masterarbeit bisher weder im In- noch im Ausland (einer Beurteilerin / einem Beurteiler zur Begutachtung) in irgendeiner Form als Prüfungsarbeit vorgelegt habe.

Weiters versichere ich, dass die von mir eingereichten Exemplare (ausgedruckt und elektronisch) identisch sind.

Datum: ..... Unterschrift: .....

Acknowledgements

The act of giving without the expectation of something in return is the true definition of kindness. Thank you for your kindness and support!

Ao. Univ.-Prof.in Mag.a Dr.in Ursula Windberger, BSc

Dr. Lukas Schwarz

Assoc.-Prof. Ing. Mag. Dr. Fabian Kanz

Renate Sparer

Ing. Mag. Rudolf Sparer

Danijela Komla

Barbara Holczmann

Monika Weiss

Patrizia Beinhofer

Kurzfassung

Diese Arbeit beschäftigt sich mit den hämorheologischen Eigenschaften und der Lagerfähigkeit von antikoaguliertem Schweinevollblut, welches in der forensischen Blutspurenmusteranalyse verwendet wird, um Tathergänge zu rekonstruieren, Sachverhalte zu veranschaulichen und Fachpersonal auszubilden. Für eine umfassende rheologische Charakterisierung wurde von zehn Schweinen EDTA-Blut gewonnen. Durch Herstellung von Verdünnungen mit 30, 40, 50 und 60 % Hämatokrit und die Durchführung von Rotationsmessungen bei 7, 12, 17, 22, 27, 32, 37 und 42 °C mit Scherraten von 1 - 1000 s^{-1} wurde der Einfluss von Hämatokrit und Temperatur auf die dynamische Scherviskosität η dargelegt. Mit Ermittlung des Speichermoduls G´ und des Verlustmoduls G´´ über Messungen im oszillierenden Scherfeld (small amplitude oscillation) konnte außerdem die Suspensionsstabilität der Proben bei unterschiedlichen Temperaturen und Hämatokrit-Verhältnissen aufgezeigt werden. Um die Lagerfähigkeit von Schweinevollblut zu verbessern und alterungsbedingte Veränderungen zu ermitteln, wurde Blut von elf Tieren mit CPDA-1 antikoaguliert, über einen Zeitraum von 32 Tagen bei Kühlschranktemperatur gelagert und jeden zweiten Tag untersucht. Rheologisch wurden dabei erneut die dynamische Scherviskosität η, sowie der Verlustfaktor tanδ (G´´/G´) mit einer Frequenz von 1 s^{-1} (vergleichbar mit 60 Herzschlägen pro Minute) bei 22 und 37 °C erhoben. Weiters wurden Blutbilder erstellt und die Konzentration von freiem Hämoglobin im Plasma bestimmt. Anhand der vorliegenden Daten wird aus hämorheologischer Sicht empfohlen, Schweinevollblut mit CPDA-1 maximal 20 Tage bei 4 °C zu lagern, wenn dieses bei forensischen Experimenten zur Anwendung kommen soll. Eine Pilot-Studie mit einfachen Simulationsexperimenten vor und nach 32-tägiger Lagerung zeigte deutliche Unterschiede hinsichtlich der entstehenden Blutspuren. Weitere Untersuchungen zur Analyse und Optimierung der Lagerfähigkeit von Schweinevollblut werden empfohlen.

Abstract

This thesis deals with the hemorheological characteristics and storability of anticoagulated pig whole blood, which is used in forensic bloodstain pattern analysis to reconstruct the circumstances of a crime, to visualize a set of facts and to train professional staff. For a comprehensive rheological characterization EDTA-blood was drawn from ten pigs. To describe the influence of hematocrit and temperature on dynamic shear viscosity η, dilutions with 30, 40, 50 and 60 % hematocrit were prepared and analysed during rotational measurements at 7, 12, 17, 22, 27, 32, 37 and 42 °C with shear rates of 1 - 1000 s^{-1}. The analysis of storage module G´ and loss module G´´ during small amplitude oscillatory shear revealed the suspension stability of porcine blood at different temperatures and hematocrit values. In order to improve storability of pig whole blood and to study age-related changes, samples from eleven animals were anticoagulated with CPDA-1, stored in the fridge for 32 days and analysed every two days. Rheological testing at 22 and 37 °C included measurements of dynamic shear viscosity η, as well as analysis of loss factor $\tan\delta$ (G´´/G´) at a frequency of 1 s^{-1} (comparable to 60 heartbeats per minute). Moreover, hemograms were prepared and the level of free hemoglobin in plasma was determined. Considering the data at hand it is recommended from a hemorheological point of view to maximum store pig whole blood with CPDA-1 at 4 °C for a period of 20 days if used for forensic experimentation. A pilot study with simple simulation experiments before and after storage for 32 days showed notable differences in the resulting bloodstain patterns. Further studies on the analysis and optimization of storability of porcine whole blood are recommended.

List of abbreviations

BPA	bloodstain pattern analysis
CSR	controlled shear rate
CSS	controlled shear stress
CPDA-1	Citrate Phosphate Dextrose Adenine anticoagulant solution
γ	deformation amplitude
η	dynamic shear viscosity
EDTA	ethylenediamine tetraacetic acid
fHb	free hemoglobin
HCT	hematocrit
HVIS	high-velocity impact blood spatter
γ_L	limiting value of the LVE range
LVE range	linear viscoelastic range
IABPA	International Association of Bloodstain Pattern Analysts
G´´	loss module
tanδ	loss factor tangent delta
LVIS	low-velocity impact blood spatter
MALDI	matrix-assisted laser desorption/ionization
MCH	mean corpuscular hemoglobin
MCHC	mean corpuscular hemoglobin concentration
MCV	mean corpuscular volume
MVIS	medium-velocity impact blood spatter
mPa*s	milli-Pascal-second
Pa*s	Pascal-second
RBC	red blood cell
s^{-1}	reciprocal second / inverse second
rpm	rounds per minute
$\dot{\gamma}$	shear rate
τ	shear stress
SAOS	small amplitude oscillatory shear
G´	storage module
SBS	synthetic blood substitute
TOF MS	time of flight mass spectrometry
WBC	white blood cell

List of key terms

blood
bloodstain pattern analysis
CPDA-1
dynamic shear viscosity
EDTA
forensic science
hematocrit
hematology
hemorheology
oscillation
pig
porcine blood
rotation
rheology
storability
storage
temperature

Contents

1. Introduction

1.1. Introduction to bloodstain pattern analysis

1.1.1. Definition and objectives

Bloodstain pattern analysis (BPA) is a discipline of forensic sciences dedicated to the detection, categorization, analysis and interpretation of blood spatter with the aim of reconstructing a course of criminologically relevant events. BPA stands in close cooperation with other scientific subjects like forensic pathology, forensic DNA analysis, forensic photography, forensic serology and computational forensics [1,2,3,4,5].

Typical issues of a forensic investigation that are worked on by BPA experts include a distinction between natural death, accident, suicide and homicide, a demand to confirm or rule out the involvement of an alleged perpetrator or an evaluation of the intensity of a criminal action. As the judicial system takes into account whether a victim was injured in a singular act or mutilated multiple times, the latter is an important aspect to legal representatives, jury members and judges in order to determine an appropriate degree of penalty [2,3,4,5].

To shed light upon the issues described, BPA analysts search for latent traces of blood, help to figure out the date or time of a crime, the type and velocity of a weapon used, the types of injuries inflicted and the positions and movements of those involved. In doing so, BPA for example might clarify whether an assailant was left or right handed and it might allow to underpin or to refute the testimony of a person on how the blood of the victim was placed on their clothing. All information gained can serve as evidence for or against an accused person, but also as a proof of exoneration for emergency responders and other persons present at the scene of a spatter-producing event [6].

Fig. 1: Logo of IABPA. [7]

Depending on local conditions, BPA is being utilized and carried out mostly in an interdisciplinary manner between police or court officials and scientific and medical personnel. The International Association of Bloodstain Pattern Analysts (IABPA), founded in 1983, serves as an umbrella organization for analysts and offers professional networking and educational programs around the world (Fig.1). The Journal of Bloodstain Pattern Analysis is being issued by the IABPA every three months on their website and features research articles, case reports, presentation abstracts and critical comments [2,3,4,5].

1.1.2. Spatter classification

The history of BPA began in 1895, when Dr. Eduard Piotrowski published a study about the bloodstain pattern resulting from blows against the head. Since then, the field of BPA has expanded enormously. One of the most important achievements, which for the first time enabled communication and consistent interpretation between BPA experts, was the implementation of a scientific classification of blood spatter [8].

The conventional taxonomic approach was orientated on the velocity of the force that has an impact on the blood source. The basic concept was, that the force applied to the source is relevant for the size and other characteristics of the resulting stains. Stains were attributed to the categories of low-velocity (LVIS), medium-velocity (MVIS) or high-velocity impact blood spatter (HVIS). LVIS were defined to be the result of a force with a velocity of up to 5 ft/s (1.5 m/s), featuring primary stains with a diameter of 4 mm or greater. This type of spatter is observed when blood is simply dripping form a wound or a blood-soaked item under the influence of gravity. MVIS were determined to be created by a force with a velocity of 5 to 25 ft/s (1.5 to 7.5 m/s) as during stabbings, arterial spurting or beatings with a blunt instrument like a baseball bat. The resulting primary stains range between 1 and 3 mm in diameter. HVIS, the type of spatter associated with gunshots or injury caused by other sorts of machinery, were defined to have a diameter of less than 1 mm and being the result of a force against the blood source with more than 100 ft/s (30 m/s). As this original terminology did not appreciate several mechanisms like expiratory bloodstains to the extent required, a newer and more holistic approach to bloodstain pattern classification has been made (Fig.2). It incorporates several other factors next to impact velocity [9].

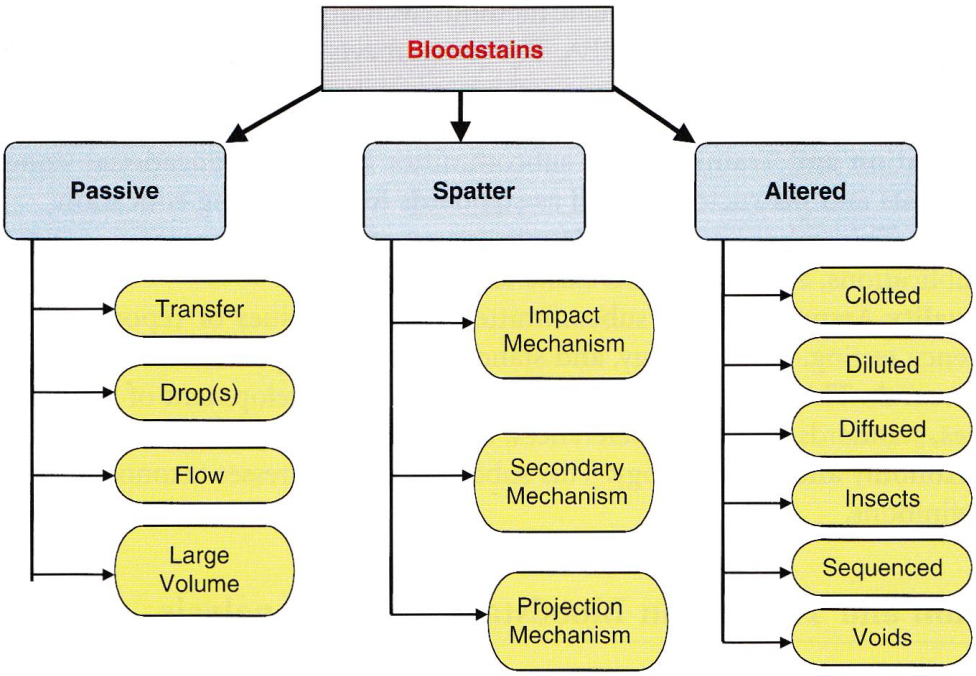

Fig. 2: Bloodstain categories and subcategories. In greater detail than the original approach, the new taxonomy includes various mechanisms of bloodstain formation and alteration [10].

Modern bloodstain classification includes the following categories:

I. **Passive patterns** are created when blood is free-falling and is influenced just by gravity, air resistance and the kind of surface which it impinges on. Subcategories of passive patterns include transfer patterns, drop patterns, flow patterns, and patterns with a large volume [11].

   a. **Transfer patterns** originate from a bloody object getting in contact with a nonbloody surface. Undeterminable transfer patterns are often referred to as blood smear, while a transfer stain with visible directionality is termed as a swipe. Sometimes there might even be recognizable transfer patterns like fingerprints, footprints, the sole of a shoe or impressions of a knife [12].

   b. **Drop patterns** are created by single free-falling drops, by multiple drops falling into each other from a stationary source or by multiple drops forming a drip trail during horizontal motion [13].

   c. **Flow patterns** are always directed and are created when blood moves across a surface from one point to another due to gravity in a singular or in multiple flows. Changes of flow direction indicate movement of the body or object on which the flow pattern is found [14].

   d. **Patterns with a large volume of blood** are either blood pools or saturation stains, both of which are associated with extensive bleeding. When a large volume of blood accumulates on a non-absorbing surface, it forms a blood pool and serum separation might be visible. Saturation stains are the result of large volumes of blood being absorbed into a surface like a carpet or bed linen [15].

II. **Spatter patterns** are created when an external force is applied to a source of blood, which is then dispersed and forms distinct spots and stains. Depending on the surface, the size of the stains might allow a determination of impact velocity on the blood source like defined in the conventional taxonomic approach to bloodstain pattern classification with the categories of LVIS, MVIS and HVIS. Also depending on the surface, the shape of the spatters might allow an evaluation of the angle of impact and therefore a determination of the location or at least the direction where the blood came from (blood source) [16].

   a. **Impact mechanism patterns** are patterns created by beating, stabbing, shooting and other sorts of trauma. In the case of gunshots, back spatter might be found on the hand of the shooter or even in the barrel of the firearm as a result of blood being dashed back towards the source of energy. The counterpart is forward spatter, which is created when a bullet leaves the body through an exit wound and blood droplets are being entrained [17].

b. **Secondary mechanism patterns** are produced when a secondary effect other than the actual bloodletting event overcomes the physical properties of blood. So when blood drops hit each other, satellite spatter is created around a parent stain in the centre of the pattern. This type of secondary mechanism pattern can often be found on clothing of a person assisting a bleeding victim and might probably be misinterpreted as an impact mechanism pattern from beating [18].

c. **Projection mechanism patterns** are patterns that are created due to other force than external impact. This type of spatter can be found when blood is exhaled, coughed or sneezed out. Patterns resulting from arterial spurting or ruptured varicose veins are also attributed to that category. Patterns resulting from exhalation through mouth, nose or wounds to the respiratory tract typically feature air bubbles and vacuoles, making a foamy impression [19].

III. **Altered patterns** are a result of any sort of alteration of the original appearance of traces of blood. This includes the mechanisms of clotting, dilution and diffusion, as well as insect activity. Moreover, sequencing of bloodstains and the phenomenon of void patterns belong to this category [20].

a. **Clotted patterns** are manifested when blood clotting leads to the formation and retraction of a clot, producing visible portions of serum. The time until clotting takes place depends on factors like blood volume, temperature, humidity, the presence of anticoagulant medication and the nature of the surface where blood is positioned [21,22].

b. **Diluted patterns** can be found at crime scenes after rain and snowfall or when clean-up attempts have been made. They have a washed-out appearance and sometimes the original stains are altered or removed to a point where analysis or even recognition with the naked eye is impossible. Offenders cleaning a surface often use water, various bleaching agents, acids or paint. Chemical enhancement can be used to search for latent bloodstains [23].

c. **Diffused patterns** are usually situated on surfaces like cotton clothing or bedding, which become saturated with blood due to capillary diffusion. In most cases, the process leads to the discolouration of large areas of cloth [24].

d. **Patterns created by insects** can be misinterpreted as impact blood spatter. When flies are feeding on decomposing bodies or pools of blood, they ingest blood and regurgitate it on another surface to allow the blood to be degraded by enzymatic activity. Later the flies return and consume some of it [25,26].

e. **Sequenced patterns** are traces of blood that have been altered by a sequence of events, often enabling conclusions regarding the chronology of two or more incidents. One of numerous examples for sequencing of bloodstains would be the presence of blood spatters on top of a pre-existing transfer pattern [27].

f. **Void patterns** describe the absence of bloodstaining in an otherwise continuous stained area. When an object or a body is relocated or completely removed a void becomes recognizable [28].

1.1.3. Chemical enhancement

While some forensic cases might include unaffected traces of blood, others might not. Offenders often wash off the blood of their victims from floors, walls and killing tools. Therefore, BPA experts use a number of ways to chemically enhance latent bloodstains, with the detection of blood employing luminol being the most prominent technique. The method is based on the presence of the metalloprotein hemoglobin, which can be found in red blood cells (RBCs). The prosthetic group for hemoglobin is heme, which upon ageing and oxidation changes to hemin. When hemin is present, it will catalyse the oxidation of luminol by hydrogen peroxide in alkaline solution, leading to the emission of strong bluish chemiluminescence for approximately 30 seconds. The reaction where luminol is sprayed on a surface can be repeated several times, does not interfere with serologic species or blood group testing and is sufficient enough to detect minutest amounts of blood even after a murder scene or an object has been cleaned from visible traces [29].

Other reagents used in BPA include Amido Black, Ninhydrin, Aqueous Leucocrystal Violet and titanium dioxide. Depending on the colour and texture of the surface, different chemicals are applied to bloody finger- and handprints, footwear impressions and other bloodstain patterns that are not clearly visible (Fig.3) [30].

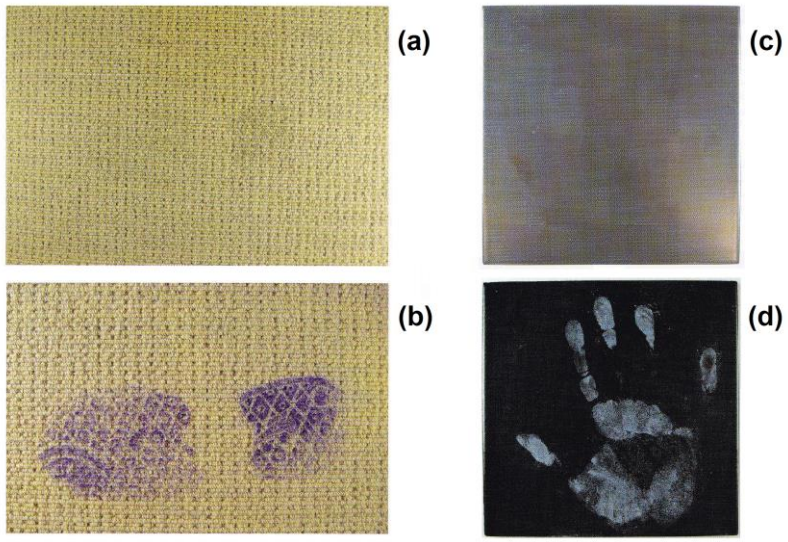

Fig. 3: Chemical enhancement in BPA. Photographs (a) and (b) show a bloody footwear impression on a carpet. Picture (a) was taken before and picture (b) was taken after enhancement with Aqueous Leucocrystal Violet. Photographs (c) and (d) exhibit a bloody handprint, that had been found on a dark kitchen tile. Picture (c) shows the untreated handprint, while picture (d) reveals the same stain after treatment with titanium dioxide. Following enhancement, the handprint is clearly visible and rich in detail [31].

1.1.4. The necessity of simulations

When approaching a bloodstain pattern case, analysts will start with an examination of the crime scene. If not possible, they will at least examine photographs taken during evidence collection by the police. Next, analysts will review reports, photographs and notes from officers, emergency medical technicians, hospital staff and autopsy personnel. Hypotheses will be formulated for each bloodstain pattern and need to be tested. Testing might include a review of past cases and past experiments or there might be a demand for actual experimentation. In general, BPA casework includes four levels of analysis (Fig.4). It must be clear that although very much dependent on experience, a correct understanding of traces of blood in a criminal case can sometimes only be achieved through experimental setups [2,32].

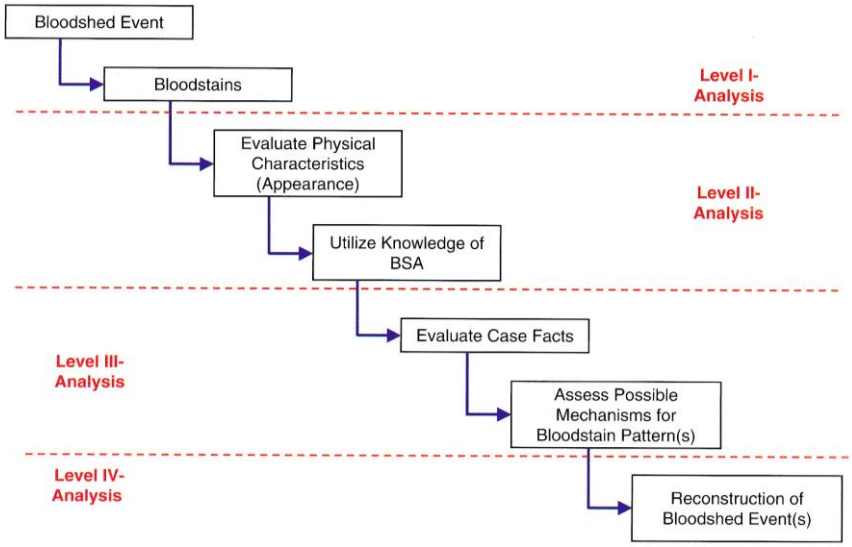

Fig. 4: Logic tree to BPA. The chart gives an overview of the four levels of BPA analysis [33].

Even when the question of fault has already been resolved, practical BPA experiments might still be in great demand. It is one thing to gain adamant evidence, but it is another to present it in court in a way so that every juror will understand the momentousness of it. In a modern world orientated more and more towards visual stimuli, demonstrative evidence can be a powerful and persuasive support to expert testimony at a trial. BPA re-enactment experiments can be videotaped beforehand or conducted directly in the courtroom with the purpose of illustrating a set of facts [34].

Next to specific case work, the training of qualified BPA professionals also requires practical simulations. Using different types of apparatuses, participants in basic and advanced BPA educational programs are able to create patterns similar to the ones present at actual crime scenes. To demonstrate back and forward spatter occurring after gunshots for example, shooting through blood-soaked polyurethane sponges is a very common procedure. Reviewing the stain patterns resulting from various types of impact is a crucial factor in understanding the dynamics and mechanisms involved in the formation of a bloodstain pattern. Trainees might even preserve patterns created on cardboard or other surfaces and use them as a point of reference in their future work [35].

1.1.5. Previous findings on suitable samples

Thinking about the area of application for practical BPA experiments and the serious consequences that might result from bad training, misinterpretation or poor visualization, it is obvious that any sort of simulation needs to employ a fluid that has physical material characteristics as similar to those of human whole blood as possible. However, due to blood-transmitted viral infections like HIV and due to a limited availability even for transfusion therapy, human blood itself can often not be used for BPA purposes. Up to date, no adequate synthetic blood substitute (SBS) meeting the physiological properties of human whole blood is available. There are computer-based programs dealing with the documentation and analysis of traces of blood at an alleged crime scene, but they have also up to date not been incorporated into routine work because of practical problems [2,3,36,37,38,39,40].

Therefore, in some countries anticoagulated animal whole blood - especially from pig - is a commonly used alternative for simulations. But although MacDonell made a comparison of samples without additives and blood drawn with ethylenediamine tetraacetic acid (EDTA) and did not find any differences in their behaviour, one has to admit, that anticoagulation always means manipulation. The only way to evade that is to perform the required experiments with living test animals. Nonetheless, as this leads to enormous extra effort and expense and brings along ethical issues, animal samples with additive solutions are used in most of the cases [2,36].

While it is general knowledge that hematocrit (HCT) and other parameters are very similar in human and pig blood, publications regarding the physical material characteristics of porcine blood in respect of forensic issues are very rare. In their 1996 publication Raymond, Smith and Liesegang analysed the viscosity of ten pig blood samples from abattoirs with EDTA using a cone plate viscometer. Analysis was conducted immediately after withdrawal and was repeated after storage at 4 °C [2].

They concluded that while HCT values of human and pig samples feature almost the same range, blood viscosity of freshly slaughtered pigs was around 20 % higher than that of fresh human samples. It was furthermore stated, that this variation extended to 60 % after the samples had been incubated at 4 °C for a period of two weeks and that some of the samples were obviously affected by contamination with bacteria or fungi. Based on these findings and considering analysis of surface tension, relative density and pattern simulations, the authors of the study postulated that it would be valid to use pig blood instead of human samples for BPA issues, even if stored at 4 °C for two weeks [2].

In 2015, data from Serp including five blood samples derived from living animals via venipuncture and five samples from abattoirs confirmed the applicability of pig blood for 11 days after withdrawal. However, it was pointed out that there are significant differences between blood samples from venipunctured and slaughtered pigs, with abattoir samples being less physiologic in comparison to human blood and with both groups undergoing significant changes during storage with EDTA. Analysis also revealed massive contamination of pig blood samples from abattoirs after storage at 4 °C for 18 days, confirming earlier findings from 1996. Meanwhile, samples collected through venipuncture did not feature a number of microorganisms to a level where they could be detected using standard agar plates [41].

1.2. Fundamental aspects of bloodshed

1.2.1. Anatomical and physiological basics

The cardiovascular system consists of the heart, blood and blood vessels. There are three types of blood vessels with different wall structures - arteries, veins and capillaries. The heart is a hollow muscular organ with two atria and two ventricles built of involuntary striated muscle. While the right heart is responsible for pulmonary circulation, the left heart actuates systemic blood flow (Fig.5). Blood pressure in the cardiovascular system depends on blood volume, cardiac output and the systemic vascular resistance. It varies between a diastolic minimum when the heart is refilling and a systolic maximum when the ventricles contract [42,43].

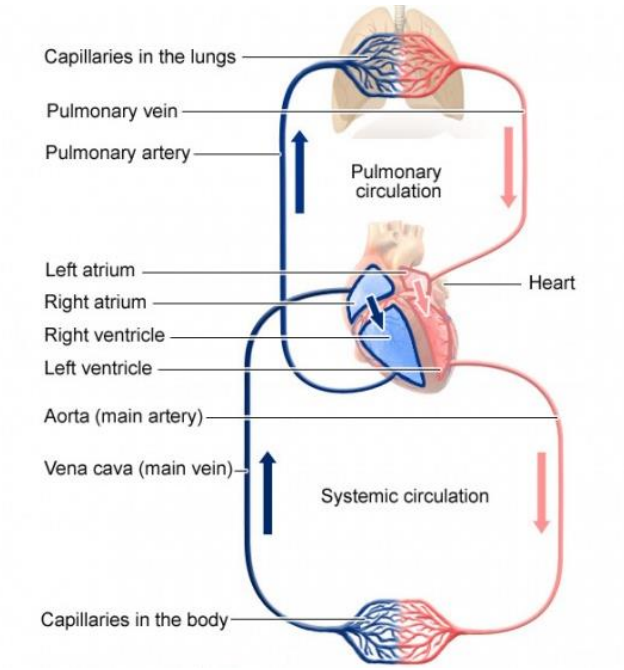

Fig. 5: The circulatory system. Blood flow in the body is divided into a pulmonary and a systemic circuit. Red lines indicate the flow of oxygen-rich blood. Blue lines represent deoxygenated blood after oxygen has been used as an oxidizing agent in cellular respiration [44].

The bloodstream proceeds as follows: superior and inferior vena cava transport oxygen deprived blood from the body into the right atrium of the cardiac muscle. It is then pumped through the tricuspid valve into the right ventricle. When the ventricle contracts, the tricuspid valve closes and blood is released through the pulmonary valve into the pulmonary arteries. In the lungs those arteries branch and merge into capillaries that are adjacent to alveoli. Carbon dioxide is exchanged for oxygen via passive diffusion and oxygenated blood is re-collected and transported to the left atrium through pulmonary veins. Next, blood enters the left ventricle through the mitral valve. The ventricle contracts and releases blood through the aortic valve into the aorta. Arteries branch into all areas of the body and merge into capillaries, where the reverse gas exchange takes place. Venous vessels then re-collect blood into the vena cava and the circulation recurs [43].

Blood is ascribed to connective tissue consisting of blood cells and a protein and electrolyte solution - the blood plasma. It has several crucial functions for the body: transport of oxygen and carbon dioxide, distribution of hormones, nutrients and metabolic waste products, regulation of body temperature, immunologic defence against pathogenic agents or tumor cells and preservation of the body's integrity by wound closure. In a healthy adult human individual, blood has a natural pH of 7.4 and amounts to 4.5 - 5.0 liters, which is approximately 8 - 9 % of the total body mass. The volume fraction of RBCs to total blood volume is referred to as HCT [45,46].

Blood plasma is a yellowish but clear liquid containing water, electrolytes, proteins and low molecular organic substances. The remaining fluid after clotting has taken place is referred to as blood serum and is missing clotting factors like fibrinogen [47].

The cellular fraction of blood can be subdivided into red blood cells (RBCs), white blood cells (WBCs) and blood platelets. Hematopoiesis, the production of blood cells, takes place in the bone marrow (Fig.6). Mature RBCs, or erythrocytes, don't have nuclei or mitochondria. The lack of these cell organelles explains their rather short life span of 120 days. RBCs contain the ferrous protein complex hemoglobin and are responsible for oxygen transport. WBCs, or leukocytes, can be subdivided into lymphocytes, monocytes and neutrophil, eosinophil and basophil granulocytes. They represent the cellular part of the body's innate immune system and fight pathogens by phagocytosis or the release of toxic granules. Through the production of antibodies WBCs also operate the adaptive immune response. Platelets, or thrombocytes, are key players of hemostasis whose cross-linkage by fibrin leads to thrombus formation [48,49].

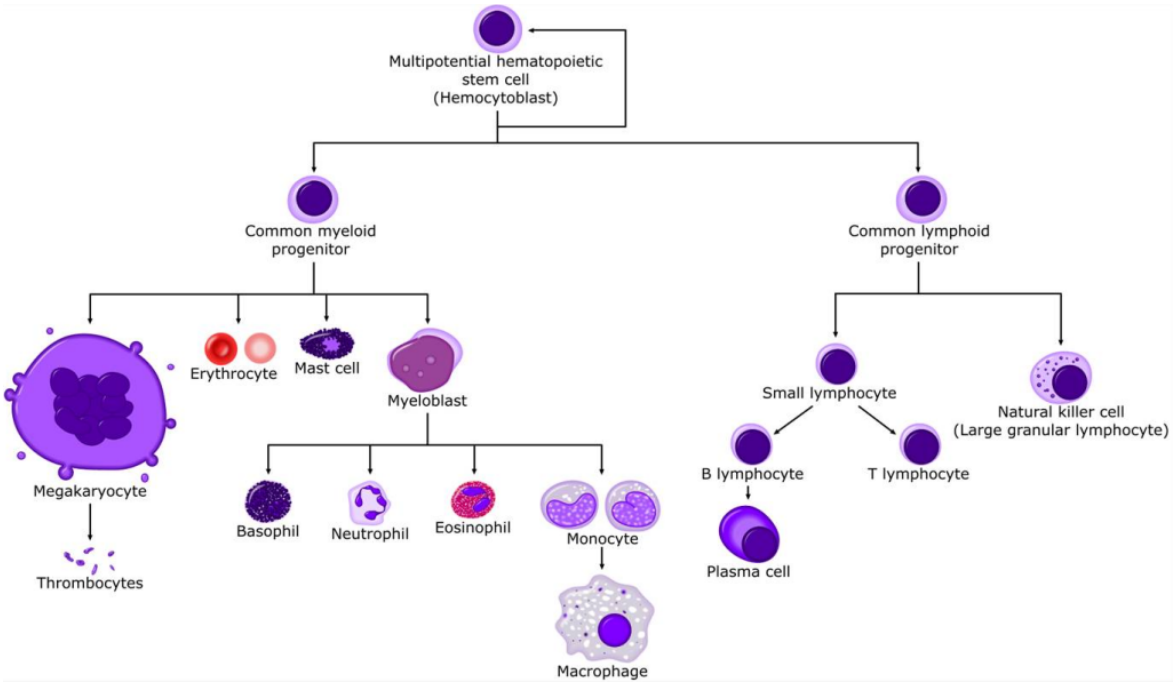

Fig. 6: Hematopoiesis in simplified terms. The overview shows multipotential hematopoietic stem cells in the bone marrow as origin of all mature blood cells. In terms of total volume and cell number in healthy peripheral whole blood, erythrocytes represent the most prominent population [50].

1.2.2. Physical properties of blood

Even though blood is connective tissue and has the function of an organ, it's physical properties are those of a liquid. Liquids, as well as gases, belong to the fluids, which are a subset of the phases of matter. The molecules in a liquid have the ability to move around freely, enabling the substance to flow and to conform to the shape of its container. Temperature and pressure have a determining influence on the physical configuration of single molecules. Commonly, the physical properties of any substance are defined by classical mechanics. There is a vast number of factors that can be used to describe the characteristics of a liquid like absorption, boiling point, density, elasticity, electrical resistivity and conductivity, opacity, refractive index, tension, thermal conductivity and viscosity [51,52].

In the field of bloodstain pattern analysis viscosity, surface tension and relative density are considered to be the most important of all physical properties, as they determine the flight characteristics of blood, which in turn directly affect the characteristics of blood spatter. In order to be able to study bloodstain formation and the resulting patterns one has to be aware of and to understand those physical properties [51,53,54].

Once a liquid comes to movement, the molecules in the substance slide against each other and are subjected to a specific force of friction. The resultant flow resistance can be described as viscosity η and is reported in Pascal-seconds (Pa*s) or milli-Pascal-seconds (mPa*s). At room temperature, honey features greater viscosity than water. The reciprocal for viscosity is fluidity. At room temperature, honey features lower fluidity than water [51,55].

There is ideal (inviscid) and non-ideal (viscous) flow behaviour. Isaac Newton first formulated that the flow resistance of a fluid would be proportional to flow velocity. Considering findings from Bernoulli, Euler and Navier, George Gabriel Stokes then postulated the law of viscosity as

$$\tau = \eta * \dot{\gamma}$$

whereas τ is shear stress, η is viscosity and $\dot{\gamma}$ is shear rate. This equation is often referred to as Newton's law of viscosity and fluids behaving according to that law are called Newtonian. They have ideal flow behaviour - meaning that viscosity is independent from the amount and duration of the shearing load (Fig.7) [51,55].

Under ordinary conditions, many gases, water or motor oil are practically Newtonian. When the speed of water molecules and layers sliding past each other is doubled, the resisting force will also be doubled - and vice versa. The harder the trigger of a water pistol is pulled, the faster the liquid will exit the gun barrel [51,55].

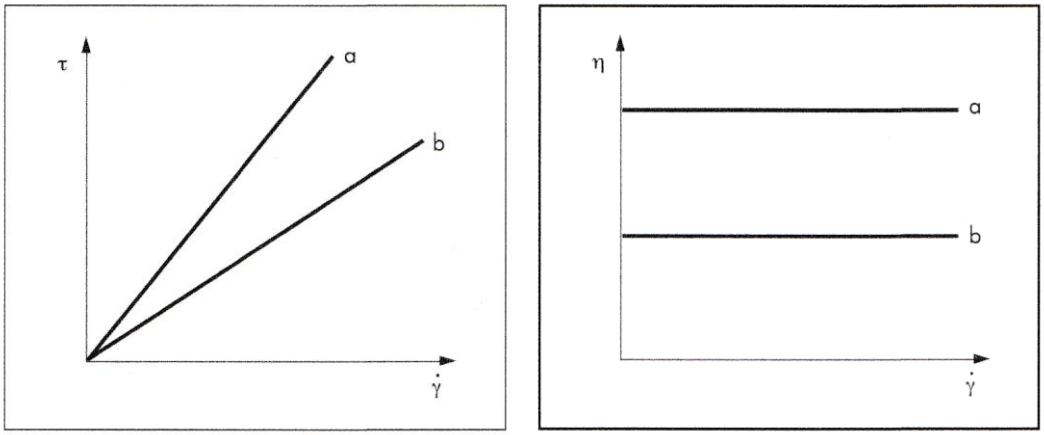

Fig. 7: Characteristics of Newtonian fluids. The left graph shows flow curves of two Newtonian fluids, a and b. Shear stress τ and shear rate $\dot{\gamma}$ are linearly proportional to each other. Reciprocal dependence is in place. The graph on the right side shows curves of viscosity of two Newtonian fluids, a and b. Viscosity η is independent from the shear rate $\dot{\gamma}$ and stays the same when the shear rate increases [55].

If a fluid in its flow behaviour in one or the other way significantly deviates from Newton's law of viscosity, it is referred to as non-Newtonian. When the speed of the molecules and layers of a non-Newtonian fluid sliding past each other is doubled, the resisting force is not doubled. In lieu, it may less than double or more than double. Non-Newtonian liquids whose viscosity increases with the rate of shear strain, are referred to as shear thickening. If viscosity decreases with the rate of shear strain, the liquid is shear thinning (Fig.8). Thixotropic liquids feature decreasing and rheopectic liquids feature increasing viscosity over time when they are shaken [51,56].

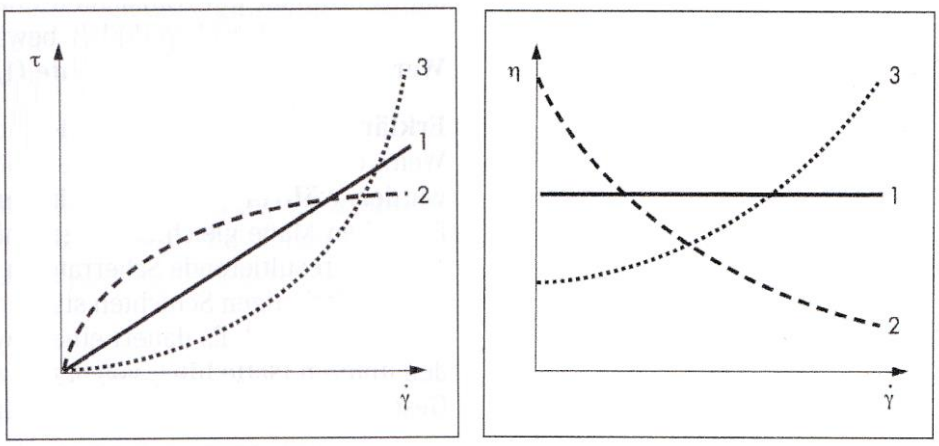

Fig. 8: Characteristics of non-Newtonian fluids. The left graph shows flow curves and the graph on the right side shows curves of viscosity. Both graphs compare the behaviour of an ideal viscous (1), a shear thinning (2) and a shear thickening fluid (3). Viscosity η of the shear thinning fluid decreases as the shear rate $\dot{\gamma}$ increases. When exposed to the same ascent of shear rate, viscosity of the shear thickening fluid increases [57].

Whole blood viscosity is a sum of the characteristics and the interaction of all the individual components of the substance. Viscosity of blood plasma is approximately twice as big as it is for water. It might be higher due to an elevated fibrinogen level. HCT is related to the number of RBCs, which in terms of number and volume are the most prominent solid particles in blood. Logically, the quantity of solid particles in a suspension does have an impact on viscosity. Earlier studies indicate that blood viscosity increases with HCT and is also influenced by temperature. Moreover, it has been shown that RBCs have the ability to change their shape to a low-drag conformation during high flow rates and are able to deform when passing narrow capillaries (Fig.9). At low flow rates or under static conditions, RBCs tend to aggregate, which is also known as rouleaux formation. The aggregates are able to disperse and deform, depending on surrounding shear forces. [53,58,59,60,61,62,63].

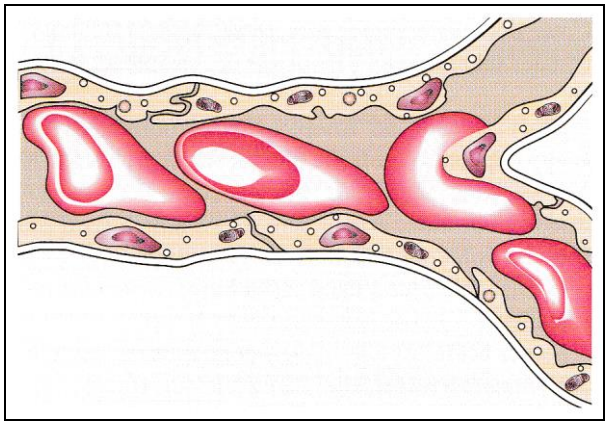

Fig. 9: RBCs passing capillaries. The cells change their shape in order to pass confined space in the circulatory system [56].

Eventually, whole blood is a shear thinning fluid and so viscosity significantly varies with the shear rate. Low shear rates are accompanied with RBC sedimentation and aggregation, as well as the formation of a clear plasma phase, causing blood to act like a non-Newtonian liquid. At high shear rates, blood behaves like a homogenous liquid and becomes Newtonian [51,53,59,60,61,63].

2. Project fundamentals

2.1. Academic void

As previous work from Raymond, Smith and Liesegang only provided viscosity measurements for pig blood at a singular shear rate and did not address the influence of temperature and HCT on viscosity to the extent required, further research was needed for a profound characterization of the substance. Moreover, the suspension stability of porcine blood - given by the number of structural elements in blood as well as the forces between those structures and the surrounding plasma - had not been analysed before and had to be assessed with rheological tests in the oscillating shear field [2,59].

Regarding storability of porcine blood, earlier studies indicated that, assuming anticoagulation with EDTA and constant storage at 4 °C, ageing samples can be used for BPA experiments up to 11-14 days after withdrawal, before displaying substantially altered material characteristics. The acquisition and storage of suitable samples in an adequate amount for simulations is a critical point for every BPA expert, both financially and logistically. In order to enable higher quality standards and to avoid distorted BPA simulations during multi-day educational programs or reconstruction experiments, an improvement of storability of pig blood must be strived after [2,41].

Considering viscosity, pig blood from abattoirs has been proven to feature greater divergences to human samples than porcine samples derived from living animals through venipuncture. These differences are present already when samples are fresh, but become considerably bigger after some days of storage. Moreover, blood from slaughtered pigs has been shown to be affected by high contamination rates of bacteria or fungi, ‘while those seem to be absent in pig blood from living animals. In order to maximize the potential of an adequate simulation of a physiological human situation during BPA experiments and to minimize the impact of microorganisms on the blood samples, future research should therefore focus on porcine whole blood gained from living animals via venipuncture [2,41].

2.2. Research questions

Regarding the academic void in the field of research described above, the following research questions were posed:

I. Rheological characterization of porcine blood

a. What impact have the factors hematocrit and temperature on pig whole blood viscosity and suspension stability?
b. What conclusions regarding the applicability of porcine whole blood for BPA re-enactment experiments can be made considering these effects?

II. Hemorheological analysis of pig blood storability

c. What hemorheological changes does pig blood show during storage at 4 °C?
d. What steps can be taken in order to prolong the storability of pig blood samples intended for BPA? How could a protocol look like?
e. To what extent can the storability of porcine blood intended for BPA be prolonged in comparison to present conservation methods with EDTA?

III. Pilot study on bloodstain pattern simulation with aged samples

f. In what way are bloodstain patterns created with aged pig blood different to patterns originating from simulations with fresh samples?

2.3. Aim of the project

The study at hand had the aim of gaining further information about the physical material characteristics of porcine blood in order to improve the use of it in the field of forensic BPA. It was designed to clarify the influence of HCT and temperature on pig whole blood viscosity and suspension stability, supplying BPA experts with essential information for an optimization and standardization of future test protocols. The elicitation of physical parameters at the same time also aimed at providing benchmark data for a possible future production of SBS products. Furthermore, the project at hand had the aim of studying the hemorheological changes that porcine blood runs through during storage at 4 °C. It strived for enhancement and elongation of storability of anticoagulated pig blood samples and was also meant to deliver data for a pilot assessment of the effect of storage and ageing on bloodstain patterns created by re-enactment experiments.

2.4. Scientific hypotheses

The following scientific hypotheses were posed in order to be rigorously tested during this project:

I. Rheological characterization of porcine blood

H_0: HCT and temperature do not influence pig whole blood viscosity and suspension stability and it is therefore not necessary to consider these factors during practical BPA experimentation.

H_1: HCT and temperature have a substantial impact on pig whole blood viscosity and suspension stability and should be taken into consideration during BPA simulations.

II. Hemorheological analysis of pig blood storability

H_0: Storage at 4 °C does not influence the hemorheological characteristics of porcine whole blood.

H_1: There are substantial changes in hemorheological characteristics of porcine whole blood during storage at 4 ° C.

III. Pilot study on bloodstain pattern simulation with aged samples

H_0: Bloodstain patterns created during simulations with aged samples feature the same physical appearance like patterns originating from re-enactment with fresh samples.

H_1: Bloodstain patterns created during simulations with aged samples are different in their physical appearance compared to patterns originating from re-enactment with fresh samples.

3. Materials and methods

3.1. Rheological characterization of porcine blood

3.1.1. Experimental setup

To study the influence of HCT and temperature on viscosity and suspension stability, blood samples were drawn from conscious pigs and anticoagulated with EDTA. HCT dilutions were prepared and subsequently analysed with a rheometer. Blood sampling and analysis was performed on ten different dates and included ten pigs.

3.1.2. Specimen collection

Samples were obtained from animals at University of Veterinary Medicine in Vienna. The withdrawal of blood from pigs for the intended purpose has been approved by the Austrian Federal Ministry of Science, Research and Economy (reference numbers: BMWF-66.009/0372-WF/V/3b/2014, BMWFW-68.205/0188-WF/V/3b/2015).

Following previous analysis of human and horse blood, a sample size of n=10 pigs was proposed. The individuals for phlebotomy were between three and six months of age, seven of them female, one male and two male neutered. Nine animals were born to hybrid parents of Large White (W) crossed with Landrace (L), both of which are breeds of domestic pig (Sus scrofa domesticus). One animal had a sire from Piétrain (P) domestic pig breed (Tab.1).

SAMPLE ID	SEX	AGE [months]	BREED
S01	female	5	WL x WL
S02	female	5	WL x WL
S03	male	6	WL x P
S04	female	3	WL x WL
S05	female	3	WL x WL
S06	female	4	WL x WL
S07	castrated	4	WL x WL
S08	female	4	WL x WL
S09	castrated	4	WL x WL
S10	female	4	WL x WL

Tab. 1: Overview showing ID, sex, age and breed of the ten pigs used for blood withdrawal.

Blood sampling was performed by a veterinarian via venipuncture of Vena cava cranialis. During the procedure, pigs were conscious and were held in place with a jaw sling. The puncture site was not disinfected. Blood was collected directly into standard 9 ml Vacuette® EDTA tubes (Greiner Bio-One®, Kremsmünster, Austria) which were swayed softly to guarantee sufficient intermixture with the buffer. From each animal a total of nine tubes was used to obtain approximately 80 ml of blood.

After phlebotomy, specimens were transferred to a lab at Medical University of Vienna for analysis. On the way to the lab, samples were kept at room temperature and processing started within one hour after withdrawal. Sample preparation and subsequent analysis took approximately 14 hours per sample, during which blood was kept in the fridge at 4 °C whenever possible.

3.1.3. Preparation of hematocrit dilutions

To be able to study the effect of HCT on rheological parameters, HCT dilutions were prepared. Plasma was separated from RBCs via centrifugation of all Vacuette® tubes for 10 min at 3,000 rpm with a Rotanta RPC® centrifuge (Hettich®, Tuttlingen, Germany). Afterwards a pipet was used to collect blood plasma from all tubes to a 50 ml Falcon® vial (BD®, Franklin Lakes, USA). Sedimented RBCs were transferred to another vial.

Next, HCT of the remaining cell concentrate was measured using a standard hematocrit centrifuge (Hettich®, Tuttlingen, Germany). A capillary tube was filled with blood for two-thirds and was caulked with a sealing kit. Separation of cells and plasma was performed by centrifugation at a speed of 10,000 rpm for 5 min. A template was then used to read off the HCT value. As a precaution, HCT analysis was always performed in doubles and was repeated if the values determined were inconsistent.

Following the measurement, the formula

$$\frac{10 * x\,[\%]}{\text{HCT of cell concentrate}\,[\%]} = y\,[\text{ml}]$$

was used to calculate the volume of the cell concentrate (y) necessary for the preparation of 10 ml of blood for each desired HCT dilution (x). So when the cell concentrate had 68 % HCT and a dilution with 30 % HCT should be prepared, the formula was

$$\frac{10 * 30\,\%}{68\,\%} = 4.41\ \text{ml}$$

and therefore 4.4 ml of the cell concentrate were mixed with 5.6 ml of plasma in a 15 ml Falcon® vial. After mixing, HCT was checked again in order to ensure optimum test conditions. If necessary, HCT was readjusted by adding either plasma or cell concentrate to the solution. From each sample dilutions with 30, 40, 50 and 60 % HCT were prepared.

3.1.4. Rheological analysis - rotational measurements

Rotational measurements can be used to characterize the complex and non-ideal flow behaviour of a wide range of fluids, solutions and emulsions [64].

To describe the effect of HCT and temperature on pig whole blood viscosity, HCT dilutions from each sample were analysed consecutively with rotational measurements at temperatures of 7, 12, 17, 22, 27, 32, 37 and 42 °C with shear rates of 1 - 1000 s^{-1} based on a logarithmic shear rate ramp starting with 1 s^{-1}.

Measurements were conducted with a Physica MCR 301® rheometer (Anton Paar®, Graz, Austria) (Fig.10), operated by Rheoplus® software (version 3.40, Anton Paar®, Graz, Austria) that had been installed on a standard computer. The device featured a stainless steel double gap concentric cylinder system with a Peltier element for electric heating and cooling, as well as a water cooling function. It was placed on a purpose-built metal table to blank out surrounding vibrations and was supplied with cold water through a flexible tube.

The system was always pre-cooled to a starting temperature of 7 °C and the Falcon® vials containing the HCT dilutions were pivoted extensively prior to analysis in order to ensure a homogenous suspension. Next, 3.5 ml of the sample were loaded into the gap with a pipette, the apparatus was brought into measuring position and analysis was started.

The rheometer was working after the Searle method, which means that one of two cylinders, the measurement cup, was immobilized, whereas the other cylinder, the measurement body, performed rotations while immersed in the sample (Fig.10). The various laminar layers of a fluid are thereby sheared against each other due to the occurring flow between the moving surfaces [64].

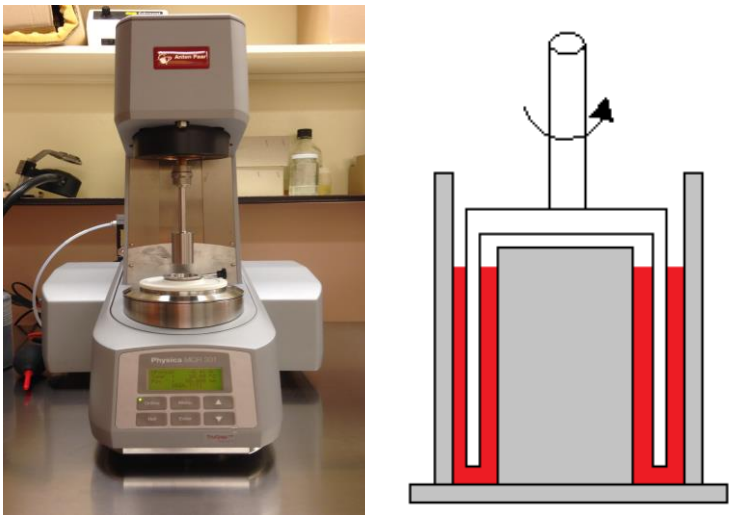

Fig. 10: Rheometer with a double gap cylinder system. The left picture shows the actual instrument used for analysis in this study. The schematic illustration on the right depicts the technical setup of the device. Blood, indicated in red, is placed in a gap and the measurement body, indicated in white, is plunged into the sample from above. During analysis the measurement body performs rotational movements. The measuring cup, indicated in grey, is immobilized at the device through a locating screw [41,65].

With an instrument like the one used, there are two different operation modes for rotational measurements. In this study, measurements were performed at controlled shear rates (CSR), where the measurement body rotates at a set speed, which determines the shear rate inside the annulus [66].

Once brought to movement in the CSR test, the sample tends to move the measurement body around. The force that is being exerted on the measurement body is called torsional moment and is recorded by the device. The torsional moment is employed to determine shear stress τ. By using the formula

$$\eta\ [\mathrm{Pa} * \mathrm{s}] = \frac{\tau\ [\mathrm{Pa}]}{\dot{\gamma}\ [s^{-1}]}$$

Rheoplus® software then calculates dynamic shear viscosity η as a quotient of shear rate $\dot{\gamma}$ and shear stress τ [66].

The other operation mode - which was not used in this study - would be a controlled shear stress (CSS) test, where the operator can adjust the torsional moment, determining the shear stress. But as ISO standard 3219 recommends to always analyse and compare viscosity at a pre-defined shear rate, pig blood was analysed with the CSR rather than CSS mode [66].

Considering the shear thinning behaviour of blood, analysis was not only performed with a single shear rate, but the shear rate was increased constantly by using a logarithmic shear rate ramp reaching from 1 s^{-1} up to 1000 s^{-1}. Data obtained for η at different shear rates were saved in tabular form and were pictured as viscosity curves [66].

It is a common procedure for measurements with synthetic resins or other products of the chemical industry to await a balance before changing from one shear rate to another, thus providing the static shear viscosity. However, this procedure could not be applied for measurements with blood. For the analysis at hand, it was necessary to change from one shear rate directly to another in order to avoid blood sedimentation. The results of this type of analysis are therefore values of dynamic shear viscosity, describing the resistance of a fluid to shearing flows, where adjacent layers move parallel to each other with different speeds. To countermand blood sedimentation and to quench any existing shear history, the following standard pre-shear interval was added to the program: 30 seconds at 300 s^{-1} followed by 10 seconds at 1 s^{-1} [60,66].

In general, flow curves are created at a constant temperature. Due to flow resistance and friction between the molecules, the sample warms up during measurement. Therefore, temperature control had to be active not only when changing between the desired temperatures, but also during the creation of each flow curve at each temperature [66].

When measurements for one HCT dilution were completed, the double gap cylinder system was removed from the machine, disassembled and blood was washed off with cold tap water. The steel parts were then carefully dried with paper towels, screwed together, re-inserted into the rheometer and filled with the next sample.

3.1.5. Rheological analysis - oscillation measurements

Oscillation measurements can be used to characterize all types of viscoelastic substances. Oscillations are repetitive variations around the mean of a state value of a system or variations between two or more different states. The process of mechanical oscillation is also described as vibration [67,68].

Oscillations always have a certain amplitude and frequency. The amplitude describes the extent of deflection of the oscillation and the frequency describes the rate at which the event occurs per time unit. When the measurement body performs oscillations with a defined frequency and amplitude, a torsional moment is recorded and is displayed together with a predefined deformation of the sample [69,70,71].

The software associated with the rheometer then calculates loss module G´´ and storage module G´ [72].

Loss module G´´ represents the deformation energy that is lost for the sample during the shearing process and is being released to the surrounding environment. That means that part of the energy is used for flowing, while another proportion is dissipated as heat. G´´ portrays the viscous behaviour of the sample [72].

Storage module G´ represents the energy being stored in the sample during shearing, which becomes fully available again after the process. This energy also serves as a driving force for re-deformation. The mechanism could be depicted with a scroll spring that elongates during deformation and then returns into its original state with a certain inertia. G´ illustrates the elastic behaviour of the sample. In blood, elastic behaviour is given by the amount of blood cells and plasma constituents, as well as by RBC parameters like size, shape, flexibility, and aggregability - the ability of RBCs to form rouleaux. Moreover, elasticity of blood is also given by the structural integration of RBCs into the surrounding colloidal protein network. It is clear that the experimental protocol like temperature and shear forces play a role for structural strength as well [72].

If G´>G´´, the elastic behaviour of the sample dominates over the viscous behaviour. The sample exhibits gel character. If G´´>G´, the viscous behaviour dominates over the elastic behaviour. The sample shows characteristics of a fluid. If G´=G´´, the sample is at the gel point, being on the boundary between liquid and gel [72].

To describe both elements of a viscoelastic material, the formula

$$\tan\delta = \frac{G''}{G'}$$

can be used for the calculation of the quotient loss factor tanδ. The higher tanδ, the more the sample has ideal viscous Newtonian behaviour. The lower tanδ, the more the sample behaves like an ideal elastic solid object. As soon as tanδ attains a value of 1, the sample features gel structure [72].

Measurements can be performed in small and large amplitude oscillatory shear (SAOS, LAOS resp.) mode. In SAOS, the applied oscillation amplitude is small enough to ensure that the material deformation is still reversible. In LAOS, the applied oscillation amplitude leads to rupturing of material structures [73].

This protocol included SAOS, which enabled a characterization of the structural strength of pig blood samples at a resting state. The maximum shear stress that can be applied to blood before it loses its stability is identified by the linear viscoelastic (LVE) range and must be determined prior to any further tests. Conclusions about a sample having more liquid or gel character as deduced from G´ and G´´ in SAOS are only valid within in linear mode [73,74].

The LVE range can be identified by amplitude sweep tests. Here, the deformation amplitude γ is steadily increased, while frequency and temperature are kept constant. In a graph with G´ and G´´ plotted against γ, a plateau of both parameters can be observed at small amplitudes - mostly at distinct levels (Fig.11). Within the plateau, the sample is deformed at a reversible level. At some point, as γ is increased further, the sample starts to disintegrate until it finally ruptures. Because of that, both shear moduli start to decrease and γ_L, the limiting value of the LVE range, is reached (Fig.11). In most cases, G´ is used for evaluation of γ_L, as it often leaves the LVE range first [74].

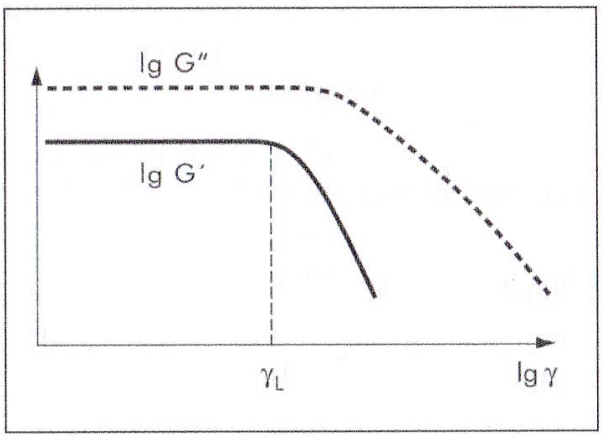

Fig. 11: Amplitude sweep test with a viscoelastic liquid. The graph with logarithmic scale shows storage module G´´ and loss module G´ at different deformation amplitudes γ. As G´´ is higher than G´, the sample features rather viscous than elastic behavior and has characteristics of a liquid. At low deformation amplitudes, a plateau - the LVE range - can be observed in both parameters. When G´ starts to decrease, the limiting value of the LVE range is reached and the sample is deformed and damaged irreversible via oscillation [74].

Instead of deformation amplitude γ, shear stress τ can also be used for determination of the LVE range. When the limit of the LVE range is reported in the form of shear stress τ, it is referred to as yield point τ_y. As long as the applied shear stress during analysis is lower than τ_y, there are no significant changes in the structure of the sample [74].

To determine the LVE range of blood samples necessary for analysis in this study, unpublished data from a pilot study were used. In the pilot study, an amplitude sweep was performed with human blood (HCT 40 %, 37 °C) at three different frequencies that may be relevant in cardiovascular physiology. Figure 12 shows the following: at 1.5 and 2 s^{-1} a G´-plateau was attained until a shear stress of about 20 mPa. At 0.5 s^{-1} the G´-curve is likely to deviate from the plateau value at lower shear stresses. Therefore, 5 - 20 mPa were defined as yield point for blood at different frequencies. Subsequent measurements were performed with 10 mPa in order to remain within the LVE range.

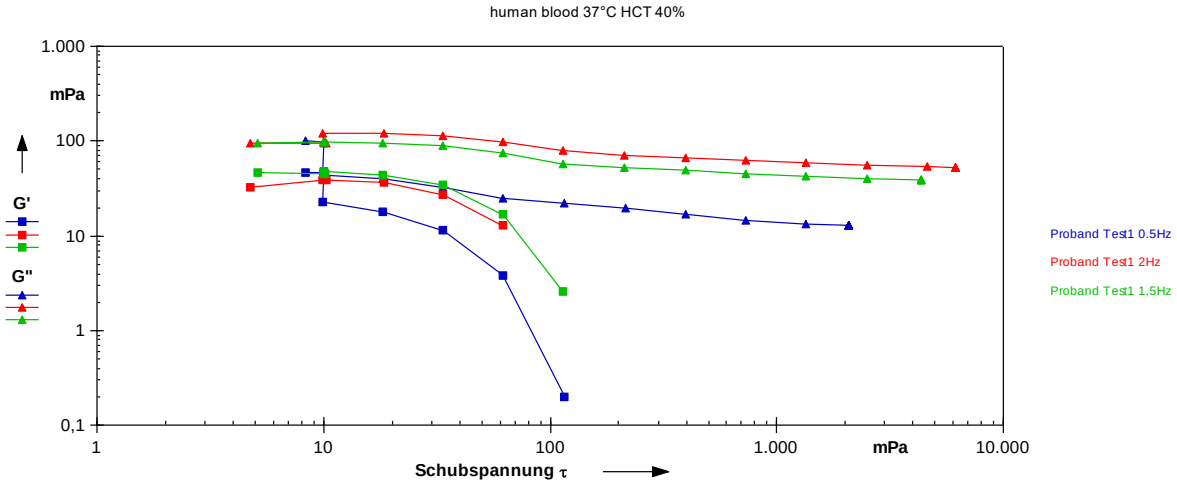

Fig. 12: Amplitude sweep tests from a pilot study. The graph shows amplitude sweep tests of human blood samples with HCT 40 % and 37 °C. Shear moduli G´ and G´´ are displayed on y-axis and shear stress τ is shown on x-axis. Yield point τ_y was defined to be 5 - 20 mPa, as G´ starts to decrease within that frame at three different frequencies [75].

After the identification of LVE range, frequency sweep tests can be used for characterisation of elasticity and suspension stability of a material. During a frequency sweep test, the frequency of oscillation varies, whereas amplitude and temperature are kept at a constant level. Frequency sweep tests describe the time-dependent deformation behaviour when the material is reversibly deformed. Low frequencies reflect structural strength of blood at rest, whereas higher frequencies reflect the suspension stability at higher impacts like during blood flow or bloodshed [76].

To analyse the suspension stability of pig whole blood within this study, HCT dilutions from each sample were analysed with SAOS measurements (frequency sweep tests) at 7, 22 and 37 °C with frequencies of 0.1 - 3.16 s^{-1}. This narrow frequency range for blood originates from the characteristic of blood being a fragile suspension and from the requirement of SAOS to maintain within the LVE range. Consequently, this frequency range probably does not cover high velocity impacts like gunshots. A pre-shear interval was added to the program: 10 seconds at 300 s^{-1} followed by 30 seconds at 1 s^{-1}.

As with rotational measurements, analysis was conducted with the Physica MCR 301® rheometer, pre-cooled to the starting temperature of 7 °C. After the samples had been intermixed thoroughly, 3.5 ml were loaded into the annulus, the measurement body was brought down into the sample and analysis was started.

3.1.6. Data evaluation

Following suitable data preparation, descriptive statistics and graphic illustrations were prepared using IBM SPSS Statistics® software (version 21, IBM®, Armonk, USA). To describe the relationship between HCT, temperature and dynamic shear viscosity of pig whole blood, master curves (contour plots) were created with SAS® software (version 9.4, SAS Institute®, Cary, USA).

3.2. Hemorheological analysis of pig blood storability

3.2.1. Experimental setup

To study and improve storability of pig whole blood for BPA simulations, blood samples from eleven pigs were anticoagulated with Citrate Phosphate Dextrose Adenine (CPDA-1) solution. They were stored at 4 °C for 32 days and analysed every second day. Analysis included rotational and oscillation measurements, hemograms and the determination of free hemoglobin (fHb). Additionally, bacteriologic screening was performed at the beginning and at the end of storage.

3.2.2. Specimen collection

Also for the second part of the project, samples were obtained from pigs at University of Veterinary Medicine in Vienna. The sample size was n=11 animals. All pigs were 4.5 months old and domestic pig crossbreds of Large White (W) and Landrace (L). Eight pigs were female and three were male neutered (Tab.2). Again, blood was taken by a veterinarian from Vena cava cranialis and animals were secured, but conscious.

As this project did not only have the aim to analyse pig whole blood storability, but also to improve the latter, reflections were made whether EDTA really was the optimum or whether better storage buffers would be available. Following literature research and consultation with the Blood Donation Center for Vienna, Lower Austria and Burgenland from the Austrian Red Cross, it was decided that CPDA-1 would be the best option for blood storage for BPA purposes.

In blood donor services, CPDA-1 is considered to be the gold standard for preservation of human whole blood or packed RBCs. The buffer was developed in 1979 and includes citric acid and sodium citrate, which both prevent coagulation by chelating calcium, monobasic sodium phosphate, which prevents a downslide of pH, dextrose (d-glucose), that supports ATP synthesis via glycolytic pathways, and adenine, which extends RBC survival by also increasing the level of ATP [77,78,79].

SAMPLE ID	SEX
A	female
B	female
C	female
D	female
E	female
F	castrated
G	female
H	female
I	female
J	castrated
K	castrated

Tab. 2: Sample overview showing ID and sex of the eleven pigs used for blood withdrawal.

Storage of pig blood for BPA purposes should be sufficient, but still with a strong practical orientation. BPA is a field of expertise that is very interdisciplinary and that might sometimes be underfunded. Simulations are conducted at different locations and laboratory equipment is not the same for every bloodstain pattern analyst. It is therefore necessary to look for simple solutions that do not imply elaborate procedures or pricy equipment. CPDA-1 is not only well established, but also inexpensive and internationally available for purchase.

Preliminary tests to this project showed that with standard blood bags containing CPDA-1, blood flow during porcine phlebotomy is very slow. Standard systems for blood donation do not have vacuum and feature a long tube attached to the actual blood bag. The animal needs to endure a very long lasting procedure and the veterinarian might have a hard time keeping the needle in place, as the animal will try to escape from the jaw sling. Furthermore, slow blood flow leads to coagulation in the line between the needle and the blood bag, as well as in the blood bag itself.

Therefore, CPDA-1 was extracted from 1-BB-500-CPDA1-LLM Fresenius Kabi® blood bags (Fresenius Kabi®, Bad Homburg vor der Höhe, Germany) by cutting open the line attached to the bag and transferring the buffer into 50 ml Falcon® vials (Tab.3).

70 ml CPDA-1
26.3 g tri-Na-citrate x 2 H_2O
3.27 g citric acid x H_2O
2.51 g NaH_2PO_4 x 2 H_2O
31.9 g glucose x H_2O
0.275 g adenine
aqua ad inj. ad 1000 ml

Tab. 3: Overview about ingredients in Fresenius Kabi® blood bag with CPDA-1.

During additional preliminary experiments 50 ml Braun® perfusor syringes (B. Braun Melsungen®, Melsungen, Germany) attached to an i.v. line and a large-bore needle proved to be a good tool for blood withdrawal from pigs (Fig.13). Syringes enable a faster blood draw, allowing the procedure to be less stressful for both the veterinarian and the pig. Also, the assumed volume of porcine blood necessary for this study was 100 ml, which was equivalent with two syringes per animal. Compared to a blood bag that needs to be filled completely, the syringes spared the withdrawal of 400 ml of blood from each pig that were not needed for analysis.

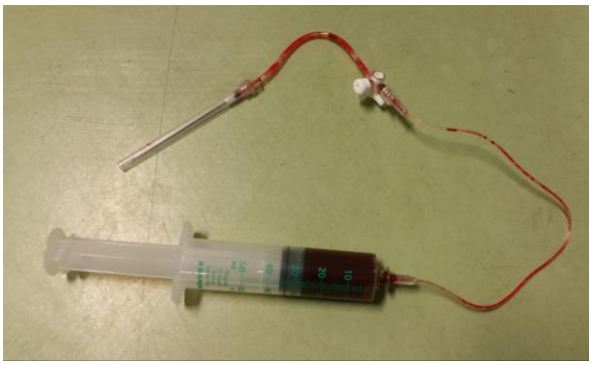

Fig. 13: Photograph of self-assembled phlebotomy set with a pre-defined amount of CPDA-1 anticoagulant solution. The set was composed of standard medical devices [78].

As blood bags from Fresenius Kabi® contain 70 ml of CPDA-1 and are designed to hold 500 ml of whole blood, the ratio has been calculated to be 0.14 ml of CPDA-1 for each millilitre of blood. Prior to blood withdrawal, perfusor syringes were therefore pre-filled with 7 ml of CPDA-1. The correct ratio would have been 6.02 ml of CPDA-1 for 43 ml of blood, but due to the fact that indications of quantity on perfusor syringes are not that accurate and blood withdrawal without vacuum is always accompanied by imprecision, the decision was made that it would be better to set the buffer volume a bit higher. The veterinarian filled syringes to the 50 ml mark. Per pig, two syringes were used.

After phlebotomy, specimens were transferred to a lab at Medical University of Vienna for analysis. Samples were transported in a cooler bag and processing started within one hour after withdrawal. In the lab samples were transferred into 50 ml Falcon® vials. Subsequently, distinct types of measurements were performed and during that time blood was kept in the fridge whenever possible.

3.2.3. Sample storage

Following the testing, Falcon® vials were stored at 4 °C for a total of 32 days, with analysis being conducted every 48 hours.

3.2.4. Bacteriologic screening

To check for microbiologic contamination of the samples caused during blood sampling or during storage, bacteriologic screening was conducted at the beginning and end of sample storage. Bacteria or fungi might not only affect RBC survival, but also bias whole blood viscosity or suspension stability of the samples.

From every sample a Columbia® agar with 5 % sheep blood and a Schaedler® agar with vitamin K1 and 5 % sheep blood from BD® were inoculated with 250 µl of blood each. Agar plates were incubated at 37 °C and examined after 24 and again after 48 hours. Columbia® agar plates were incubated in an aerobic milieu and Schaedler® plates were packed with an additive to create anaerobic conditions.

Both types of culture media are non-selective media recommended for primary isolation and cultivation of bacteria and fungi from clinical samples. Columbia® agar is a blood agar with yeast extract and two different peptones that provide vitamin B, enabling faster and better growth of bacterial colonies than on other blood agars. Schaedler® agar contains hemin and vitamin K and has been designed to fit the needs of obligate anaerobic germs [81,82,83].

Identification of microorganisms was performed with a Microflex LT® system (Bruker®, Billerica, USA), which is a device for matrix-assisted laser desorption/ionization time of flight mass spectrometry (MALDI-TOF MS).

For identification with MALDI-TOF MS, a small amount of germ material is applied onto a metal target and is covered with an acidic matrix solution. Within some minutes, the organic solvent vaporizes, leading to co-crystallization of matrix and analyte. Next, a high energetic laser pulse is sent onto the sample, leading to explosive detachment (desorption) and ionization of analyte molecules. The molecules are accelerated by an electric ion accelerator and launched into vacuum in a flight tube. During flight, the ions separate depending on their molecular mass. A reflectron, consisting of electrodes producing an electric field with a gradient, is interposed to reduce the influence of kinetic energy distribution on flight time. In the reflectron, ions are slowed down and accelerated again into the opposite direction. At the end of the flight tube, molecules are detected by a photomultiplier. The signal is sent through an analogue to digital converter and is displayed as a spectrum, whereas y-axis displays intensity and x-axis displays the time of flight of analyte ions (Fig.14) [84,85].

Finally, flexControl® 3.0 software (Bruker®, Billerica, USA) correlates the spectrum with other spectra in a data base. The identified microorganism is then displayed together with a score index to describe the quality of the measurement. The fundament for identification via MALDI-TOF MS are the positively charged ribosomal proteins, which constitute most of the analyte substance and are specific for various bacteria or fungi [84,85].

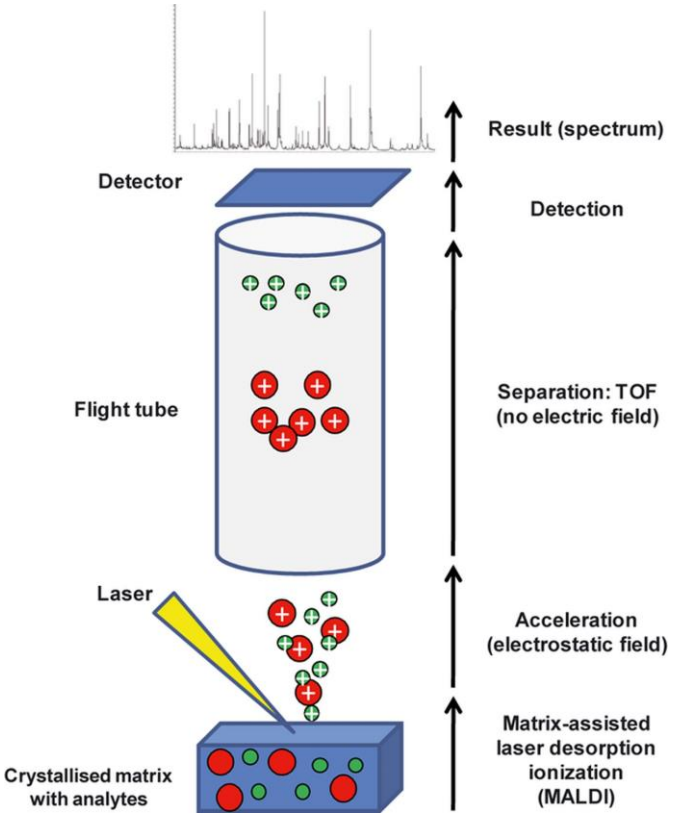

Fig. 14: The MALDI-TOF MS principle. The image shows the steps of MALDI-TOF MS analysis. Analyte molecules are split off from the target and are ionized due to high energetic laser impact. Acceleration in an electric field takes place. The flight tube allows separation of ions according on their molecular mass. The image does not show a reflectron. After detection of analyte ions, a spectrum is created [84].

To check upon possible biological hazards, detected germs were also subjected to antibiotic susceptibility testing. During agar diffusion tests, discs loaded with antibiotic agents are placed onto agar plates that have been inoculated with a bacterial suspension of a pre-defined concentration. If an antibiotic substance kills bacteria or stops them from growing, a zone of inhibition will be visible around the disc. The diameter of the zone is measured and according to specific guidelines bacteria are classified as sensitive, intermediate or resistant to the antibiotic substance [86].

Germ suspensions were prepared with NaCl and adjusted to a 0.5 McFarland standard with a DensiCHECK Plus® instrument (bioMérieux®, Marcy-l'Étoile, France). Using a Sensorturn pro® turntable (WLD-TEC®, Göttingen, Germany) and a sterile swab, the suspension was distributed onto Mueller Hinton II® agar plates from BD®. Mueller Hinton II® is the recommended agar used for the standardized disc diffusion procedure [87].

Next, antibiotic discs from Oxioid® (Thermo Fisher Scientific®, Waltham, USA) were applied to the Petri dishes with a stamper. Depending on the identified microorganisms a standard set of antibiotics was chosen like used for analysis of clinical samples in the microbiology lab at Jakob Erdheim Institute for Pathology and Clinical Bacteriology in Vienna. Samples were then incubated at 37 °C for 24 hours. Interpretation of inhibition zones was performed according to current guidelines (version 6.0) provided by the European Committee On Antimicrobial Susceptibility Testing (EUCAST®) [88].

3.2.5. Hematologic testing

Hematologic analysis in this study was conducted with an ADVIA 2120i® system (Siemens®, Berlin, Germany). The device performs simultaneous multiparametric analysis to create standard hemograms from approximately 300 µl of blood. As RBCs are the most prominent component of whole blood next to blood plasma and are believed to have a major influence on whole blood viscosity and suspension stability, the time-dependent course of selected erythrocyte indices was of peculiar interest: RBC count, HCT, mean cell volume (MCV), mean corpuscular hemoglobin (MCH) and mean corpuscular hemoglobin concentration (MCHC) [89].

In general, automated cell counting and assignment to a specific cell type is performed with flow cytometry. This type of analysis is a biophysical technology that combines optical laser-based and impedance-based measurements [89].

During optical measurement, the sample is diluted with physiologic saline solution and is sucked through a thin capillary into a measurement cuvette (flow cell). Single cells are channelled through the flow cell by insertion into a stream of sheath fluid (hydrodynamic focusing) and are subjected to a laser beam with a specific wavelength. By passing the laser beam, cells disperse light that is detected with a photomultiplier. Light at a narrow angle to the laser beam is referred to as forward scatter. The amount of forward scatter correlates with cell volume. Light dispersed at a 90° angle to the laser beam is called sideward scatter. It correlates with cell granularity and size and shape of the nucleus [89].

Simultaneously to laser-based analysis, impedance measurement with alternating current is performed. When the sample is sucked into the flow cell, it passes between a positively and a negatively charged electrode. With every cell passing, electrical conductivity in the electric field between the electrodes changes. The increase in electric resistance correlates with the size and concentration of the cell [89].

The ADVIA 2120i® system features five different reaction chambers: Hb, Baso, RBC, Retic and Perox [89].

In the Hb reaction chamber, Hb is measured via photometry. RBCs are lysed, Hb fractions are oxidized and measured as monoaquomonohydroxyferri-porphyrin at a wavelength of 565 nm. Contrary to older systems, ADVIA 2120i® uses a cyanide-free reagent for oxidation [89].

In the RBC chamber, RBCs are iso-volumetrically sphered (brought to spherical shape). During measurement of RBCs in the flow cell, forward scatter is detected at two different ranges: high-angle light scatter (5 - 15°) is converted to MCHC, low-angle light scatter (2 - 3°) is used for determination of MCV [89].

While RBC count, MCV and MCHC are determined via flow cytometry measurements and Hb is determined via photometric analysis, the parameters HCT and MCH are calculated by the ADVIA 2120i® software (Tab.4) [89].

PARAMETER	METHOD
RBC count	measured via flow cytometry
Hb	measured via photometry after lysis of RBCs
HCT	calculated as HCT = RBC * MCV
MCV	measured via flow cytometry
MCH	calculated as MCH = (Hb * 10) / RBC
MCHC	measured via flow cytometry

Tab. 4: Overview about RBC parameters of interest during this study and how they were determined with the ADVIA 2120i® system.

Prior to hematologic analysis, blood was adjusted to room temperature and was mixed thoroughly for several minutes. As the system is able to handle blood from humans and various animals, pig was selected as the target species. Furthermore, sample ID was entered into the software, the aspiration port of the device was inserted into the sample and measurement was started.

Since hemograms are by default created with EDTA blood and hematologic systems are not designed to work with CPDA-1, the Siemens® company provided the formula

$$X = \frac{\text{total sample volume (blood + anticoagulation buffer) [ml]}}{\text{volume of blood [ml]}}$$

to calculate a conversion factor X to be used for an adjustment of all results of hematologic analysis. In this study, 43 ml of pig blood were mixed with 7 ml of CPDA-1 to a total sample volume of 50 ml. Therefore, a conversion factor of 1.16 was applied.

3.2.6. Analysis of free hemoglobin

Hemoglobin is a metalloprotein that can be found in RBCs. When RBCs rupture due to mechanical stress or ageing, hemoglobin is released. Thus, the level of fHb in blood plasma can be used as an indicator of RBC destruction [29,48,49].

Analysis of fHb was performed with a colorimetric method on a Cobas c 311® analyser (Roche®, Basel, Switzerland).

Prior to actual measurement, 750 µl of each blood sample were transferred to a 1.5 ml Eppendorf® micro-centrifuge tube (Eppendorf®, Hamburg, Germany). Samples were centrifuged for 10 min at 3,000 rpm with a Rotanta RPC® centrifuge. Afterwards a pipet was used to collect 250 µl of blood plasma to a plastic cuvette, which was then inserted into the analyser.

As hemoglobin shows pseudo-peroxidase behaviour, it catalyses the reduction of hydrogen peroxide with 4-aminophenazone and phenol. The product of the chemical reaction is 4-(p-benzoquinone-monoimino)-phenazone, which upon formation has an influence on absorbance of light by the sample, thus enabling a quantification of free hemoglobin in blood plasma [90].

First, the analyser incubates the plasma sample together with a reagent (containing 4-aminophenazone and phenol) and a diluent (water). In a second step, hydrogen peroxide is added to the cuvette and following further incubation, absorbance is measured at a wavelength of 500 nm. A reagent blank serves as a point of reference [90].

3.2.7. Rheological analysis - rotational measurements

Every two days, viscosity curves of the ageing blood samples were created with a logarithmic shear rate ramp of 1 - 1000 s^{-1} as described before (section 3.1.4.). Measurements were performed at 22 and 37 °C only. To reveal changes in viscosity of pig whole blood over storage time, dynamic shear viscosity was assessed at shear rates of 1, 10, 100 and 1000 s^{-1}.

3.2.8. Rheological analysis - oscillation measurements

Frequency sweep tests at a shear stress of 10 mPa were performed every two days as described before (section 3.1.5.). Measurements were conducted at 22 and 37 °C only. For the analysis of suspension stability (elasticity) of big whole blood over storage time, storage module G´, loss module G´´ and loss factor tanδ were assessed at a frequency of 1 s^{-1}.

3.2.9. Data evaluation

Following suitable data preparation, graphic illustrations of all parameters were prepared using IBM SPSS Statistics® software.

3.3. Pilot study on bloodstain pattern simulation with aged samples

3.3.1. Experimental setup

As a pilot project, four pig blood samples were anticoagulated with CPDA-1 and were used for the creation of a bloodstain pattern immediately after withdrawal and again after 32 days of storage at 4 °C. A template with concentric bands was used to check whether the resultant patterns were different before and after storage.

3.3.2. Specimen collection

Samples were obtained from pigs at University of Veterinary Medicine in Vienna. The sample size was n=4 pigs and the individuals were between 3 and 3.5 months old. Two of the animals were male, one was female and one male but castrated. Three pigs were born to hybrid parents of Large White (W) crossed with Landrace (L) and one animal had a sire from Piétrain (P) domestic pig breed (Tab.4).

SAMPLE ID	SEX	AGE [months]	BREED
V	female	3	W x L
W	castrated	3	W x L
X	male	3.5	W x L
Y	male	3.5	W x P

Tab. 5: Overview showing ID, sex, age and breed of the four pigs used for spatter creation.

Blood sampling was performed like described before (section 3.1.2.), but blood was collected into standard 15 ml Falcon® vials loaded with CPDA-1. According to the ratio calculated earlier (section 3.2.2.), 2 ml of CPDA-1 were used for anticoagulation of 12 ml of porcine whole blood.

After phlebotomy, specimens were transferred to a lab at Medical University of Vienna for analysis. On the way to the lab, samples were kept at room temperature and processing started within one hour after withdrawal.

3.3.3. Sample storage

Samples were stored in the fridge at 4 °C for a period of 32 days and were mixed thoroughly at least every five days.

3.3.4. Bloodstain pattern production

Due to a lack of specific equipment for bloodstain pattern production, a simple model was applied. A drop pattern associated with a secondary mechanism - producing satellite spatter around a parent stain - was created on a glass plate. The procedure was performed before and after storage, enabling a comparison of the physical appearance of bloodstain patterns created with the same blood samples.

Since several pre-tests showed, that the surface, the drop height, the diameter of the pipe outlet and the velocity of blood drop formation all influence the resulting stains, these factors were standardized for pattern production before and after storage.

Prior to actual experimentation, blood samples were mixed thoroughly and acclimatized to room temperature. A standard i.v. line was mounted to a standard 50 ml Braun® perfusor syringe and the whole system was filled with blood. Air bubbles occurring within the line were removed by hand via soft shaking and pushing. The free end of the i.v. line was fixed to a stative and was placed above a clean and dry glass plate. The height between blood outlet and glass surface was 50 cm. Next, the syringe was inserted into a Combimat 2000® perfusor (B. Braun Melsungen®, Melsungen, Germany), which was set to a velocity of 15 ml per hour (Fig.15).

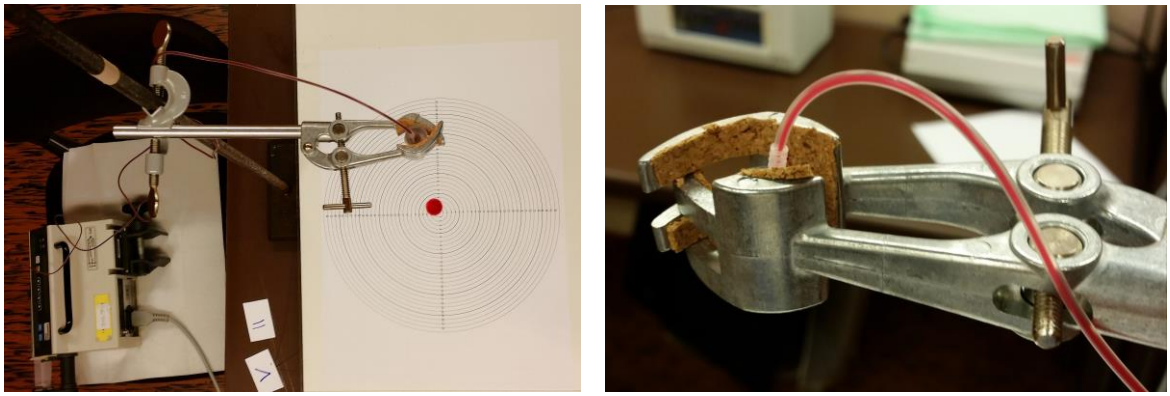

Fig. 15: Apparatus for standardized production of a simple bloodstain pattern. The pictures show the experimental setup used in this pilot study. The self-assembled apparatus was built of an i.v. line, a syringe, a perfusor and a stative and provided reproducible experimental conditions, thus allowing to reveal the influence of storage and ageing on bloodstain patterns [80].

The perfusor was started and the first drop exiting the outlet was discarded. Blood spatter was formed by using the second and third drop falling into each other on the glass plate. Bloodstain creation was conducted three times with each sample before and after storage at 4 °C.

In order to enable a standardized evaluation of the parent stain diameter and the distance between the parent stain and surrounding satellite spatter, a self-made template with concentric bands was placed under the glass plate. The spacing between the bands was 0.5 cm each. After producing blood spatter, the parent stain was centred on the template by moving the glass plate.

3.3.5. Photography

The patterns created during experimentation were documented with a Canon EOS 5D Mark II® reflex camera (Canon®, Tokyo, Japan) equipped with a Tamron® SP 90 mm f/8 macro lens (Tamron®, Saitama, Japan). The camera was mounted to a stative and placed as vertical to the glass plate as possible. Photosensitivity was set to 800 ISO. No flash was used and shutter release was operated through a remote in order to reduce camera shake. Photographs of the patterns were cut and aligned with Adobe Photoshop® software (version CC 2015, Adobe Systems®, San José, USA).

3.3.6. Comparative analysis

In order to evaluate possible differences in bloodstain patterns due changes of blood samples related to ageing and storage, the diameter of the parent stain, the number of spatters within the first 14 bands of the template (within 7 cm around the point of impact), the number of spatters between bands 14 and 28 (between a distance of 7 and 14 cm from the point of impact), as well as the total number of spatters within 28 bands (within 14 cm around the point of impact) were assessed.

The parent stain, spatter directly connected to (flowing together with) the parent stain and spatter outside of band 28 were not included into the counting process. Spatter lying on band 14 were either assigned to the inner or the outer half of the template, depending on where the major part of the stain was located. Likewise, spatter lying on band 28 were either counted to the outer half of the template or not included at all.

4. Results

4.1. Rheological characterization of porcine blood

4.1.1. Rheological analysis - rotational measurements

During the rheological characterization with rotational measurements, dynamic shear viscosity increased with HCT increments and decreased with temperature increments.

Figures 17 to 20 show contour plots revealing the HCT-temperature-dependency of dynamic shear viscosity of fresh pig whole blood anticoagulated with EDTA at shear rates of 1, 10, 100 and 1000 s^{-1}. The graphs indicate that a specific viscosity value is given at many combinations of HCT and temperature. Figure 16 is a comparison of all contour plots. It illustrates the impact of shear rate on dynamic shear viscosity. Dynamic shear viscosity of pig whole blood, thus, is not a fixed value but varies with HCT, temperature and shear rate.

Tables 6 to 9 depict mean values and 95 % confidence intervals for dynamic shear viscosity at all HCT and temperature combinations tested in this study.

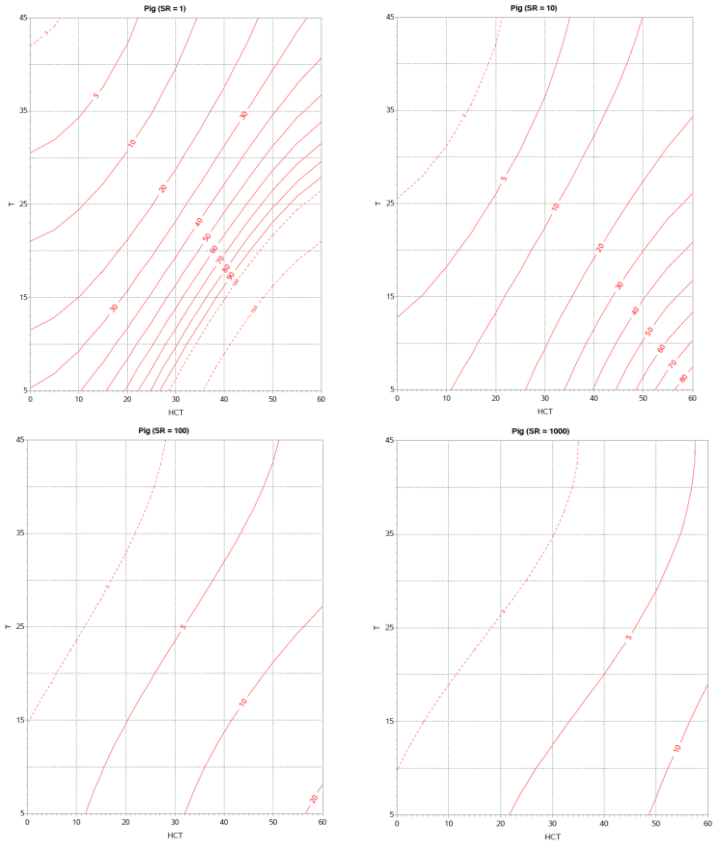

Fig. 16: Overview of all contour plots. The comparison reveals the impact of shear rate [s^{-1}] on dynamic shear viscosity [mPa*s] of pig whole blood. Depending on the shear rate applied to the samples, identical HCT-temperature-combinations feature different values for dynamic shear viscosity.

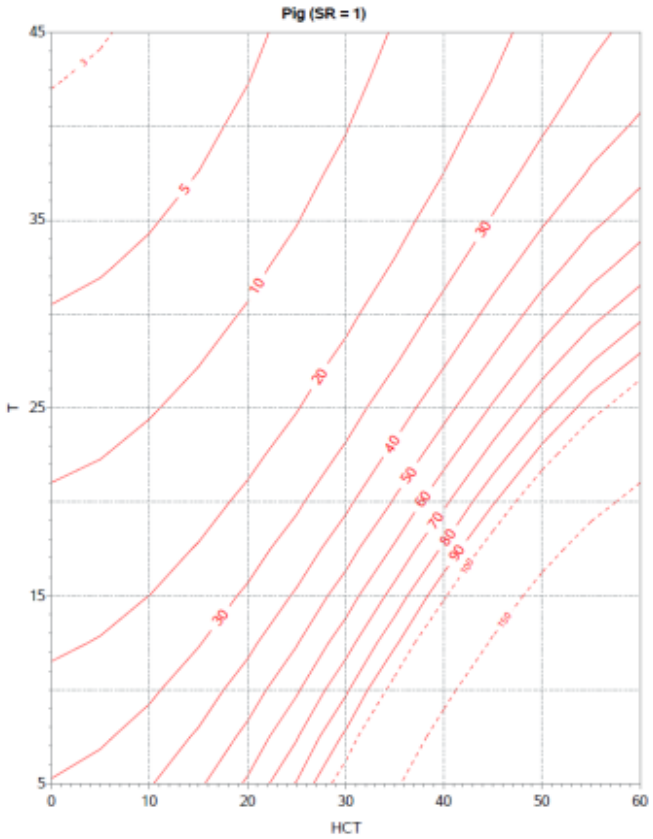

Fig. 17: Contour plot with 1 s^{-1}. The red lines depict the HCT-temperature-dependency of pig whole blood viscosity [mPa*s] at a shear rate of 1 s^{-1}.

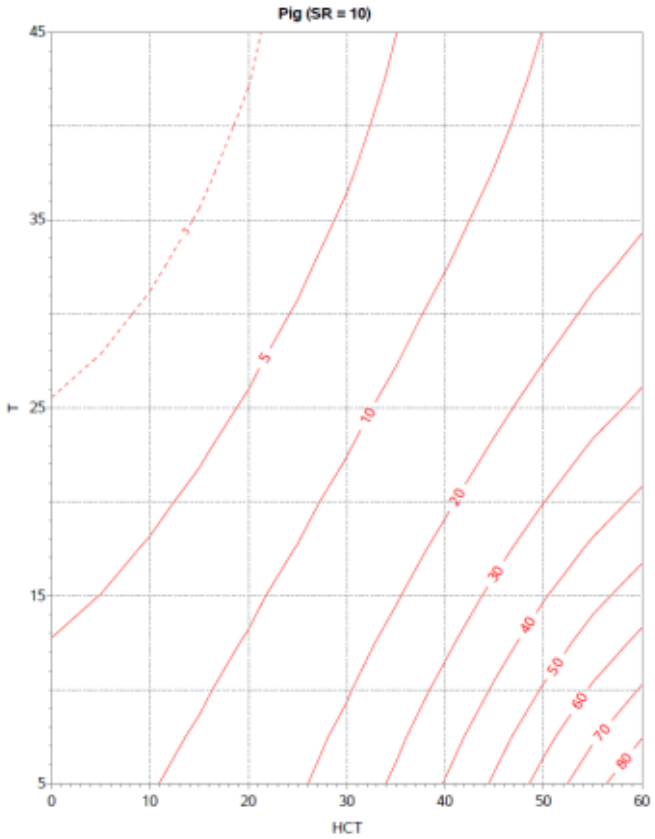

Fig. 18: Contour plot with 10 s^{-1}. The red lines depict the HCT-temperature-dependency of pig whole blood viscosity [mPa*s] at a shear rate of 10 s^{-1}.

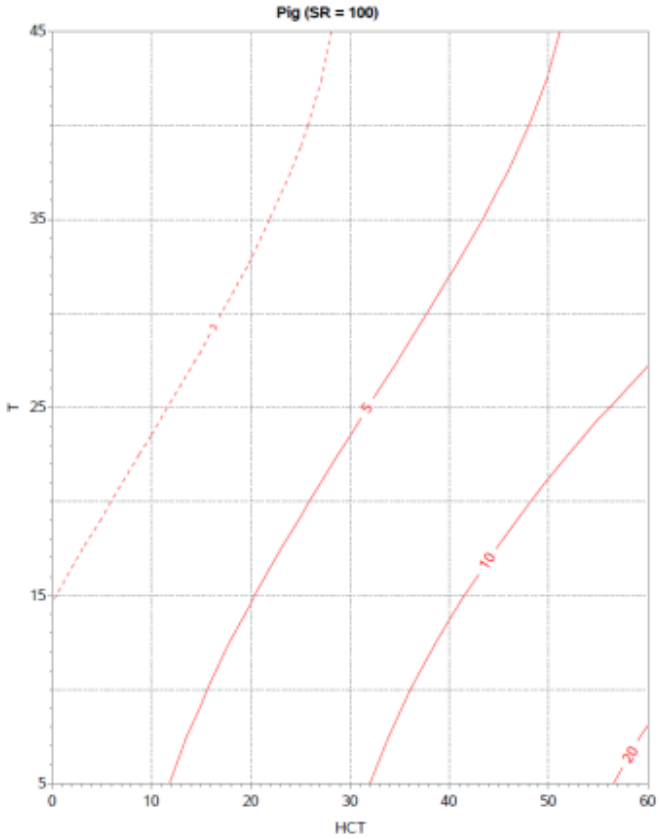

Fig. 19: Contour plot with 100 s^{-1}. The red lines depict the HCT-temperature-dependency of pig whole blood viscosity [mPa*s] at a shear rate of 100 s^{-1}.

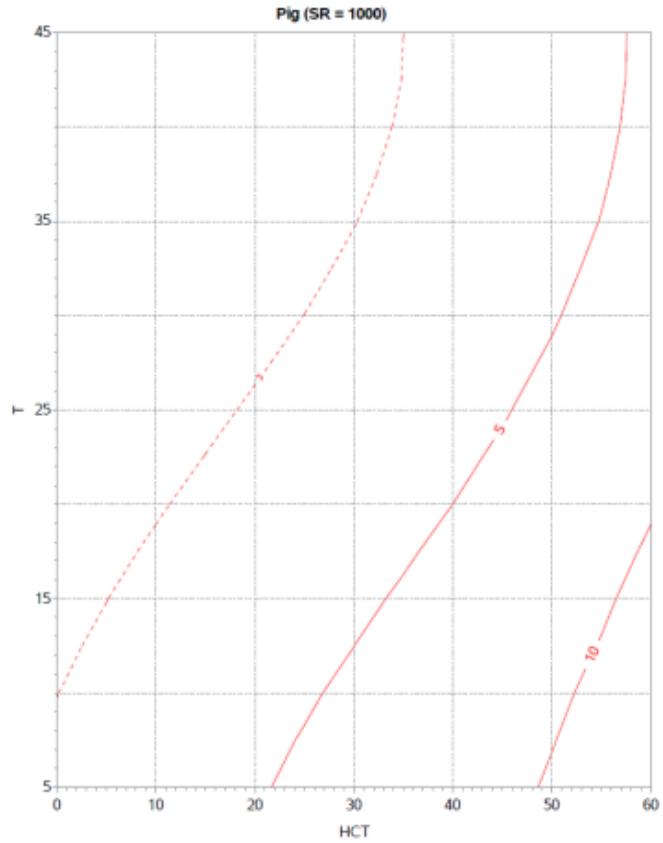

Fig. 20: Contour plot with 1000 s^{-1}. The red lines depict the HCT-temperature-dependency of pig whole blood viscosity [mPa*s] at a shear rate of 1000 s^{-1}.

1 s^{-1} [95%CI]	HCT 30 %	HCT 40 %	HCT 50 %	HCT 60 %
7 °C	103.66 [81.40;125.92]	152.10 [136.74;167.46]	207.10 [185.99;228.21]	302.30 [277.00;327.60]
12 °C	83.13 [61.93;104.33]	120.66 [104.03;137.29]	168.00 [146.05;189.95]	247.00 [224.40;269.60]
17 °C	60.54 [44.34;76.74]	91.05 [77.00;105.10]	125.53 [105.83;145.23]	187.90 [168.75;207.05]
22 °C	39.01 [26.99;51.03]	65.57 [55.51;75.63]	92.78 [77.32;108.24]	145.90 [126.24;165.56]
27 °C	27.41 [14.26;40.56]	44.22 [33.52;54.92]	68.46 [55.89;81.03]	110.26 [94.10;126.42]
32 °C	19.29 [7.59;30.99]	30.09 [22.20;37.98]	48.34 [43.72;52.96]	86.04 [70.83;101.25]
37 °C	16.64 [3.52;29.75]	22.97 [17.87;28.07]	35.61 [30.67;40.56]	68.49 [50.97;86.01]
42 °C	12.39 [4.13;20.64]	17.10 [13.85;20.35]	26.29 [22.29;30.29]	48.20 [34.70;61.70]

Tab. 6: Overview about mean values and 95% confidence intervals for dynamic shear viscosity [mPa*s] of EDTA pig blood at different HCT-temperature-combinations at a shear rate of 1 s^{-1}.

10 s^{-1} [95%CI]	HCT 30 %	HCT 40 %	HCT 50 %	HCT 60 %
7 °C	23.32 [20.42;26.22]	37.94 [34.91;40.97]	55.63 [51.30;59.96]	80.89 [73.61;88.17]
12 °C	18.12 [15.70;20.54]	29.83 [27.31;32.35]	43.84 [40.29;47.39]	62.57 [58.06;67.08]
17 °C	14.03 [12.22;15.84]	23.22 [21.38;25.06]	34.09 [31.40;36.78]	48.50 [45.68;51.32]
22 °C	10.64 [9.50;11.77]	17.90 [16.65;19.15]	26.51 [24.43;28.59]	37.81 [35.55;40.07]
27 °C	8.30 [7.09;9.51]	13.80 [12.69;14.91]	20.73 [19.01;22.45]	29.53 [27.37;31.69]
32 °C	6.26 [5.39;7.13]	10.44 [9.42;11.45]	16.05 [14.84;17.26]	23.15 [21.15;25.15]
37 °C	5.22 [4.17;6.26]	8.34 [7.41;9.28]	12.35 [11.29;13.41]	18.31 [16.51;20.11]
42 °C	4.31 [3.28;5.34]	6.59 [5.82;7.35]	9.91 [9.04;10.78]	16.38 [14.35;18.41]

Tab. 7: Overview about mean values and 95% confidence intervals for dynamic shear viscosity [mPa*s] of EDTA pig blood at different HCT-temperature-combinations at a shear rate of 10 s^{-1}.

100 s^{-1} [95%CI]	HCT 30 %	HCT 40 %	HCT 50 %	HCT 60 %
7 °C	9.37 [8.84;9.90]	13.25 [12.64;13.86]	16.59 [15.79;17.39]	21.37 [19.83;22.91]
12 °C	7.78 [7.32;8.23]	10.98 [10.44;11.52]	13.78 [13.10;14.46]	17.43 [16.42;18.44]
17 °C	6.49 [6.13;6.86]	9.15 [8.71;9.59]	11.46 [10.90;12.02]	14.39 [13.73;15.05]
22 °C	5.43 [5.15;5.72]	7.65 [7.28;8.02]	9.54 [9.04;10.05]	12.02 [11.57;12.47]
27 °C	4.55 [4.30;4.79]	6.35 [6.05;6.65]	7.91 [7.51;8.31]	10.14 [9.78;10.50]
32 °C	3.78 [3.58;3.97]	5.20 [4.92;5.47]	6.48 [6.15;6.82]	8.62 [8.29;8.95]
37 °C	3.14 [2.95;3.34]	4.20 [3.96;4.45]	5.28 [4.99;5.58]	7.46 [7.07;7.85]
42 °C	2.63 [2.45;2.81]	3.47 [3.25;3.70]	4.58 [4.30;4.87]	6.85 [6.37;7.34]

Tab. 8: Overview about mean values and 95% confidence intervals for dynamic shear viscosity [mPa*s] of EDTA pig blood at different HCT-temperature-combinations at a shear rate of 100 s^{-1}.

1000 s^{-1} [95%CI]	HCT 30 %	HCT 40 %	HCT 50 %	HCT 60 %
7 °C	6.19 [5.96;6.41]	8.00 [7.71;8.29]	10.28 [9.93;10.62]	14.65 [13.74;15.56]
12 °C	5.23 [5.05;5.42]	6.66 [6.43;6.88]	8.55 [8.27;8.83]	12.19 [11.45;12.92]
17 °C	4.29 [4.14;4.45]	5.43 [5.24;5.62]	7.06 [6.82;7.29]	10.20 [9.56;10.83]
22 °C	3.77 [3.64;3.91]	4.71 [4.54;4.87]	6.17 [5.96;6.37]	8.86 [8.31;9.40]
27 °C	3.12 [3.01;3.23]	3.92 [3.78;4.06]	5.24 [5.07;5.42]	7.62 [7.13;8.12]
32 °C	2.77 [2.67;2.87]	3.50 [3.37;3.63]	4.74 [4.56;4.93]	6.84 [6.38;7.29]
37 °C	2.27 [2.18;2.36]	2.97 [2.84;3.09]	4.13 [3.88;4.38]	6.06 [5.62;6.51]
42 °C	2.07 [2.00;2.15]	2.73 [2.57;2.90]	3.79 [3.57;4.00]	5.79 [5.26;6.33]

Tab. 9: Overview about mean values and 95% confidence intervals for dynamic shear viscosity [mPa*s] of EDTA pig blood at different HCT-temperature-combinations at a shear rate of 1000 s^{-1}.

4.1.2. Rheological analysis - oscillation measurements

During frequency sweep tests with shear stress of 10 mPa, shear moduli G´ and G´´ increased with HCT enlargement and decreased with rise in temperature.

Figures 22 to 33 show boxplots of results for both shear moduli at different HCT-temperature-combinations at distinct frequencies. Figure 21 depicts a synopsis of all frequency sweep tests.

Tables 10 to 12 show mean values with 95 % confidence intervals of G´, G´´ and tanδ at a frequency of 1 s^{-1} at all HCT and temperature combinations tested in this study.

At 7 °C in all HCT dilutions (Fig.22-25), as well as at 22 °C in the 60 % HCT dilution (Fig.29), storage module G´ was bigger than loss module G´´ and likewise, at 1 s^{-1} tanδ was below 1 (Tab.12). Under these conditions, pig blood samples featured the characteristics of a viscoelastic solid, representing a jelly-like material. In the remaining HCT-temperature-combinations, pig whole blood can be described as a viscoelastic liquid.

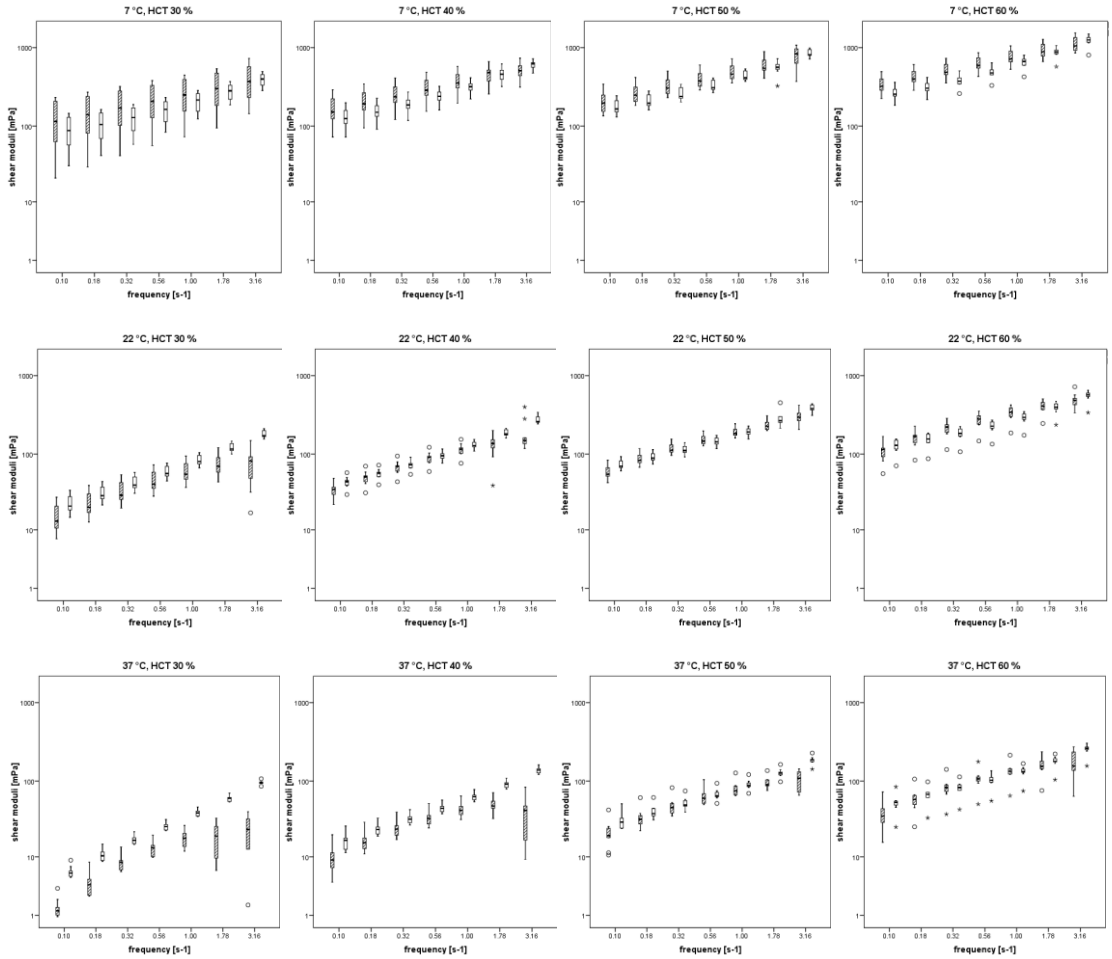

Fig. 21: Overview of frequency sweep tests. The graphs show shear moduli G´ and G´´ [mPa] at different frequencies [s^{-1}] in distinct HCT-temperature-combinations.

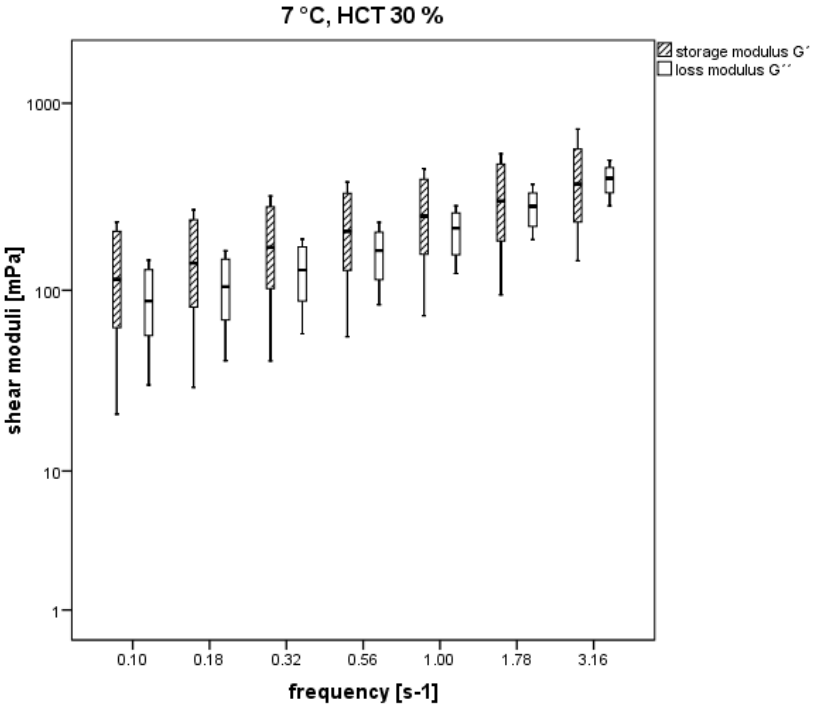

Fig. 22: Frequency sweep test with the 30 % HCT dilution at 7 °C. Shear moduli G´ and G´´ reveal characteristics of a viscoelastic solid for pig blood under these conditions.

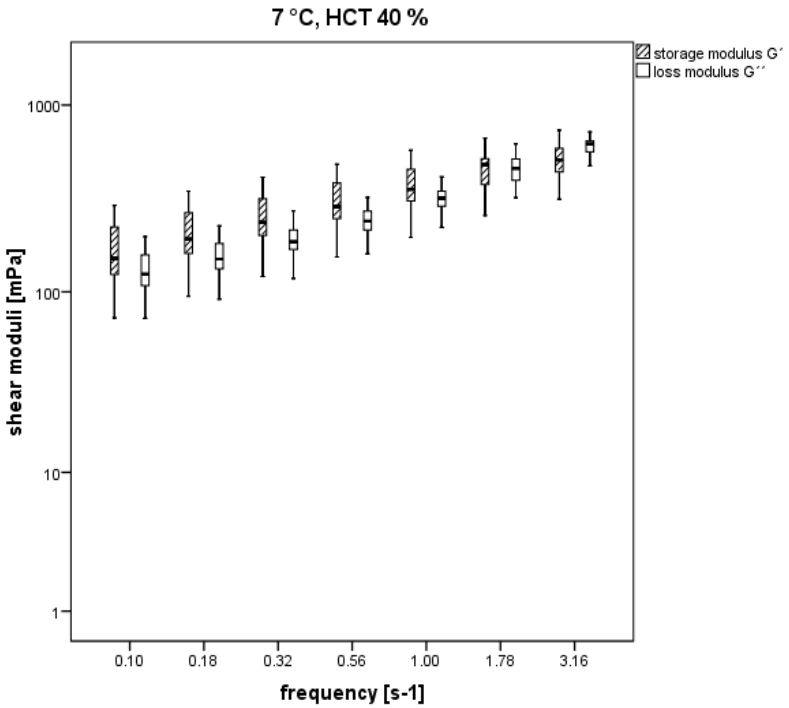

Fig. 23: Frequency sweep test with the 40 % HCT dilution at 7 °C. Shear moduli G´ and G´´ reveal characteristics of a viscoelastic solid for pig blood under these conditions.

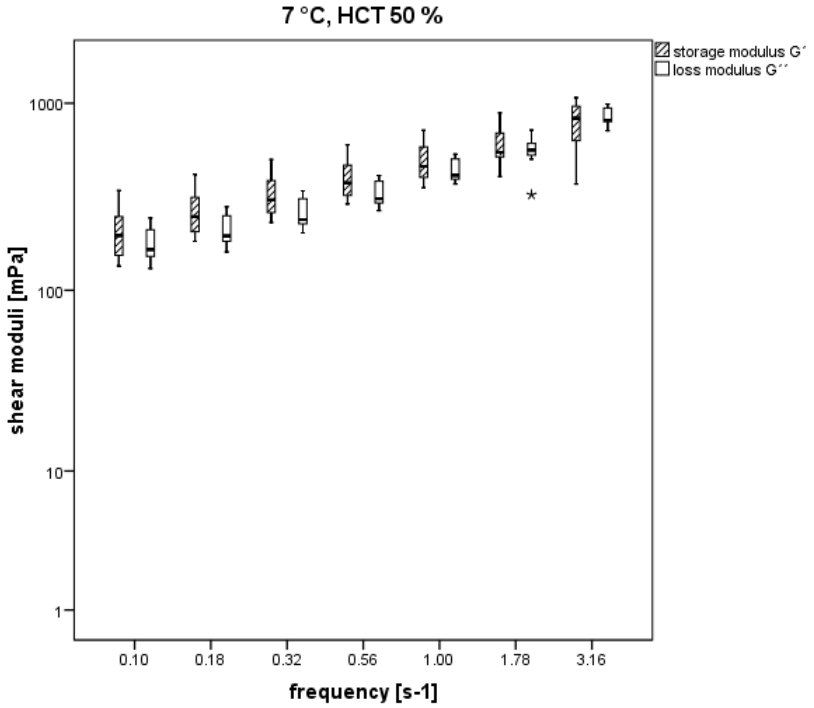

Fig. 24: Frequency sweep test with the 50 % HCT dilution at 7 °C. Shear moduli G´ and G´´ reveal characteristics of a viscoelastic solid for pig blood under these conditions.

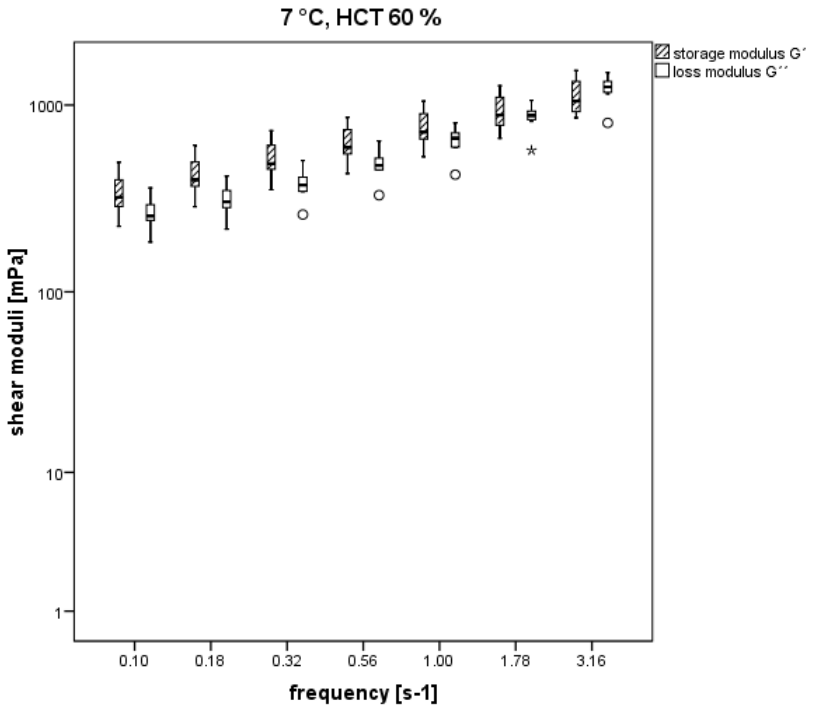

Fig. 25: Frequency sweep test with the 60 % HCT dilution at 7 °C. Shear moduli G´ and G´´ reveal characteristics of a viscoelastic solid for pig blood under these conditions.

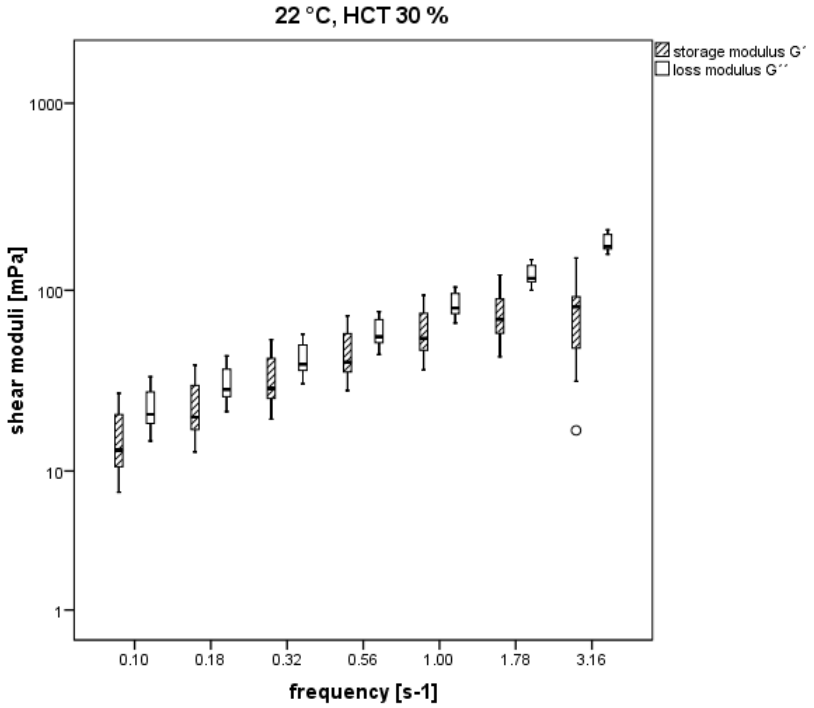

Fig. 26: Frequency sweep test with the 30 % HCT dilution at 22 °C. Shear moduli G´ and G´´ reveal characteristics of a viscoelastic liquid for pig blood under these conditions.

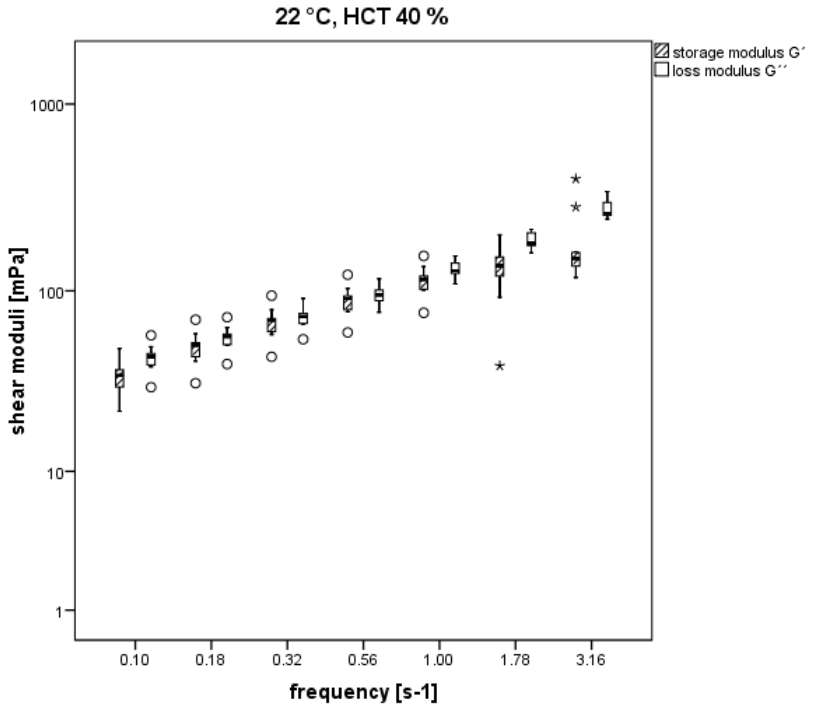

Fig. 27: Frequency sweep test with the 40 % HCT dilution at 22 °C. Shear moduli G´ and G´´ reveal characteristics of a viscoelastic liquid for pig blood under these conditions.

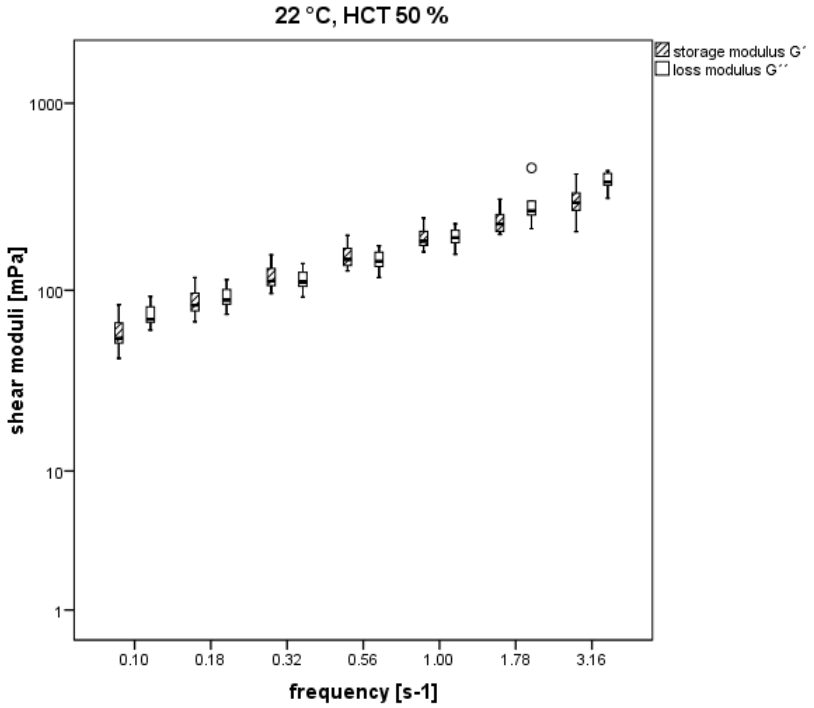

Fig. 28: Frequency sweep test with the 50 % HCT dilution at 22 °C. Shear moduli G´ and G´´ reveal characteristics of a viscoelastic liquid for pig blood under these conditions.

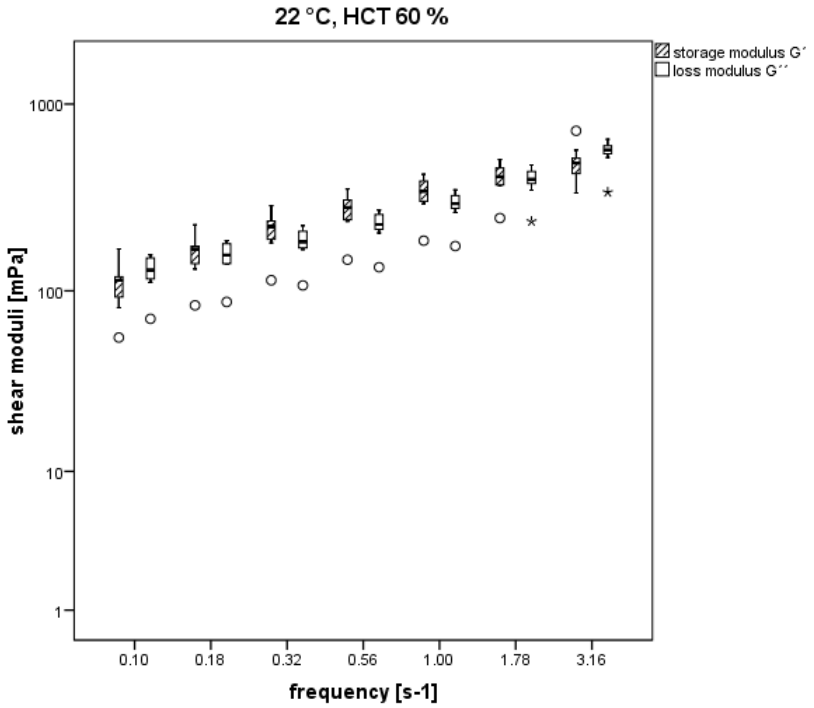

Fig. 29: Frequency sweep test with the 60 % HCT dilution at 22 °C. Shear moduli G´ and G´´ reveal characteristics of a viscoelastic solid for pig blood under these conditions.

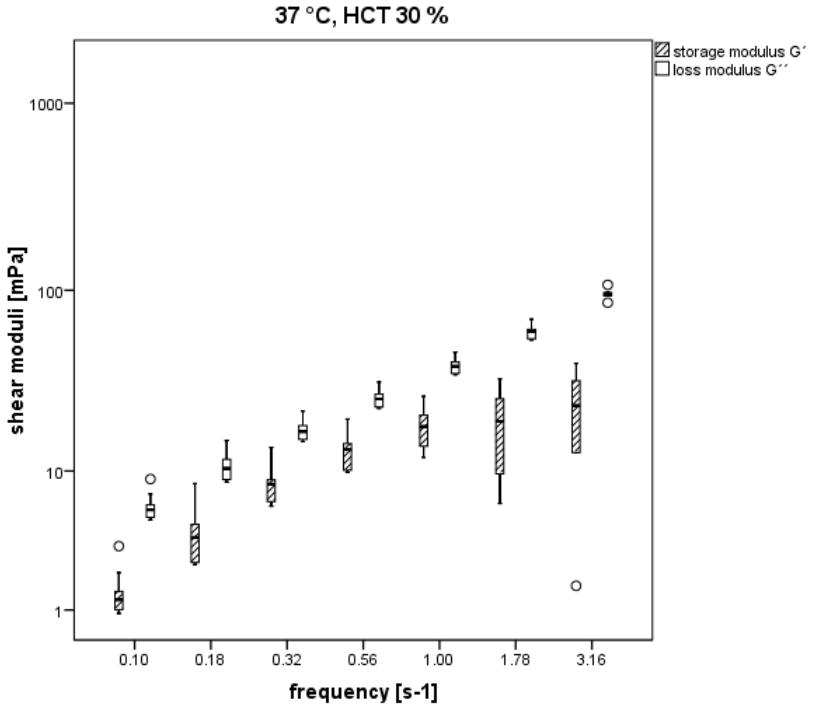

Fig. 30: Frequency sweep test with the 30 % HCT dilution at 37 °C. Shear moduli G´ and G´´ reveal characteristics of a viscoelastic liquid for pig blood under these conditions.

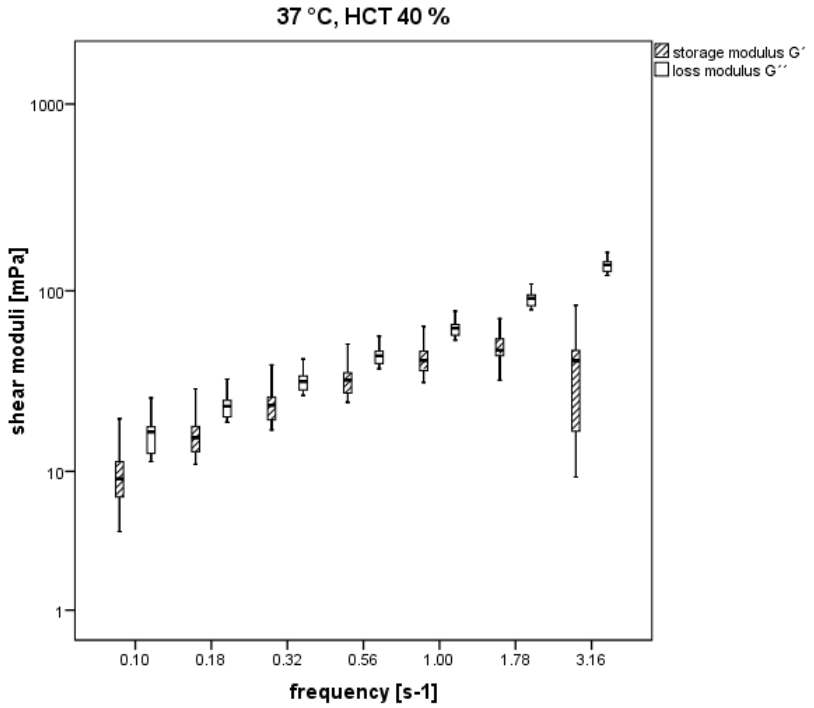

Fig. 31: Frequency sweep test with the 40 % HCT dilution at 37 °C. Shear moduli G´ and G´´ reveal characteristics of a viscoelastic liquid for pig blood under these conditions.

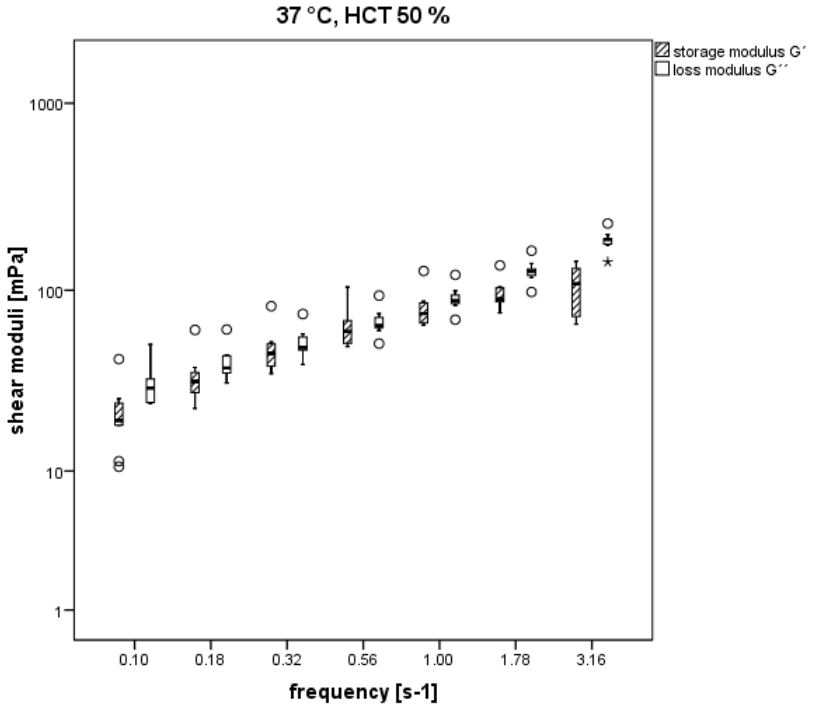

Fig. 32: Frequency sweep test with the 50 % HCT dilution at 37 °C. Shear moduli G´ and G´´ reveal characteristics of a viscoelastic liquid for pig blood under these conditions.

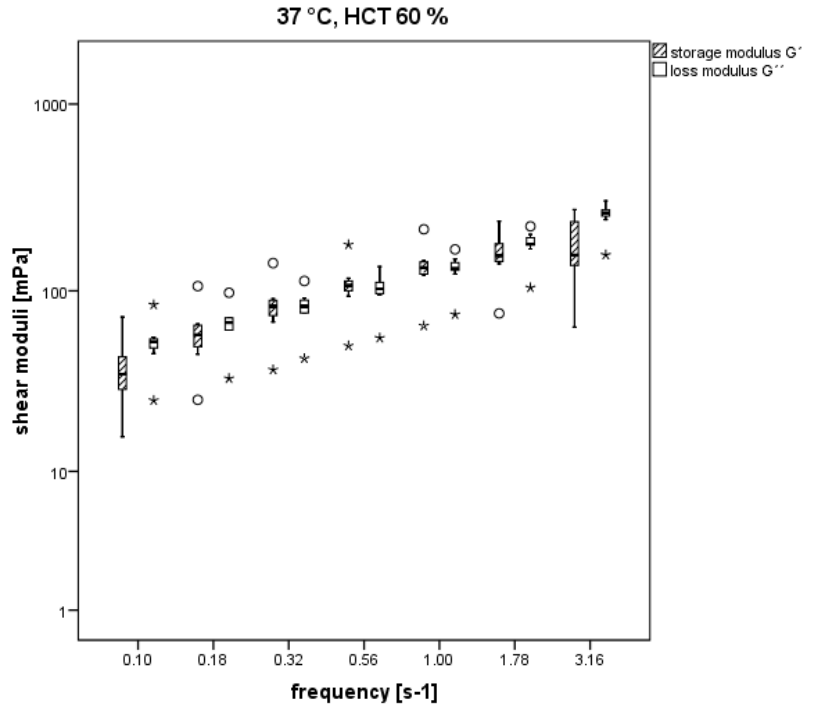

Fig. 33: Frequency sweep test with the 60 % HCT dilution at 37 °C. Shear moduli G´ and G´´ reveal characteristics of a viscoelastic liquid for pig blood under these conditions.

G´ [95%CI] at 1 s^{-1}	HCT 30 %	HCT 40 %	HCT 50 %	HCT 60 %
7 °C	266.49 [168.70;364.28]	380.70 [297.82;463.58]	496.60 [412.29;580.91]	752.90 [632.01;873.79]
22 °C	59.87 [46.50; 73.24]	115.01 [100.21;129.81]	193.80 [172.54;215.06]	335.90 [287.55;384.25]
37 °C	17.75 [14.41;21.09]	43.33 [36.77;49.89]	80.24 [67.05;93.43]	134.47 [108.54;160.40]

Tab. 10: Overview of mean values with 95 % confidence intervals of storage module G´ at a frequency of 1 s^{-1} at all HCT-temperature-combinations tested in this study.

G´´ [95%CI] at 1 s^{-1}	HCT 30 %	HCT 40 %	HCT 50 %	HCT 60 %
7 °C	211.30 [168.57;254.03]	321.80 [282.35;361.25]	435.80 [392.87;478.73]	652.10 [577.35;726.85]
22 °C	82.84 [73.92;91.76]	131.30 [121.86;140.74]	193.00 [177.36;208.64]	290.10 [254.76;325.44]
37 °C	38.74 [36.23;41.25]	62.56 [57.60;67.52]	90.48 [80.95;100.01]	131.55 [114.61;148.49]

Tab. 11: Overview of mean values with 95 % confidence intervals of loss module G´´ at a frequency of 1 s^{-1} at all HCT-temperature-combinations tested in this study.

tanδ [95%CI] at 1 s^{-1}	HCT 30 %	HCT 40 %	HCT 50 %	HCT 60 %
7 °C	0.9292 [0.6930;1.1654]	0.8805 [0.7837;0.9773]	0.8968 [0.8239;0.9698]	0.8857 [0.7696;1.0018]
22 °C	1.4472 [1.2767;1.6176]	1.1590 [1.0747;1.2432]	1.0018 [0.9580;1.0455]	0.8705 [0.8331;0.9080]
37 °C	2.2801 [1.9678;2.5925]	1.4698 [1.3626;1.5770]	1.1444 [1.0672;1.2215]	1.0016 [0.9219;1.0812]

Tab. 12: Overview of mean values with 95 % confidence intervals of loss factor tanδ at a frequency of 1 s^{-1} at all HCT-temperature-combinations tested in this study.

4.2. Hemorheological analysis of pig blood storability

4.2.1. Bacteriologic screening

From 11 pig blood samples screened for bacteria and fungi immediately after withdrawal only one sample (sample ID: H) featured two bacterial colonies on the Columbia® screening agar, which had been incubated under aerobic conditions. Bacteria were identified with MALDI-TOF MS as Corynebacterium stationis. With an inoculation volume of 250 µl per plate, the two colonies measure up to 8 colony forming units per millilitre. Due to the fact that Corynebacterium stationis was only present in one of 11 samples in minor concentration, no antibiotic susceptibility testing was performed. All other ten samples analysed immediately after blood withdrawal were germ free in both aerobic and anaerobic screening after incubation at 37 °C for 48 hours.

After storage at 4 °C for 32 days, blood samples were again screened for bacteria and fungi. This time, Columbia® and Schaedler® agars from all samples both featured massive bacterial growth already after 24 hours. The presence of a dense bacterial lawn in many cases made it difficult to distinguish and identify distinct microorganisms with MALDI-TOF MS. Nevertheless, three different bacterial species were identified: Staphylococcus xylosus was found in eight samples (sample IDs: A, B, C, D, E, F, H, J), Pantoea agglomerans was present in four samples (sample IDs: G, I, J, K) and Staphylococcus sciuri was identified in one sample (sample ID: G).

ANTIBIOTIC	STAPH. XYLOSUS	STAPH. SCIURI
Penicillin	-	-
Flucloxacillin	+	+
Amoxicillin / Clavulanic acid	+	+
Ampicillin / Sulbactam	+	+
Cefazolin	+	+
Gentamicin	+	+
Erythromycin	+	+
Clindamycin	+	-
Rifampicin	+	+
Fusidic acid	-	-
Moxifloxacin	+	+
Sulfamethoxazole / Trimethoprim	+	+
Minocycline	+	+

Tab. 13: Antibiograms for Staphylococci found in pig blood after storage.

As shown in tables 13 and 14, standard susceptibility testing with antibiotic discs according to current EUCAST® guidelines revealed antibiograms within normal limits. The antibiotic substances chosen for testing match standard sets of antibiotics like used in a microbiology lab in one of the major hospitals in Vienna.

ANTIBIOTIC	PANTOEA AGGLOMERANS
Ampicillin	+
Ampicillin / Sulbactam	+
Piperacillin / Tazobactam	+
Aztreonam	+
Ertapenem	+
Meropenem	+
Cefuroxime	+
Cefotaxim	+
Ceftazidim	+
Cefepime	+
Gentamicin	+
Trimethoprim	+
Ciprofloxacin	+

Tab. 14: Antibiogram for Pantoea agglomerans found in pig blood after storage.

4.2.2. Hematologic testing

Over storage time, RBC count fell from more than 7.25 to less than 7 million cells per millilitre. The decline was not constant, but a clear trend was noted (Fig.34).

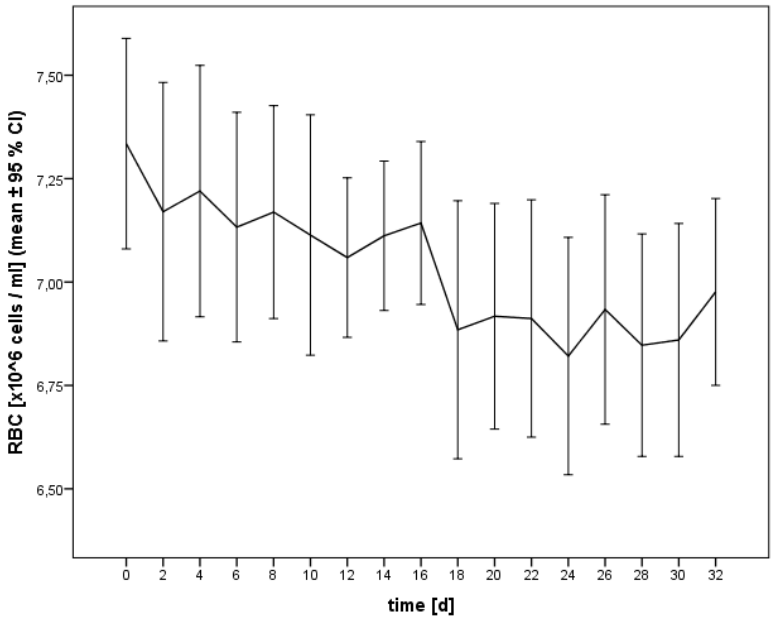

Fig. 34: RBC count over storage time. The graph shows mean values with error bars (95 % confidence intervals) for RBC count [x10^6 cells / ml] at all time points.

HCT increased during the first four days of storage and showed sort of a plateau until day 16 before descending to a level approximately 2 % beyond the inital value (Fig.35).

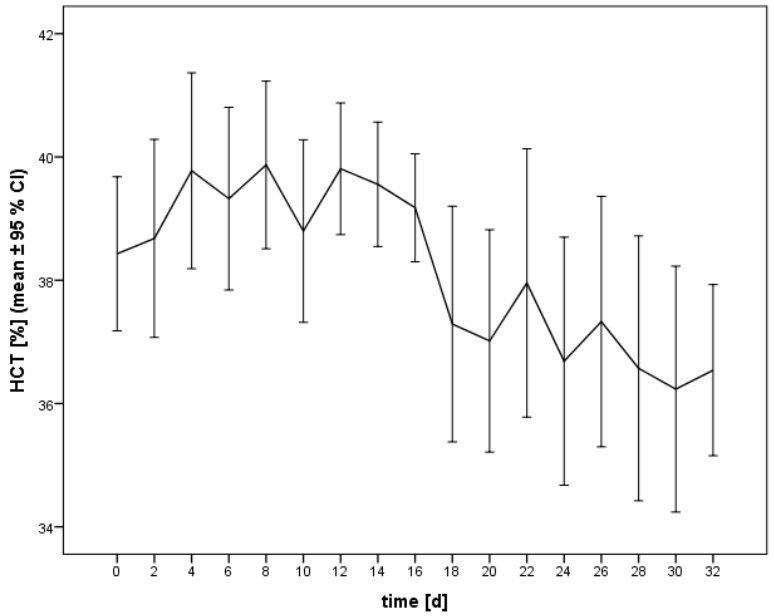

Fig. 35: HCT over storage time. The graph shows mean values with error bars (95 % confidence intervals) for HCT [%] at all time points.

Wilcoxon signed-rank test (significance level: 0.05) was used to compare HCT values of day 0 with day 32. It revealed a statistical significance of 0.003, leading to the rejection of H_0. This means that the population mean rank was significantly lower after storage.

MCV of blood samples displayed an ascent until day 12 and afterwards lowered back to approximately the same level like observed at the beginning of storage (Fig.36).

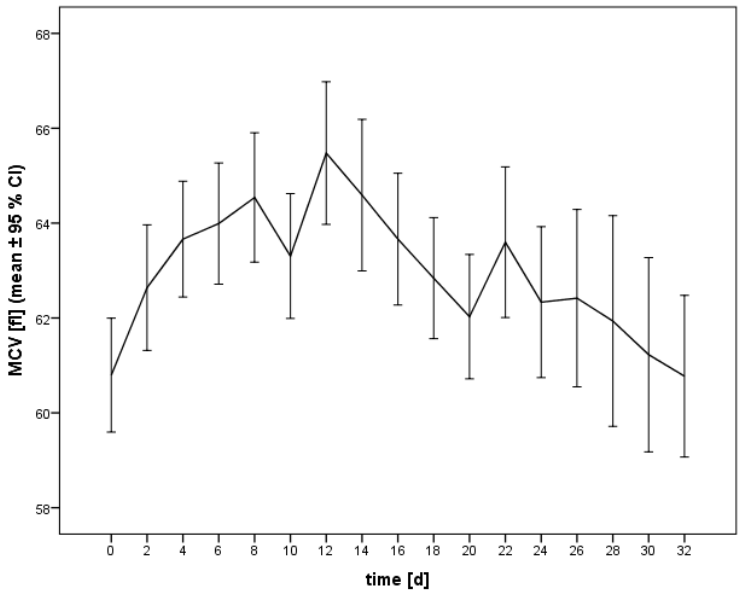

Fig. 36: MCV over storage time. The graph shows mean values with error bars (95 % confidence intervals) for MCV [fl] at all time points.

MCH during storage at 4 °C featured an almost constant upward movement (Fig.37).

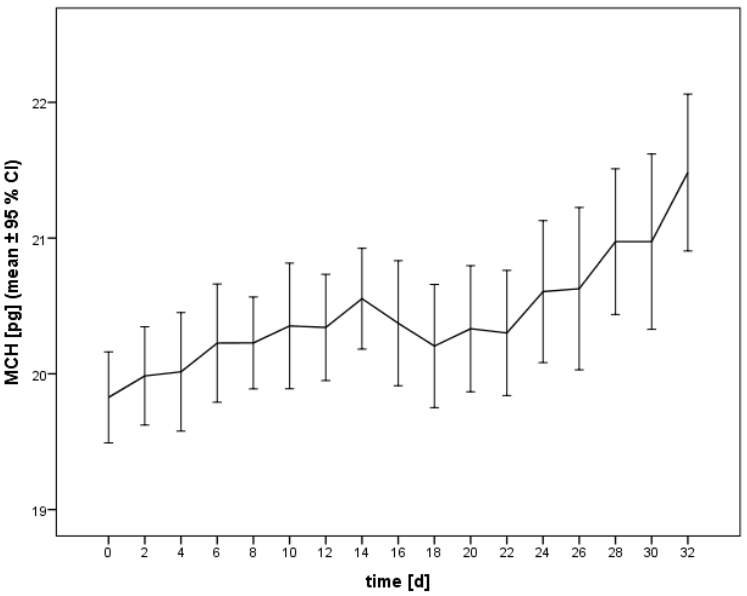

Fig. 37: MCH over storage time. The graph shows mean values with error bars (95 % confidence intervals) for MCH [pg] at all time points.

MCHC decreased almost 2 g/dl during the first four days of storage, remained at the low level for some days and began a constant uprise at day 12 (Fig.38).

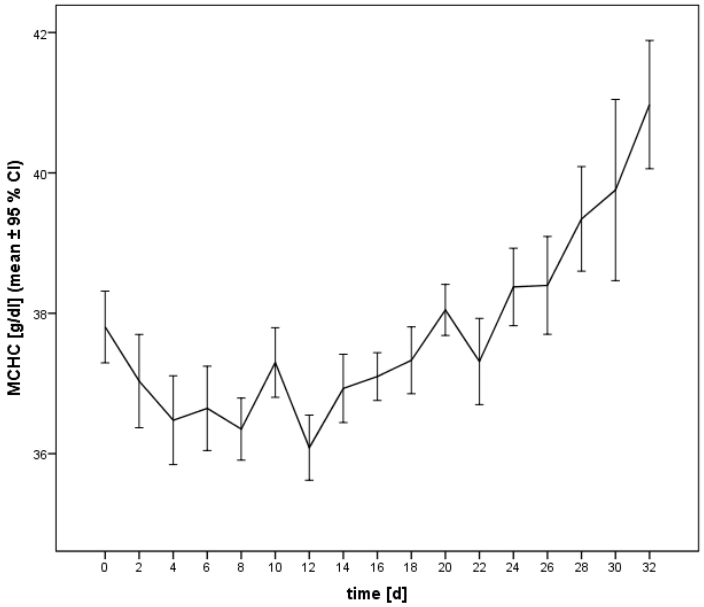

Fig. 38: MCHC over storage time. The graph shows mean values with error bars (95 % confidence intervals) for MCHC [g/dl] at all time points.

4.2.3. Analysis of free hemoglobin

Analysis of fHb revealed a steady increase over the passage of storage time. Following day 26, a remarkable leap of fHb was observed (Fig.39).

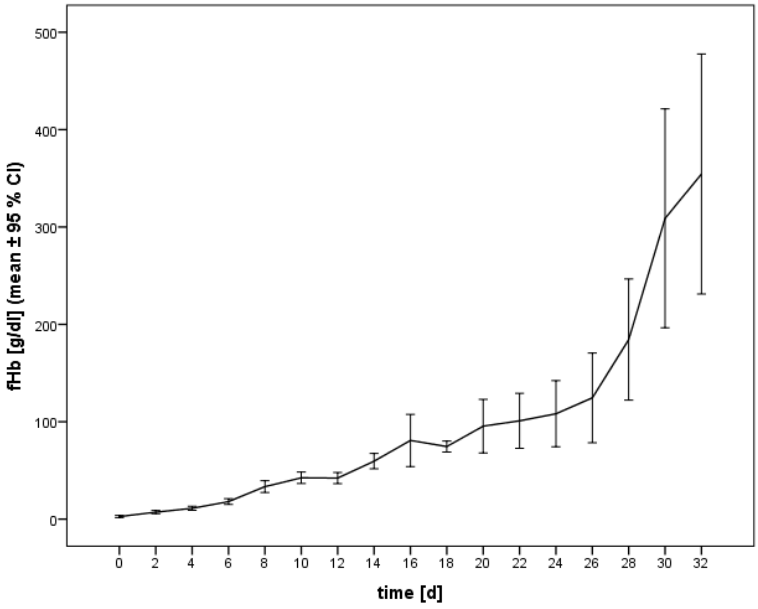

Fig. 39: fHb over storage time. The graph shows mean values with error bars (95 % confidence intervals) for fHb [g/dl] at all time points.

4.2.4. Rheological analysis - rotational measurements

Dynamic shear viscosity showed different courses during ageing, depending on the shear rate applied on the sample. Whereas at low shear rate (1 s^{-1}) viscosity showed a biphasic course, at high shear rate (1000 s^{-1}) viscosity displayed a constant increase.

Figure 40 gives an overview about dynamic shear viscosity of pig blood with CPDA-1 at different shear rates over storage at 4 °C for 32 days. Figures 41 to 48 display the course of dynamic shear viscosity at specific temperature-shear-rate-combinations in detail.

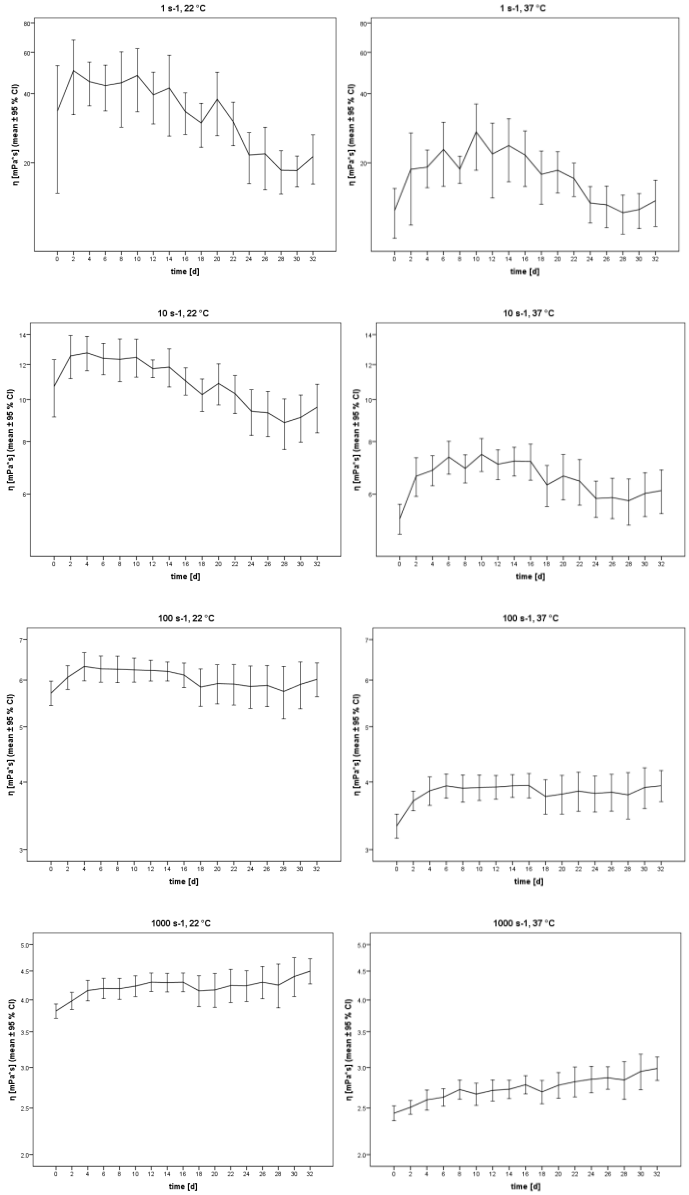

Fig. 40: Dynamic shear viscosity of pig whole blood with CPDA-1 over storage time.
The overview gives an impression of how different the influence of storage on dynamic shear viscosity is, when distinct shear rates are applied on the blood sample at different temperatures. The change of dynamic shear viscosity over time is different in each constellation. The graphs display mean values with 95 % confidence intervals for dynamic shear viscosity.

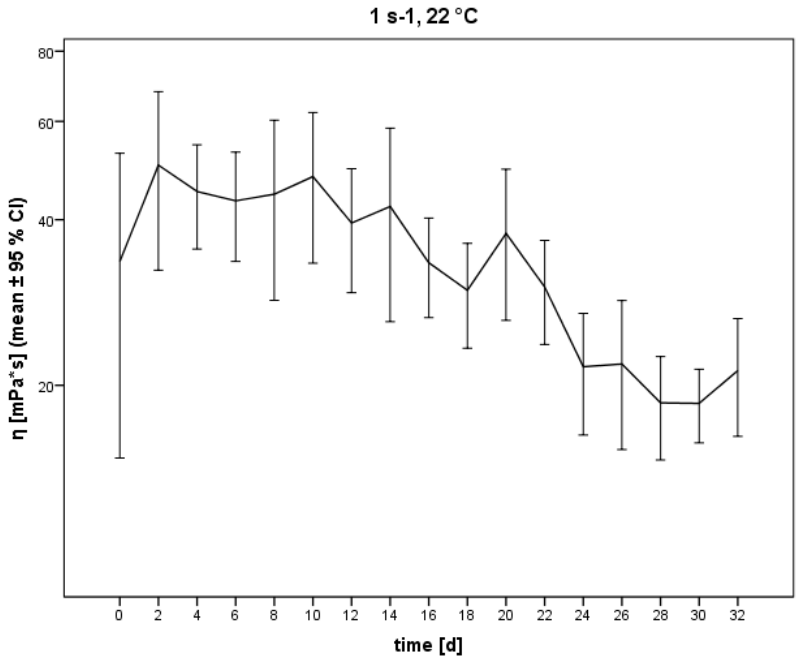

Fig. 41: Dynamic shear viscosity at 22 °C and 1 s^{-1}. The graph shows mean values with error bars (95 % confidence intervals) for dynamic shear viscosity [mPa*s] over storage time.

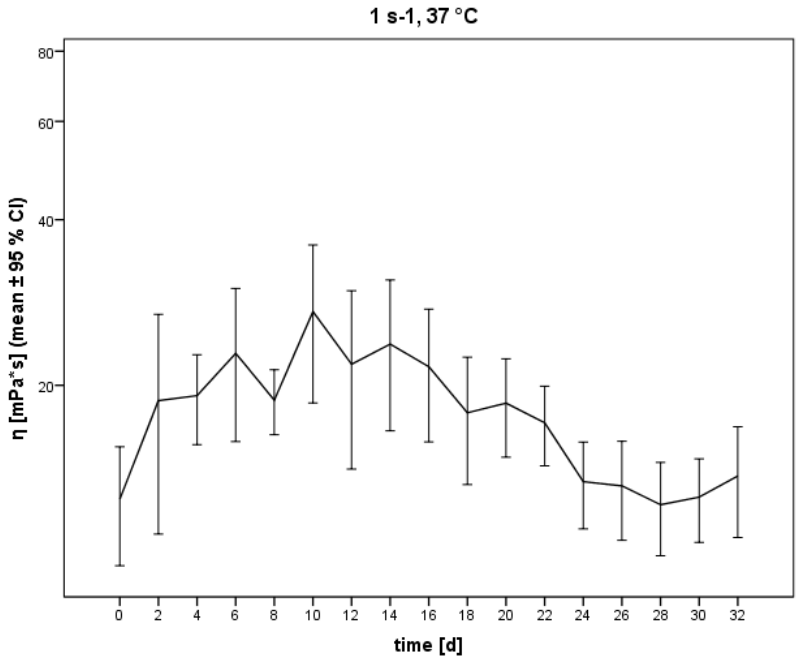

Fig. 42: Dynamic shear viscosity at 37 °C and 1 s^{-1}. The graph shows mean values with error bars (95 % confidence intervals) for dynamic shear viscosity [mPa*s] over storage time.

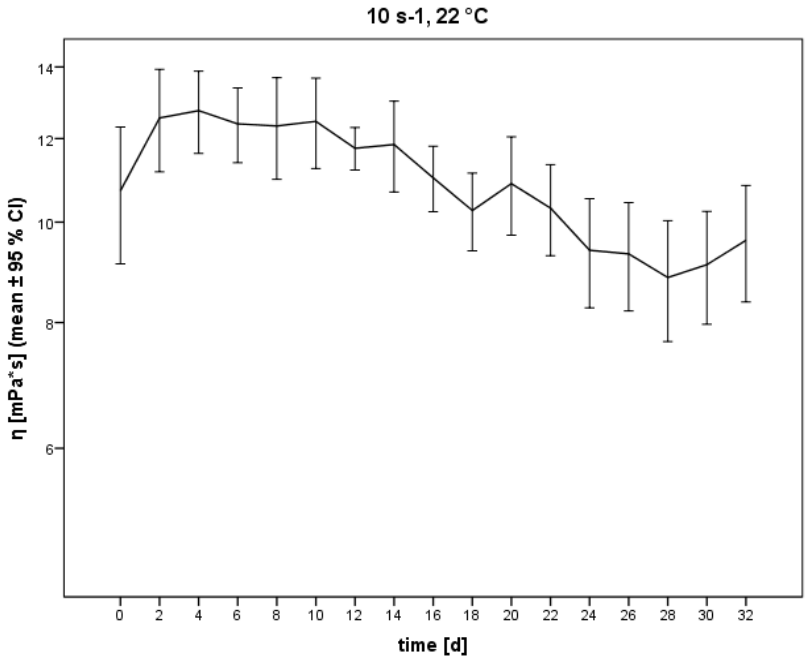

Fig. 43: Dynamic shear viscosity at 22 °C and 10 s^{-1}. The graph shows mean values with error bars (95 % confidence intervals) for dynamic shear viscosity [mPa*s] over storage time.

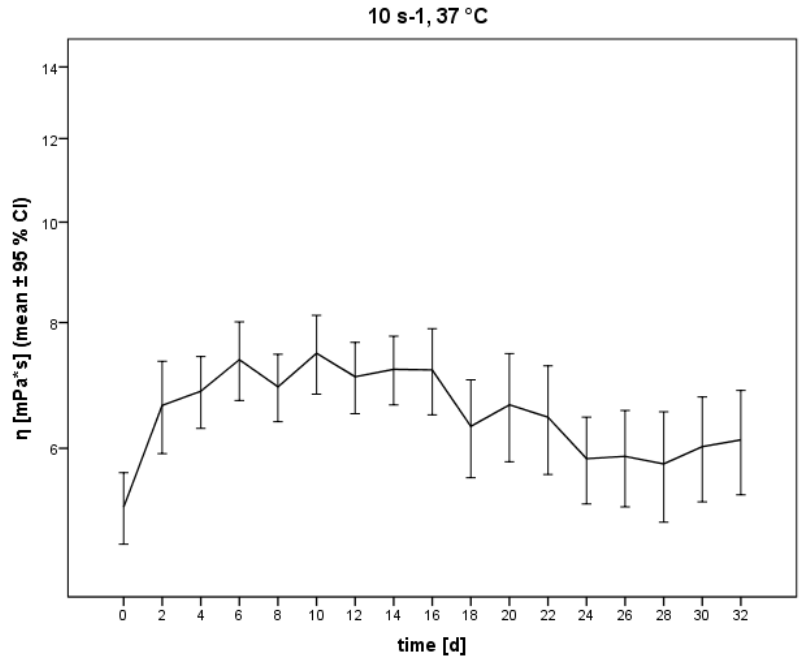

Fig. 44: Dynamic shear viscosity at 37 °C and 10 s^{-1}. The graph shows mean values with error bars (95 % confidence intervals) for dynamic shear viscosity [mPa*s] over storage time.

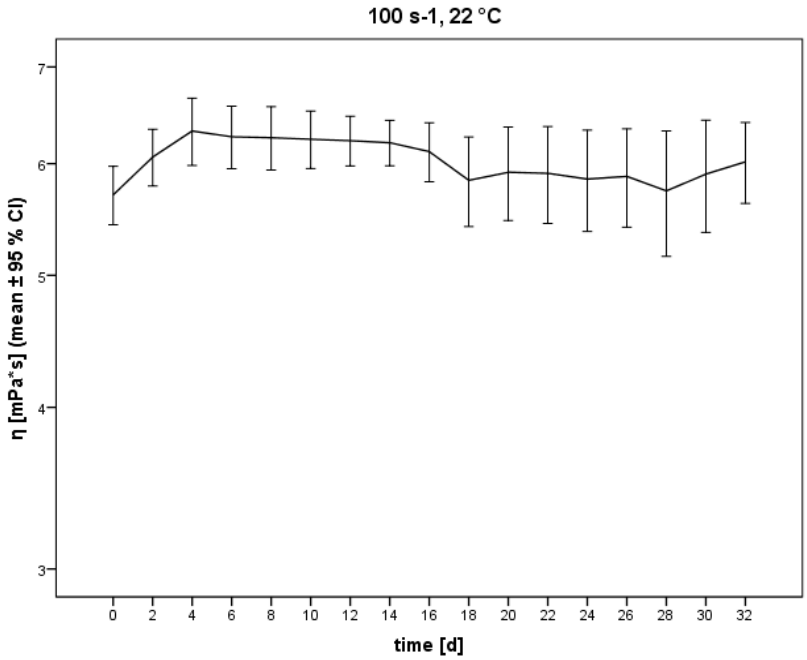

Fig. 45: Dynamic shear viscosity at 22 °C and 100 s^{-1}. The graph shows mean values with error bars (95 % confidence intervals) for dynamic shear viscosity [mPa*s] over storage time.

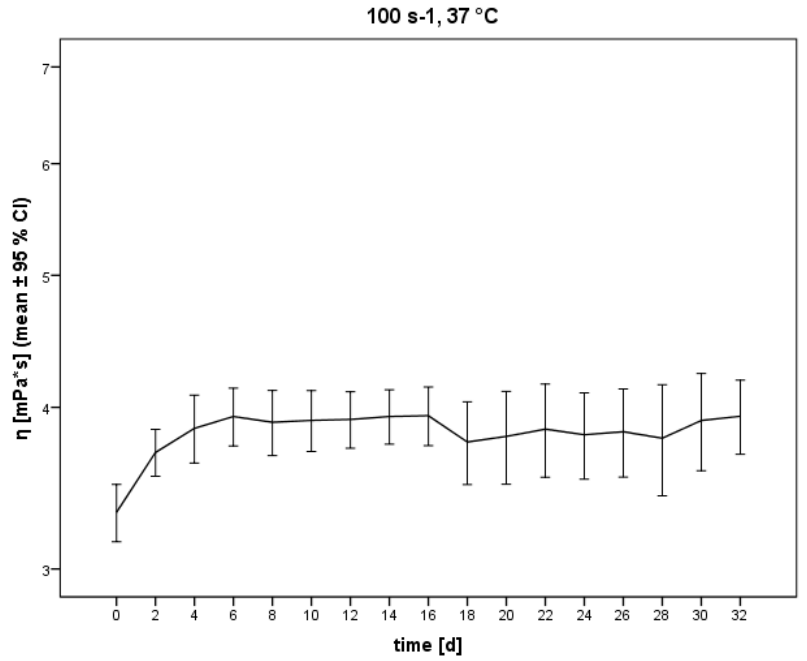

Fig. 46: Dynamic shear viscosity at 37 °C and 100 s^{-1}. The graph shows mean values with error bars (95 % confidence intervals) for dynamic shear viscosity [mPa*s] over storage time.

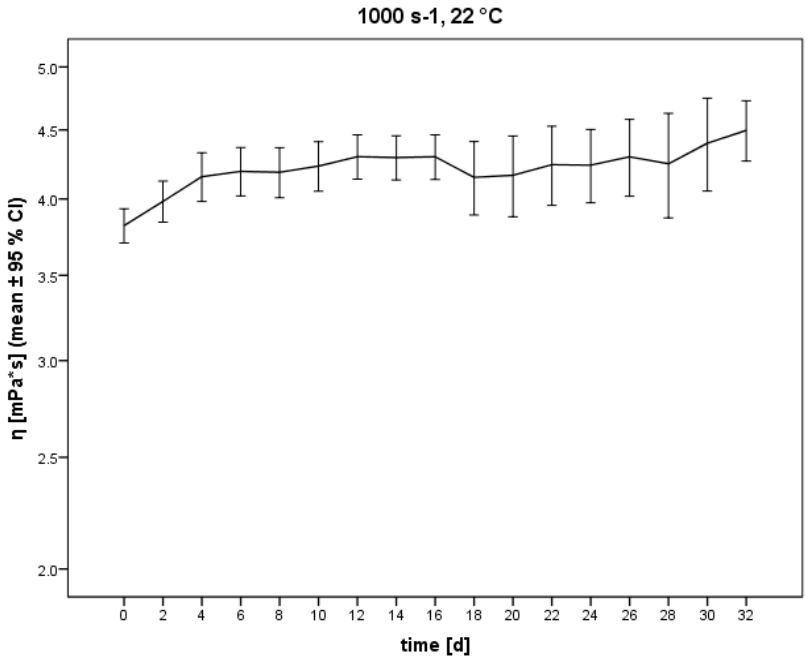

Fig. 47: Dynamic shear viscosity at 22 °C and 1000 s^{-1}. The graph shows mean values with error bars (95 % confidence intervals) for dynamic shear viscosity [mPa*s] over storage time.

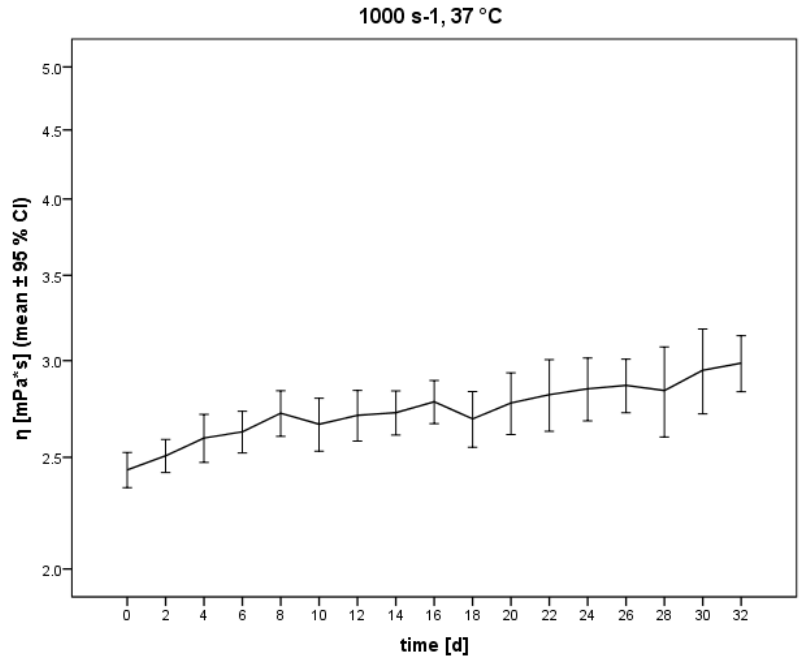

Fig. 48: Dynamic shear viscosity at 37 °C and 1000 s^{-1}. The graph shows mean values with error bars (95 % confidence intervals) for dynamic shear viscosity [mPa*s] over storage time.

4.2.5. Rheological analysis - oscillation measurements

Frequency sweep tests revealed a progressivity of loss factor tanδ at 1 s^{-1} during storage. The ascent was pronounced when samples were measured at 22 °C, starting between day 20 and 22 (Fig.49). At 37 °C, slight progressivity started between day 16 and 18. A pronounced increase was then noted between day 22 and 24 (Fig.50).

Wilcoxon signed-rank test (significance level: 0.05) was used to compare tanδ values at 1 s^{-1} of day 0 with day 32. It revealed a statistical significance of 0.004 (22 °C) and 0.033 (37 °C). In both cases, H_0 was rejected. Thus, the population mean rank was significantly higher after storage.

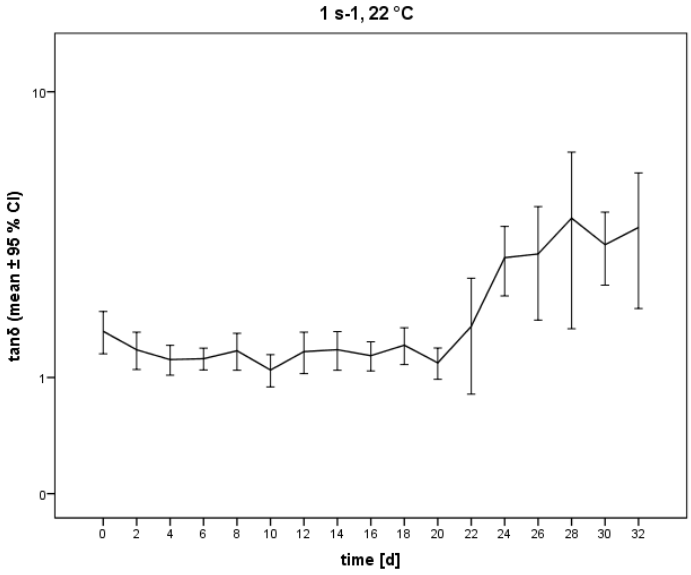

Fig. 49: Loss factor tanδ at 22 °C and 1 s^{-1}. The graph shows mean values with error bars (95 % confidence intervals) for tanδ over storage time.

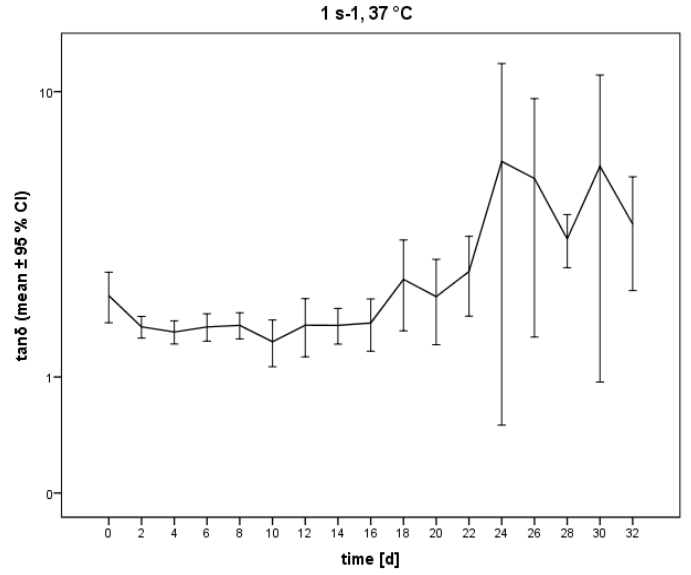

Fig. 50: Loss factor tanδ at 37 °C and 1 s^{-1}. The graph shows mean values with error bars (95 % confidence intervals) for tanδ over storage time.

4.3. Pilot study on bloodstain pattern simulation with aged samples

4.3.1. Photography

With four pig blood samples and three simulation experiments per sample, 12 photographs were obtained before and after storage each. A total of 24 pictures was therefore included for comparative analysis in this pilot study. Figures 51 and 52 exemplify one bloodstain pattern from each sample before and after storage.

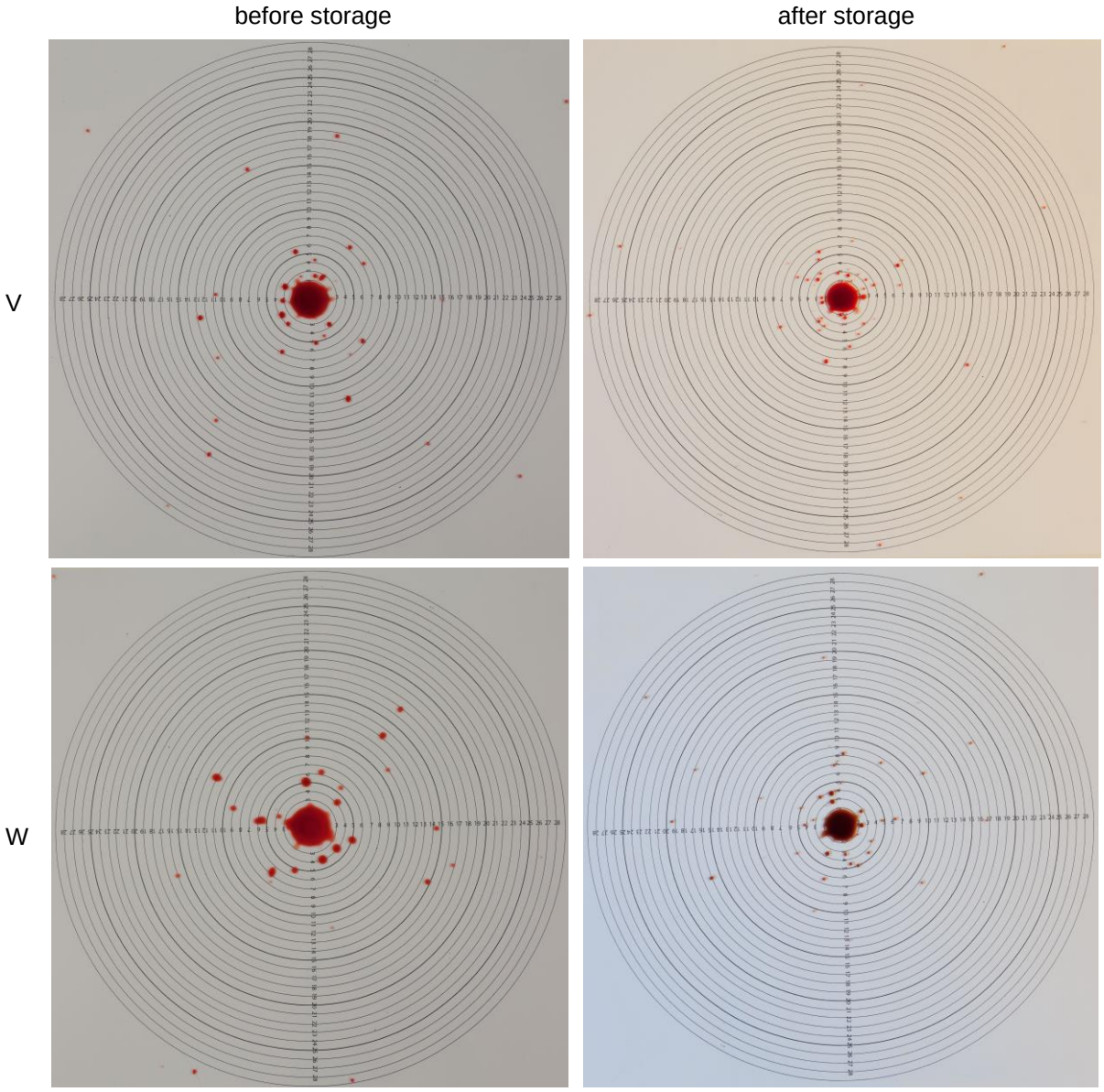

Fig. 51: Bloodstain patterns of samples V and W. The photographs show spatter resulting from two drops of blood falling into each other under standardized conditions before and after storage at 4 °C for 32 days.

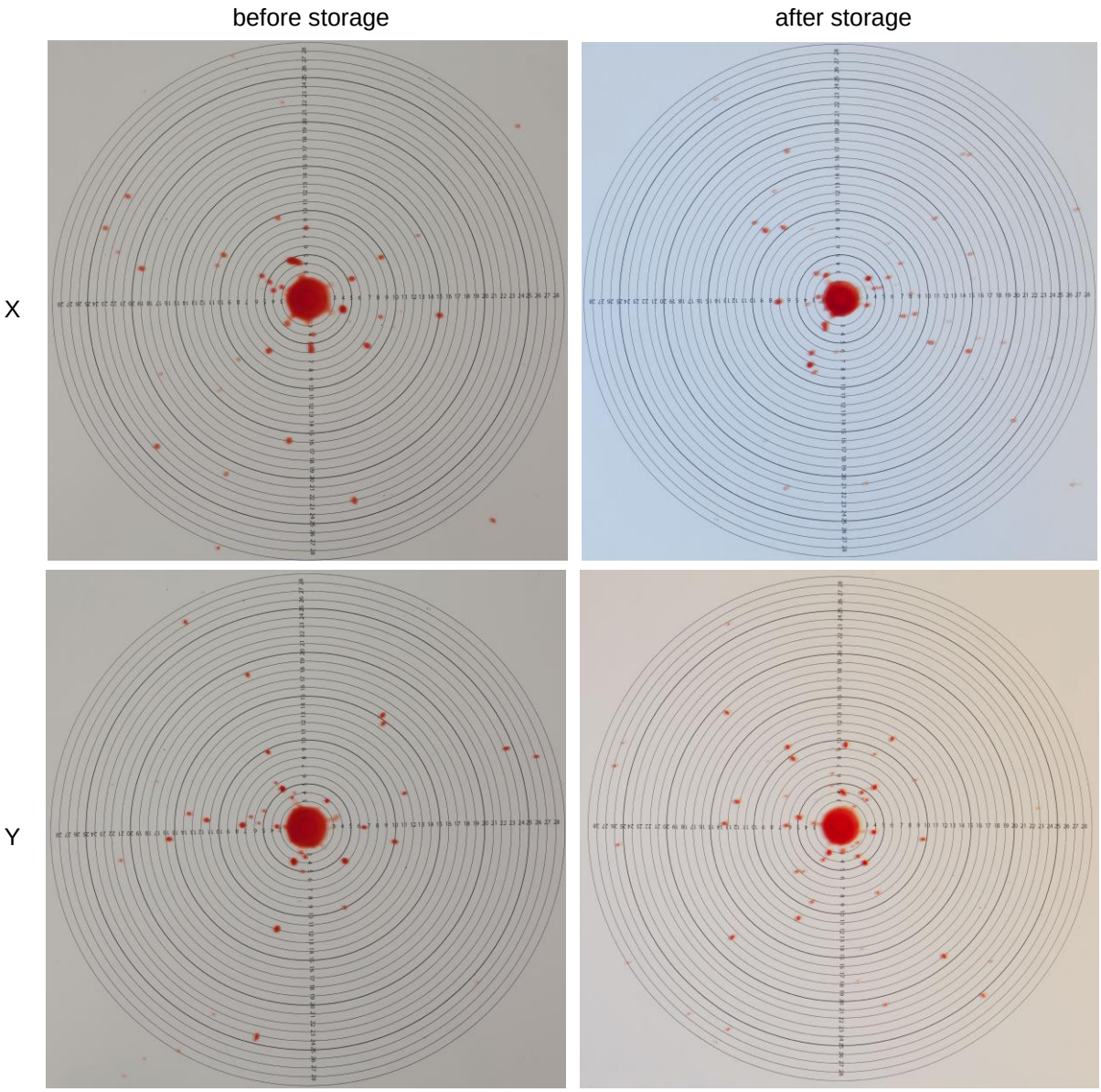

Fig. 52: Bloodstain patterns of samples X and Y. The photographs show spatter resulting from two drops of blood falling into each other under standardized conditions before and after storage at 4 °C for 32 days.

4.3.2. Comparative analysis

The comparison of bloodstain patterns before and after storage revealed changes in all parameters that were taken into account.

Parent stains before storage were either showing a diameter identical to the second band (diameter of 1 cm) or a diameter between bands 2 and 3 (diameter between 1 and 1.5 cm). After storage, parent stains of samples V and W featured a smaller diameter in all experiments. The stains were smaller than the second band, meaning that the diameter was less than 1 cm in all six cases. The parent stains of samples X and Y were smaller in two simulations each, as well as approximately the same size as before storage in one case each.

Thus, being smaller in 10 of 12 simulations, parent stains by tendency were smaller after storage at 4 °C for 32 days than shortly after withdrawal. Figure 53 exemplifies the decrease in parent stain diameter as observed in this pilot study.

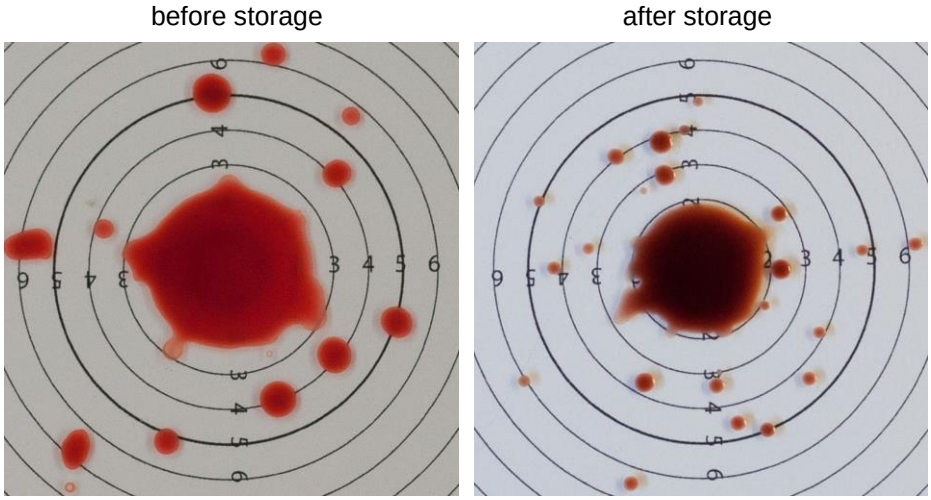

Fig. 53: Parent stains of simulations with sample W before and after storage. The photographs reveal the decrease of parent stain diameter after storage as observed during simulations in 10 of 12 cases. The pictures also reveal a change in size of satellite spatter, which was visible in some, but not in all comparisons.

The number of spatters within the first 14 bands of the template (within 7 cm around the point of impact) was higher after storage than before (Tab.15).

SAMPLE ID	BEFORE STORAGE	AFTER STORAGE	DIFFERENCE
V	20.33	31.00	+ 10.67
W	22.00	28.66	+ 6.66
X	20.66	33.00	+ 12.34
Y	22.66	32.33	+ 9.67

Tab. 15: Overview about the mean number of stains within the first 14 bands (within 7 cm around the point of impact) before and after storage.

The number of spatters between bands 14 and 28 (between a distance of 7 and 14 cm from the point of impact) after storage was slightly lower at experiments with three samples and higher at simulations with one sample compared to blood spatter produced directly after withdrawal (Tab.16).

SAMPLE ID	BEFORE STORAGE	AFTER STORAGE	DIFFERENCE
V	8.00	5.33	- 2.67
W	7.33	7.00	- 0.33
X	13.33	17.33	+ 4.00
Y	12.00	12.33	- 0.33

Tab. 16: Overview about the mean number of stains between bands 14 and 28 (between a distance of 7 and 14 cm from the point of impact) before and after storage.

The total number of spatters within 28 bands (within 14 cm around the point of impact) was higher in all experiments after storage than before (Tab.17).

SAMPLE ID	BEFORE STORAGE	AFTER STORAGE	DIFFERENCE
V	28.33	36.33	+ 8.00
W	29.33	35.66	+ 6.33
X	34.00	50.33	+ 16.33
Y	34.66	44.66	+ 10.00

Tab. 17: Overview about the mean total number of stains within 28 bands (within 14 cm around the point of impact) before and after storage.

In summary it can be stated that aged big blood in this pilot study showed a decrease in parent stain diameter and an increase of satellite spatter. The increase of satellite stains in numbers takes place rather in proximity to the parent stain than further afar. In some of the comparisons, a decrease of satellite spatter size was observed.

5. Discussion

5.1. Rheological characterization of porcine blood

For this part of the study, two research questions were posed:

a. What impact have the factors hematocrit and temperature on pig whole blood viscosity and suspension stability?

To study the influence of HCT and temperature on pig whole blood viscosity, different HCT dilutions (30, 40, 50, 60 %) of samples with EDTA (n=10) were analysed at various temperatures (7, 12, 17, 22, 27, 32, 37, 42 °C) with rotational measurements at distinct shear rates (1, 10, 100, 1000 s^{-1}).

In order to assess the influence of HCT and temperature on pig whole blood suspension stability (elasticity), the same HCT dilutions were analysed with oscillation measurements at different temperatures (7, 22, 37 °C). Frequency sweep tests (0.1 - 3.16 s^{-1}) were performed in SAOS mode with reversible material deformation at constant shear stress of 10 mPa.

Data obtained in this study indicate that dynamic shear viscosity of pig whole blood varies with HCT, temperature and shear rate. The measurement parameter increased with HCT increments, decreased with temperature ascent and was reduced with shear rate enlargement.

Results also reveal that storage module G´ and loss module G´´ increase with HCT increments and decrease with rise in temperature. Loss factor tanδ acts contrariwise. At 7 °C in all HCT dilutions and at 22 °C in the 60 % HCT dilution, pig blood featured the characteristics of a viscoelastic solid. In the other HCT-temperature-combinations, samples showed liquid viscoelastic behaviour.

As was expected, HCT and temperature thus have a striking impact on both pig whole blood viscosity and suspension stability. The influence of these two parameters has partly been observed in previous experiments, but was assessed and described in detail in this study for the first time [2,41].

b. What conclusions regarding the applicability of porcine whole blood for BPA re-enactment experiments can be made considering these effects?

In respect of the far reaching legal and emotional consequences for offenders, victims and relatives, which might result from insufficient BPA educational programs, error-prone BPA expert assessments and poor courtroom simulations, it seems inconceivably important to equip practical work of BPA with maximum quality and accurateness.

The physical properties of blood droplets - like viscosity and surface tension - influence blood spatter formation [2,52].

As confirmed and characterized in this study, HCT and temperature have a notable impact on pig whole blood viscosity and suspension stability. In order to accomplish optimum results and commensurableness, an international standardization of those two parameters in BPA experiments is highly recommended.

Experimentation with blood samples should orientate on the conditions under which an alleged crime occurred. Samples should therefore be warmed up to body temperature of 37 °C prior to usage. If available, HCT of the samples should be customized according to medical records of the victim. Leastwise, HCT of the samples should be adjusted to gender and age. Infants exhibit a dissimilar range of HCT values than adults and characteristically, values for males and females are also unlike [46].

Moreover, it should be pointed out that anticoagulation always means manipulation of the physiological situation. Data presented in this study are suitable for describing the physical material characteristics of pig blood anticoagulated with EDTA. Behaviour of native human whole blood during an act of bloodshed is believed to be alike, but might just as well differ. Unfortunately, conventional rheological analysis is not suitable for measurements of native whole blood. Further research is recommended in order to test the applicability of pig blood for BPA and to appreciate possible changes in physical behaviour due to anticoagulation additives.

Prior to the project, the following hypotheses were posed:

H_0: HCT and temperature do not influence pig whole blood viscosity and suspension stability and it is therefore not necessary to consider these factors during practical BPA experimentation.

H_1: HCT and temperature have a substantial impact on pig whole blood viscosity and suspension stability and should be taken into consideration during BPA simulations.

Considering the information obtained in this study, H_0 was rejected and H_1 was accepted.

5.2. Hemorheological analysis of pig blood storability

Regarding storability of pig blood for BPA, three research questions were introduced:

c. What hemorheological changes does pig blood show during storage at 4 °C?

Storability of pig whole blood was assessed with refrigerated storage and periodic multi-parametric analysis of samples anticoagulated with CPDA-1 (n=11) during a period of 32 days.

In consequence of troubles with bacterial contamination during earlier studies, samples were tested for microorganisms with routine screening agars at the beginning and end of storage at 4 °C. To embrace hematological characteristics over storage time, hemograms were created every two days with an automatic cell counter. Additionally, fHb was determined. Rotational measurements and measurements in the oscillating shear field were performed at two different temperatures (22, 37 °C) like described before.

Upon storage, RBC count diminished noticeably. As flow cytometry only counts intact cells, RBC decay may be accepted. Continuously increasing values for fHb corroborate this assumption. Presumably, the rise in fHb might in fact be linear and not exponential like observed in this study. As already known, haptoglobin, an acute phase protein, binds fHb in order to avoid iron loss and prevent highly reactive heme groups from causing tissue damage. The haptoglobin-hemoglobin-complex is not recorded with the colorimetric method used to determine fHb. At the time when all haptoglobin molecules are spent for complex formation, a remarkable leap of fHb is observed [90,92,93,94].
MCV increased during the first days of storage and decreased back to the original value afterwards. Conceivably, osmotic Na^+-influx leads to RBC swelling in the early phase of storage and the formation of echinocytes plays a role during later stages. Echinocytes, which are characteristic for RBC ageing, are RBCs featuring protrusions and a loss of the typical biconcave disc morphology [95,96].

MCH featured an almost constant upward movement throughout the storage process. This can be explained by the fact that MCH is calculated as MCH = (Hb * 10) / RBC. Hemoglobin measurement is a photometrical method performed after RBC lysis. As the number of intact RBCs lowers over storage time, MCH goes up [89].

MCHC decreased during the first days of storage. When RBC swelling takes place, the ratio between cell size and cellular Hb volume changes - reflecting in a decrease of MCHC. Likewise, cell shrinkage during a later phase of storage also had an impact on MCHC, which in this study showed constant progressivity following day 12. Thus, MCV and MCHC exhibit an opposing course.

HCT increased during the first days of storage, then displayed sort of a plateau and went down again below the original value afterwards. As HCT is calculated as HCT = RBC * MCV, it is determined by two hematological variables featuring contrasting progression.

Depending on the shear rate applied on the pig blood samples, dynamic shear viscosity showed different courses during ageing. While at a very low shear rate (1 s^{-1}) it showed a biphasic course, at high shear rate (1000 s^{-1}) the parameter increased constantly. Thus, upon storage, blood partially lost its shear thinning behaviour, approaching towards the characteristics of a Newtonian liquid.

Previous projects indicate that HCT is the major influence determining whole blood viscosity. The biphasic course of dynamic shear viscosity at low shear rate can therefore be associated to the increase of HCT in the early phase of ageing. However, the initial increase of HCT was in this case not related to cell count, but rather to a gain of RBC mass. Viscosity at high shear rate seems less prone to changes in HCT - regardless of its origin. Hence, the use of high rather than low shear rate is recommended for ageing analysis [41,52,97].

The reasons for the increase of dynamic shear viscosity at high shear rate in spite of a decrease of HCT over time can only be speculated. Rheology is a macroscopic method, characterizing the overall physical behaviour of blood. The effects of microscopic mechanisms like cell-cell-interactions are not described. Presumably, a number of factors might play a role: morphological changes of RBCs or a gain of cell debris in the sample might hinder the gliding of cells past each other during shear. Functional modifications like changes of the RBC surface charge might result in a modification of the interaction between cells and surrounding molecules. Finally, protein clusters in blood plasma due to damaged protein folding are also conceivable reasons.

In summary, a loss of structural strength over time is likely to occur. This assumption was confirmed by SAOS. During frequency sweep tests, a progressivity of loss factor tanδ at 1 s^{-1} (equivalent to 60 heartbeats per minute) was observed. When samples were measured at 22 °C, a pronounced ascent started between day 20 and 22. At 37 °C, slight progressivity started between day 16 and 18 and a pronounced ascent was noted between day 22 and 24. The increase of tanδ reflects an increase of fluidity and indicates that the formation of structures is impaired. Again, aged samples change their physical properties and approach towards Newtonian behaviour, which is not common for blood.

Results of bacteriological screening in this study cannot be regarded generally valid, but as BPA simulations might include resembling samples and similar steps of sample processing, the approach to microbiological issues presented in this study appears to be realistic. Screening after withdrawal was negative, showing only an insignificant volume of bacteria in a single sample. Screening procedure after storage revealed massive bacterial contamination.

However, bacteria that were identified via MALDI-TOF MS were the same in most of the samples. This indicates sample carryover. It is conceivable that bacteria were spread from one specimen cup to another during various working steps, but it is remarkable that these germs were not present when screening was first performed on the day of blood withdrawal. It is therefore suggested that bacterial contamination originated from the suction tube of the automated hematology analyser or from the pipet that was used to fill the annulus of the rheometer. Both elements were not disinfected and were also used by other research groups working with different animal species.

Anyway, bacteria found in this study are presumably no health risk to forensic personnel. Staphylococcus xylosus and Staphylococcus sciuri are both gram-positive colonisers of human and animal skin with little-known human pathogenic behaviour. Pantoea agglomerans belongs to the group of Enterobacteriaceae, which are unaspiring gram-negative germs. This species is often found in plants and is facultative human pathogenic - it has only been proven to be a cause of disease in rare cases [98,99].

Furthermore, antibiotic susceptibility testing for all three types of bacteria was within normal limits. Still, the effect of bacterial contamination on rheological behaviour remains unanswered and has to be assessed in future research.

d. What steps can be taken in order to prolong the storability of pig blood samples intended for BPA? How could a protocol look like?

As described in the methods section, CPDA-1 is a well-established and wide-spread anticoagulant buffer for whole blood preservation. Citrate inactivates blood clotting and Phosphate, Dextrose and Adenine help to enhance RBC survival. EDTA, which is currently often used for anticoagulation of samples intended for BPA experiments, does not trigger energy supply for RBCs. Thus, CPDA-1 seems more suitable for BPA issues [79,100].

In blood donor services, blood components are separated from each other and are stored under different conditions. For transfusion medicine, this strategy has proven to be most effective in terms of storability. Nevertheless, the procedure involves costly centrifuges and other utensils, which might not be available for BPA. In contrast, CPDA-1 is commercially available and can easily be adopted for venipuncture with inexpensive standard equipment. Furthermore, the effects of separated storage and reunion of blood components on structural strength have not been explored [96].

Surprisingly, blood withdrawal from pigs in a non-sterile stable seems to be barely susceptible to bacterial contamination. Presumably, blood withdrawal with a standard needle, i.v. line and perfusor syringe is therefore sufficiently dimensioned for BPA issues. If desired, antibiotics could be added to the samples in order to eliminate bacterial growth upon storage at 4 °C.

Previous findings indicate that the nature and quality of the container in which blood is stored has an impact on storability. In this study, standard 50 ml Falcon® vials were used for storage, because they are inexpensive and widely used in medical laboratories. Further research is recommended to compare different storage containers that could extend storability of whole blood samples intended for BPA [101].

e. To what extent can the storability of porcine blood intended for BPA be prolonged in comparison to present conservation methods with EDTA?

Raymond, Smith and Liesegang (1996) stated that it would be valid for BPA issues, to store pig blood anticoagulated with EDTA at 4 °C for a period of 14 days. Serp (2015) confirmed these findings.

Based on the course of loss factor tanδ (increase between day 20 and 22 at 22 °C, as well as slight increase between day 16 and 18, followed by a pronounced ascent between day 22 and 24 at 37 °C), a maximum storability of 20 days is postulated. This applies to pig whole blood that has been anticoagulated with CPDA-1, is stored at 4 °C and is gently mixed every second day. That implies a storability gain of one week, if blood is processed as described. Further research including practical simulations at regular intervals during storage is recommended.

Prior to analysis of pig blood storability, the following hypotheses were posed:

H_0: Storage at 4 °C does not influence the hemorheological characteristics of porcine whole blood.

H_1: There are substantial changes in hemorheological characteristics of porcine whole blood during storage at 4 ° C.

Based on the findings described, H_0 was rejected and H_1 was accepted

5.3. Pilot study on bloodstain pattern simulation with aged samples

For this part of the project, the following research question was posed:

f. In what way are bloodstain patterns created with aged pig blood different to patterns originating from simulations with fresh samples?

In order to assess possible changes of bloodstain patterns due to sample ageing, blood anticoagulated with CPDA-1 was used to create simple drop patterns under standardized conditions before and after storage at 4 °C for 32 days. The resulting stains were photographed and with the help of a template, the diameter of the parent stain, as well as the number and spreading width of satellite spatter was examined.

Analysis revealed that blood spatters originating from aged samples were different to patterns that had been created when specimens were fresh. A clear tendency towards a decrease of parent stain diameter and an increase of the number of satellite spatter in proximity to the parent stain was noted. With some simulations, a decrease of satellite spatter size was observed.

The trend towards smaller parent stains after storage has already been observed by Raymond, Smith and Liesegang (1996), but was first detected for blood with CPDA-1 in this study. The fact that the number of satellite spatters was elevated and the size of the particular spatters was smaller correlates with a loss or defect in structure formation like indicated by the course of the rheological parameter tanδ [2].

In general, results of the pilot project indicate that hemorheological changes in the sample are not only reflected in a change of various measuring parameters, but also have a practical relevance. It can be concluded that samples for BPA re-enactment experiments should in fact not exceed a certain duration of storage or otherwise distorted patterns might occur. It will be a task of future research to check, whether the postulated storability of 20 days for anticoagulated samples with CPDA-1 can be confirmed with appropriate simulations during the ageing process. For this, special equipment for the production of bloodstain patterns, which was not available during this pilot study, is to be employed.

At the beginning of the pilot study on bloodstain patterns originating from aged samples, the following hypotheses were established:

H_0: Bloodstain patterns created during simulations with aged samples feature the same physical appearance like patterns originating from re-enactment with fresh samples.

H_1: Bloodstain patterns created during simulations with aged samples are different in their physical appearance compared to patterns originating from re-enactment with fresh samples.

Although sample size in this pilot study was very small, conclusive differences in bloodstain patterns depending on sample age were observed. Thus, H_0 was rejected and H_1 was accepted.

6. Conclusio

BPA is a discipline of forensic sciences, contributing greatly to the clearance of criminal cases. A correct understanding of traces of blood can sometimes only be achieved with re-enactment and the training of qualified BPA professionals also requires practical simulations. Due to risk of infection and a shortage of adequate human samples, anticoagulated pig blood is a commonly used alternative during practical BPA experimentation [3,4,5,102].

Previous work showed that blood collected from abattoirs features less physiologic, in other words altered, material characteristics compared to blood collected from living animals via venipuncture. Only little was known about the influence of HCT and temperature on pig whole blood viscosity and suspension stability. The applicability of aged pig blood for BPA issues after storage at 4 °C had hardly been addressed in previous studies and literature. To gain further information, a study with three sub-projects was designed [41].

Following a comprehensive rheological characterization at different HCT variations, temperatures and shear rates, the impact of these influencing variables on dynamic shear viscosity and suspension stability of pig whole blood with EDTA was described. Furthermore, the relevance of these findings for BPA practice was discussed.

A project on storability of porcine blood was used to assess hemorheological changes during sample ageing. Anticoagulation with CPDA-1 was introduced as a potential improvement in terms of storage quality. Analysis revealed a continuous increase of high shear blood viscosity over time that was independent from changes of RBC mass. By this effect, shear thinning behaviour was reduced in aged samples, which is a clear sign for a loss of blood quality. In addition, a gradual loss of structural strength was observed upon storage. Since this effect became significant after 20 days, this time point was postulated to represent the maximum storability of porcine CPDA-1-blood for BPA issues at 4 °C.

The effect of blood ageing on spatter patterns was assessed in a pilot study with simple drop pattern simulations. A comparison of bloodstains created before and after sample storage revealed remarkable differences and thus underlined the necessity of future research on storage of pig blood for BPA issues.

List of figures

List of tables

List of references

1. **James, S. H., Kish, P. E. & Sutton, T. P.** *Principles of Bloodstain Pattern Analysis: Theory and Practice.* 1 (CRC Press, Boca Raton, 2005).
2. **Raymond, M. A., Smith, E. R. & Liesegang, J.** The physical properties of blood - forensic considerations. *Science & Justice* **36**, 153-160 (1996).
3. **Peschel, O., *et al.*** Blood stain pattern analysis. *Forensic Sci Med Pathol* **7** (3), 257-270 (2011).
4. **Kunz, S. N., Klawonn, T., Grove, C.** Möglichkeiten und Grenzen der forensischen Blutspurenmusterverteilungsanalyse. *Wien Med Wochenschr* **164** (17-18), 358-362 (2014).
5. **Brodbeck, S.** Introduction to Bloodstain Pattern Analysis. *SIAK* **2** (2012), 51-57 (2012).
6. **James, S. H., Kish, P. E. & Sutton, T. P.** *Principles of Bloodstain Pattern Analysis: Theory and Practice.* 108 (CRC Press, Boca Raton, 2005).
7. International Association of Bloodstain Pattern Analysts. IABPA Logo. [URL: http://www.iabpa.org/] download 12th of August 2016.
8. **James, S. H., Kish, P. E. & Sutton, T. P.** *Principles of Bloodstain Pattern Analysis: Theory and Practice.* 3 (CRC Press, Boca Raton, 2005).
9. **James, S. H., Kish, P. E. & Sutton, T. P.** *Principles of Bloodstain Pattern Analysis: Theory and Practice.* 7-8 (CRC Press, Boca Raton, 2005).
10. **James, S. H., Kish, P. E. & Sutton, T. P.** *Principles of Bloodstain Pattern Analysis: Theory and Practice.* 10 (CRC Press, Boca Raton, 2005).
11. **James, S. H., Kish, P. E. & Sutton, T. P.** *Principles of Bloodstain Pattern Analysis: Theory and Practice.* 71 (CRC Press, Boca Raton, 2005).
12. **James, S. H., Kish, P. E. & Sutton, T. P.** *Principles of Bloodstain Pattern Analysis: Theory and Practice.* 88-89/92 (CRC Press, Boca Raton, 2005).
13. **James, S. H., Kish, P. E. & Sutton, T. P.** *Principles of Bloodstain Pattern Analysis: Theory and Practice.* 76/79 (CRC Press, Boca Raton, 2005).
14. **James, S. H., Kish, P. E. & Sutton, T. P.** *Principles of Bloodstain Pattern Analysis: Theory and Practice.* 84 (CRC Press, Boca Raton, 2005).
15. **James, S. H., Kish, P. E. & Sutton, T. P.** *Principles of Bloodstain Pattern Analysis: Theory and Practice.* 87 (CRC Press, Boca Raton, 2005).
16. **James, S. H., Kish, P. E. & Sutton, T. P.** *Principles of Bloodstain Pattern Analysis: Theory and Practice.* 99-100 (CRC Press, Boca Raton, 2005).
17. **James, S. H., Kish, P. E. & Sutton, T. P.** *Principles of Bloodstain Pattern Analysis: Theory and Practice.* 119/136/138 (CRC Press, Boca Raton, 2005).
18. **James, S. H., Kish, P. E. & Sutton, T. P.** *Principles of Bloodstain Pattern Analysis: Theory and Practice.* 108-110/114 (CRC Press, Boca Raton, 2005).

19. **James, S. H., Kish, P. E. & Sutton, T. P.** *Principles of Bloodstain Pattern Analysis: Theory and Practice.* 149/158/160/164 (CRC Press, Boca Raton, 2005).
20. **James, S. H., Kish, P. E. & Sutton, T. P.** *Principles of Bloodstain Pattern Analysis: Theory and Practice.* 179 (CRC Press, Boca Raton, 2005).
21. **James, S. H., Kish, P. E. & Sutton, T. P.** *Principles of Bloodstain Pattern Analysis: Theory and Practice.* 188-189 (CRC Press, Boca Raton, 2005).
22. **Chen, R., et al.** Blood drop patterns: Formation and applications. *Adv Colloid Interface Sci* **231**, 1-4 (2016).
23. **James, S. H., Kish, P. E. & Sutton, T. P.** *Principles of Bloodstain Pattern Analysis: Theory and Practice.* 194-197 (CRC Press, Boca Raton, 2005).
24. **James, S. H., Kish, P. E. & Sutton, T. P.** *Principles of Bloodstain Pattern Analysis: Theory and Practice.* 179-180 (CRC Press, Boca Raton, 2005).
25. **James, S. H., Kish, P. E. & Sutton, T. P.** *Principles of Bloodstain Pattern Analysis: Theory and Practice.* 206-207 (CRC Press, Boca Raton, 2005).
26. **Benecke, M., Barksdale, L.** Distinction of bloodstain patterns from fly artifacts. *Forensic Sci Int* **137**, 152-159 (2003).
27. **James, S. H., Kish, P. E. & Sutton, T. P.** *Principles of Bloodstain Pattern Analysis: Theory and Practice.* 212-213 (CRC Press, Boca Raton, 2005).
28. **James, S. H., Kish, P. E. & Sutton, T. P.** *Principles of Bloodstain Pattern Analysis: Theory and Practice.* 210 (CRC Press, Boca Raton, 2005).
29. **James, S. H., Kish, P. E. & Sutton, T. P.** *Principles of Bloodstain Pattern Analysis: Theory and Practice.* 369-373 (CRC Press, Boca Raton, 2005).
30. **James, S. H., Kish, P. E. & Sutton, T. P.** *Principles of Bloodstain Pattern Analysis: Theory and Practice.* 398/408/416 (CRC Press, Boca Raton, 2005).
31. **James, S. H., Kish, P. E. & Sutton, T. P.** *Principles of Bloodstain Pattern Analysis: Theory and Practice.* 410/418 (CRC Press, Boca Raton, 2005).
32. **James, S. H., Kish, P. E. & Sutton, T. P.** *Principles of Bloodstain Pattern Analysis: Theory and Practice.* 422-432 (CRC Press, Boca Raton, 2005).
33. **James, S. H., Kish, P. E. & Sutton, T. P.** *Principles of Bloodstain Pattern Analysis: Theory and Practice.* 68 (CRC Press, Boca Raton, 2005).
34. **James, S. H., Kish, P. E. & Sutton, T. P.** *Principles of Bloodstain Pattern Analysis: Theory and Practice.* 460-461 (CRC Press, Boca Raton, 2005).
35. **James, S. H., Kish, P. E. & Sutton, T. P.** *Principles of Bloodstain Pattern Analysis: Theory and Practice.* 9/145 (CRC Press, Boca Raton, 2005).
36. **James, S. H., Kish, P. E. & Sutton, T. P.** *Principles of Bloodstain Pattern Analysis: Theory and Practice.* 56-57 (CRC Press, Boca Raton, 2005).
37. **Attinger, D. *et al.*** Fluid dynamics topics in bloodstain pattern analysis: Comparative review and research opportunities. *Forensic Sci Int* **231** (1-3), 375-396 (2013).
38. **Stotesbury, T. *et al.*** A Commentary on Synthetic Blood Substitute Research and Development. *Journal of Bloodstain Pattern Analysis* **31**, 3-6 (2015).

39. **Stotesbury, T., et al.** A Commentary on Synthetic Blood Substitute Research and Development. *Journal of Bloodstain Pattern Analysis.* **31** (2), 3-6 (2015).

40. **Vitiello, A., et al.** Bloodstain pattern analysis as optimisation problem. *Forensic Sci Int* Epub ahead of print (2016).

41. **Serp, B.** Die Verwendung von Schweineblut in der Blutspurenmusteranalyse: Hämatologische und hämorheologische Eigenschaften von alterndem Schweineblut. Bachelor thesis, Bachelor degree course Biomedical Sciences, FH Campus Wien (Vienna, 2015).

42. **James, S. H., Kish, P. E. & Sutton, T. P.** *Principles of Bloodstain Pattern Analysis: Theory and Practice.* 11-13 (CRC Press, Boca Raton, 2005).

43. **Thews, G., Mutschler, E. & Vaupel, P.** *Anatomie Physiologie Pathophysiologie des Menschen.* 168-170/213 (Wissenschaftliche Verlagsgesellschaft mbH, Stuttgart, 1999).

44. U.S. National Library of Medicine. How does the blood circulatory system work? [URL: http://www.ncbi.nlm.nih.gov/pubmedhealth/PMH0072434/] download 14th of August 2016.

45. **James, S. H., Kish, P. E. & Sutton, T. P.** *Principles of Bloodstain Pattern Analysis: Theory and Practice.* 41-43 (CRC Press, Boca Raton, 2005).

46. **Thews, G., Mutschler, E. & Vaupel, P.** *Anatomie Physiologie Pathophysiologie des Menschen.* 109/143 (Wissenschaftliche Verlagsgesellschaft mbH, Stuttgart, 1999).

47. **Thews, G., Mutschler, E. & Vaupel, P.** *Anatomie Physiologie Pathophysiologie des Menschen.* 109 (Wissenschaftliche Verlagsgesellschaft mbH, Stuttgart, 1999).

48. **James, S. H., Kish, P. E. & Sutton, T. P.** *Principles of Bloodstain Pattern Analysis: Theory and Practice.* 41-45 (CRC Press, Boca Raton, 2005).

49. **Thews, G., Mutschler, E. & Vaupel, P.** *Anatomie Physiologie Pathophysiologie des Menschen.* 115/129/134 (Wissenschaftliche Verlagsgesellschaft mbH, Stuttgart, 1999).

50. Shaikh, A., Bhartiya, D. Hematopoiesis in bone marrow. [URL: http://www.intechopen.com/books/blood-cell-an-overview-of-studies-in-hematology/pluripotent-stem-cells-in-bone-marrow-and-cord-blood] download 14th of August 2016.

51. **James, S. H., Kish, P. E. & Sutton, T. P.** *Principles of Bloodstain Pattern Analysis: Theory and Practice.* 48-49 (CRC Press, Boca Raton, 2005).

52. **Laan, N.** Impact of blood droplets. PhD thesis. University of Amsterdam (Amsterdam, 2016).

53. **Attinger, D., et al.** Fluid dynamics topics in bloodstain pattern analysis: comparative review and research opportunities. *Forensic Sci Int* **231** (1-3), 375-396 (2013).

54. **Adam, C. D., et al.** Fundamental studies of bloodstain formation and characteristics. *Forensic Sci Int* **219** (1-3), 76-87 (2012).

55. **Mezger, T. G.** *Das Rheologie Handbuch: Für Anwender von Rotations- und Oszillations-Rheometern.* 29/31-32 (Vincentz Network, Hannover, 2012).

56. **Mezger, T. G.** *Das Rheologie Handbuch: Für Anwender von Rotations- und Oszillations-Rheometern.* 40/47 (Vincentz Network, Hannover, 2012).

57. **Mezger, T. G.** *Das Rheologie Handbuch: Für Anwender von Rotations- und Oszillations-Rheometern.* 37-38 (Vincentz Network, Hannover, 2012).

58. **Thews, G., Mutschler, E. & Vaupel, P.** *Anatomie Physiologie Pathophysiologie des Menschen.* 221-222 (Wissenschaftliche Verlagsgesellschaft mbH, Stuttgart, 1999).

59. **Baskurt, O. K., Meiselman, H. J.** Blood Rheology and Hemodynamics. *Seminars in Thrombosis and Hemostasis* **29** (5), 435-450 (2003).

60. **Merrill, E. W.** Rheology of Blood. *Physiological Reviews* **49** (4), 863-888 (1969).

61. Sochi, T. Cornell University Library. Non-Newtonian Rheology in Blood Circulation. [URL: http://arxiv.org/abs/1306.2067] download 25th of March 2016.

62. **Windberger, U., et al.** Measurement of whole blood of different mammalian species in the oscillating shear field: influence of erythrocyte aggregation. *unpublished manuscript* Medical University of Vienna (2016).

63. **Baskurt, O. K., Meiselman, H. J.** Blood rheology and hemodynamics. *Semin Thromb Hemost* **29** (5), 435-450 (2003).

64. **Mezger, T. G.** *Das Rheologie Handbuch: Für Anwender von Rotations- und Oszillations-Rheometern.* 35 (Vincentz Network, Hannover, 2012).

65. National Institute of Standards and Technology - U.S. Department of Commerce. Guide to Rheological Nomenclature: Measurements in Ceramic Particulate Systems. [URL: http://ciks.cbt.nist.gov/~garbocz/SP946/node14.htm] download and edit 25th of March 2016.

66. **Mezger, T. G.** *Das Rheologie Handbuch: Für Anwender von Rotations- und Oszillations-Rheometern.* 35-38 (Vincentz Network, Hannover, 2012).

67. **Mezger, T. G.** *Das Rheologie Handbuch: Für Anwender von Rotations- und Oszillations-Rheometern.* 138 (Vincentz Network, Hannover, 2012).

68. **Magnus, K., Popp, K. & Sextro, W.** *Schwingungen: Eine Einführung in die physikalischen Grundlagen und die theoretische Behandlung von Schwingungsproblemen.* 13 (Vieweg + Teubner, Wiesbaden, 2008).

69. **Mezger, T. G.** *Das Rheologie Handbuch: Für Anwender von Rotations- und Oszillations-Rheometern.* 143/149/163 (Vincentz Network, Hannover, 2012).

70. **Knopp, K., Bagemihl, F.** *Theory of Functions, Parts I and II.* 3 (Dover Publications, Mineola, 1996).

71. **Pohl, R., Lüders, K.** *Pohls Einführung in die Physik. Band 1: Mechanik, Akustik und Wärmelehre.* 8 (Springer, Berlin Heidelberg, 2008).

72. **Mezger, T. G.** *Das Rheologie Handbuch: Für Anwender von Rotations- und Oszillations-Rheometern.* 143/150/151 (Vincentz Network, Hannover, 2012).

73. **Mezger, T. G.** *Das Rheologie Handbuch: Für Anwender von Rotations- und Oszillations-Rheometern.* 159-161 (Vincentz Network, Hannover, 2012).

74. **Mezger, T. G.** *Das Rheologie Handbuch: Für Anwender von Rotations- und Oszillations-Rheometern.* 150/155 (Vincentz Network, Hannover, 2012).

75. Windberger, U. unpublished data (2016).

76. **Mezger, T. G.** *Das Rheologie Handbuch: Für Anwender von Rotations- und Oszillations-Rheometern.* 163-164 (Vincentz Network, Hannover, 2012).

77. **Smith, J.**E., Mahaffey, E. & Board, P. A new storage medium for canine blood. *J Am Vet Med Assoc* **172** (6), 701-703 (1978).

78. **Price, G. S., et al.** Evaluation of citrate-phosphate-dextrose-adenine as a storage medium for packed canine erythrocytes. *J Vet Intern Med* **2** (3), 126-132 (1988).

79. **Beutler, E.**, West, C. The storage of hard-packed red blood cells in citrate-phosphate-dextrose (CPD) and CPD-adenine (CPDA-1). *Blood* **54** (1), 280-284 (1979).

80. Sparer, A. personal photograph (2016).

81. **Ellner, P. D., et al.** A new culture medium for medical bacteriology. *Am J Clin Pathol* **45** (4), 502-504 (1966).

82. Becton, Dickinson and Company (BD). Gebrauchsanweisung: Columbia Agar with 5% Sheep Blood. [URL: http://www.bd.com/resource.aspx?IDX=8609] download 21st of August 2016.

83. Becton, Dickinson and Company (BD). Gebrauchsanweisung: Schaedler Agar with Vitamin K1 and 5% Sheep Blood. [URL: https://www.bd.com/resource.aspx?IDX=8626] download 21st of August 2016.

84. **Croxatto, A. Prod´hom, G. & Greub, G.** Applications of MALDI-TOF mass spectrometry in clinical diagnostic microbiology. *FEMS Microbiol Rev* **36** (2), 380-407 (2012).

85. **Schubert, S., Wieser, A.** MALDI-TOF-MS in der mikrobiologischen Diagnostik. *BIOspektrum* **07.10**, 760-762 (2010).

86. **Bonev, B., Hooper, J. & Parisot, J.** Principles of assessing bacterial susceptibility to antibiotics using the agar diffusion method. *J Antimicrob Chemother* **61** (6), 1295-1301 (2008).

87. Becton, Dickinson and Company (BD). Gebrauchsanweisung: Mueller Hinton II Agar. [URL: https://www.bd.com/ds/technicalCenter/inserts/L007393(11)(0706).pdf] download 23rd of August 2016.

88. European Committee On Antimicrobial Susceptibility Testing. Breakpoint tables for interpretation of MICs and zone diameters. Version 6.0. [URL: http://www.eucast.org/fileadmin/src/media/PDFs/EUCAST_files/Breakpoint_tables/v_6.0_Breakpoint_table.pdf] download 15th of August 2016.

89. Siemens. ADVIA® 2120/2120i Hematology Systems. Operator's Guide. [URL: http://photos.medwrench.com/equipmentManuals/2029-4080.pdf] download 27th of August 2016.

90. **Bauer, K.** Determination of free haemoglobin in serum by an automated assay using 4-aminophenazone and the Cobas Bio System. *J Clin Chem Clin Biochem* **19** (9), 971-976 (1981).
91. Sparer, A. personal photograph (2016).
92. **Wassell, J.** Haptoglobin: function and polymorphism. *Clin Lab* **46** (11-12), 547-552 (2000).
93. **Andersen, C. B., et al.** Structure of the haptoglobin-haemoglobin complex. *Nature* **489** (7416), 456-459 (2012).
94. **Alayash, A. I., et al.** Haptoglobin: the hemoglobin detoxifier in plasma. *Trends Biotechnol* **31** (1), 2-3 (2013).
95. **Wong, K. H., et al.** The Role of Physical Stabilization in Whole Blood Preservation. *Sci Rep* **6:21023**, 1-9 (2016).
96. **D'Alessandro, A., et al.** Red blood cell storage: the story so far. *Blood Transfus* **8** (2), 82-88 (2010).
97. **Pöschl, C***.* Die Vollblutviskosität in Abhängigkeit von Hämatokrit und Temperatur. Diploma thesis, Diploma degree programme Medicine, Medical University of Vienna (Vienna, 2016).
98. **Murray, P. R., et al.** *Manual of Clinical Microbiology. 9th edition. Volume 1.* 659/700 (American Society for Microbiology, Washington, 2007).
99. **Neumeister, B., et al.** *Mikrobiologische Diagnostik: Bakteriologie - Mykologie - Virologie - Parasitologie.* 336-337/431-432 (Thieme, Stuttgart, 2009).
100. **Banfi, G., Salvagno, G. L. & Lippi, G.** The role of ethylenediamine tetraacetic acid (EDTA) as in vitro anticoagulant for diagnostic purposes. *Clin Chem Lab Med* **45** (5), 565-576 (2007).
101. **Prowse, C. V., et al.** Commercially available blood storage containers. *Vox Sang* **160** (1), 1-13 (2014).
102. **James, S. H., Eckert, W. G.** Interpretation of Bloodstain Evidence at Crime Scenes. Second Edition. 11 (CRC Press, Boca Raton, 1998).